ELECTRON SPIN RESONANCE OF SEVERAL MOLECULES IN THE SOLID STATE

Thesis by

O. Hayes Griffith

In Partial Fulfillment of the Requirements

For the Degree of

Doctor of Philosophy

California Institute of Technology

Pasadena, California

1965

(Submitted December 17, 1964)

To my parents

Osbie and Mary Belle Griffith

and my grandmother

the late Mattie Hayes Neathery

whose foresight and encouragement

made this thesis possible

GENERAL ACKNOWLEDGMENTS

The presence of seven acknowledgment sections instead of one in this thesis indicates the large amount of help received from others. Here I will only mention the names of those whose contributions were of too broad a nature to accompany any one topic of the thesis.

I am deeply indebted to Professor H. M. McConnell, my scientific advisor, for his encouragement and detailed help on both theoretical and experimental problems. It is difficult to express my appreciation for the individual attention and cooperation received while a member of Professor McConnell's research group.

I would also like to thank Dr. Alvin Kwiram, Dr. Harris Silverstone, and Dr. Pier Luigi Nordio for innumerable discussions. Proofreading of the thesis by Robert Metzger, Charles Christenson and Mrs. Siri Buckman is sincerely appreciated.

My graduate studies were made possible by a Woodrow Wilson Foundation Fellowship, three National Science Foundation Fellowships, a tuition scholarship, and support from the National Science Foundation and the Shell Companies Foundation.

ABSTRACT

Single crystals of ester-urea, ketone-urea, and ether-urea inclusion compounds were X-irradiated and investigated by electron spin resonance. Eleven inclusion compounds formed between urea and the straight-chain alkyl esters yielded radicals of the type $RCH_2\dot{C}HCOOR'$. The α and β proton coupling constants of two radicals were studied over the temperature range 352°K to 7°K. The splittings caused by the alcohol (R') protons were resolved in many cases. Information regarding the structure of the inclusion compounds was obtained. The long-lived radical $RCH_2\dot{C}HCOR'$ was detected in all six ketone-urea crystals. The spin density in the 2p orbital adjacent to the carbonyl group is 0.81 ± .04. The ether radicals were of the type $R\dot{C}HOR'$ and the spin density on the carbon atom is approximately 0.70 ± .08. The ketone radical and ether radical spin distributions obtained from the π-electron theory are in qualitative agreement with the experimental spin distributions. In addition, single crystals of fumaric acid-urea were X-irradiated and studied by electron spin resonance. The dominant radical ($HO_2CCH_2\dot{C}HCO_2H$) in this case is formed by addition of a hydrogen atom (rather than by removal of a hydrogen atom, as above). The fumaric acid-urea crystal is not a hexagonal inclusion compound. The major orientations of the radical were determined with respect to the external crystal morphology.

Electron spin resonance studies of the triplet state of pyrene and triplet exciton states in ion radical salts are also briefly reported. The

approximate g values and zero field parameters for pyrene in a fluorene matrix at 100°K are $g_{xx} = 2.0033$, $g_{yy} = 2.0026$, $g_{zz} = 2.0033$, $D(xy)/hc = \pm 0.0806\ cm^{-1}$, $D(z)/hc = \pm 0.0810\ cm^{-1}$, and $E/hc = \mp 0.0182\ cm^{-1}$. The estimated errors in the g values, D, and E are ± 0.005, ± 0.0012, and ± 0.0009, respectively. The relation between triplet excitons and magnetically dilute radicals in the $(\varphi_3PCH_3)^+ (TCNQ)_2^-$ and $(\varphi_3AsCH_3)^+ (TCNQ)_2^-$ ion radical salts was investigated. The temperature-dependent broadening of the radical line is apparently caused by an exciton-radical exchange interaction. At 77°K the exciton line width is proportional to the free radical impurity line width, which suggests that unresolved nuclear hyperfine interactions contribute greatly to the exciton line width at this temperature.

TABLE OF CONTENTS

Page

ELECTRON SPIN RESONANCE OF SEVERAL MOLECULES IN THE SOLID STATE

I. ELECTRON SPIN RESONANCE AND MOLECULAR MOTION OF THE $RCH_2\dot{C}HCOOR'$ RADICALS IN X-IRRADIATED ESTER-UREA INCLUSION COMPOUNDS .. 2

A. Introduction 4

B. Proton Coupling Constants 6

a. The β-Proton Coupling Constants 7

b. The α-Proton Coupling Constants 14

C. Experimental 16

D. Identification of the Ester Radicals 18

E. Temperature Variations of the Ethyl Heptanoate Radical Spectra 27

F. Discussion of the Room-Temperature Ester Radical Spectra 32

G. The Carboxylic Acid-Urea Inclusion Compounds 36

H. Spectroscopic Splitting Factor Data 42

I. Summary 43

J. Acknowledgments 45

K. References 46

II. ELECTRON SPIN RESONANCE OF $R\dot{C}HCOR'$ RADICALS IN X-IRRADIATED KETONE-UREA INCLUSION COMPOUNDS 51

A. Introduction 52

B. Experimental 53

C. Radical Identification 54

TABLE OF CONTENTS (continued)

Page

D. Experimental Determination of the Spin Density ρC_2^{π}

a. From α-Proton Coupling Constant Data 62

b. From β-Proton Coupling Constant Data 65

c. Effects of Temperature Changes on the ESR Spectra 67

E. Molecular Orbital Calculations of Spin Density 71

F. Acknowledgments 75

G. References 77

III. ELECTRON SPIN RESONANCE AND ELECTRONIC STRUCTURE OF THE RĊHOR' ETHER RADICALS 81

A. Introduction 81

B. Experimental 82

C. Radical Identification 83

D. Experimental Spin Distribution

a. From α-Proton Coupling Constant Data 92

b. From β-Proton Coupling Constant Data 94

E. Theoretical Spin Density Distribution

a. Hückel MO Method 95

b. Configuration Interaction 97

c. Valence Bond Model 104

F. Acknowledgments 105

G. References 106

IV. AN ELECTRON SPIN RESONANCE STUDY OF X-IRRADIATED FUMARIC ACID-UREA CRYSTALS 110

A. Introduction 111

TABLE OF CONTENTS (continued)

Page

B. Experimental 112

C. Results 115

D. Discussion

a. The Relation Between the Free Radical Axes and the Crystal Coordinates 121

b. The β-Proton Coupling Constants 122

c. Comparison of the Fumaric Acid-Urea Crystal With Other Dicarboxylic Acid-Urea Crystals 123

E. Acknowledgments 127

F. References 128

V. MAGNETIC RESONANCE OF THE TRIPLET STATE OF ORIENTED PYRENE MOLECULES 133

VI. TRIPLET EXCITONS AND MAGNETICALLY DILUTE RADICALS IN $(\varphi_3PCH_3)^+$ $(TCNQ)_2^-$ AND $(\varphi_3AsCH_3)^+$ $(TCNQ)_2^-$ ION RADICAL SALTS 140

A. Introduction 140

B. Experimental 142

C. Radical-Exciton Spin Exchange 142

D. Anisotropy of Exciton and Radical Line Widths at 77°K 152

E. Acknowledgments 156

F. References 157

APPENDIXES 159

I. SUPPLEMENTARY REMARKS ON APPARATUS AND METHODS 160

II. ETHER RADICAL CI MATRIX ELEMENTS 171

TABLE OF CONTENTS (continued)

Page

III. RADICAL AND TRIPLET SPIN HAMILTONIANS

A. Radical Hyperfine Structure Hamiltonian 174

B. Triplet State Fine Structure Hamiltonian 176

PROPOSITIONS 183

ELECTRON SPIN RESONANCE OF SEVERAL MOLECULES IN THE SOLID STATE

I. ELECTRON SPIN RESONANCE AND MOLECULAR MOTION OF THE $RCH_2\dot{C}HCOOR'$ RADICALS IN X-IRRADIATED ESTER-UREA INCLUSION COMPOUNDS*

O. Hayes Griffith†

Gates and Crellin Laboratories of Chemistry ††
California Institute of Technology
Pasadena, California

Single crystals of the inclusion compounds formed between long-chain alkyl esters and urea were X-irradiated at room temperature and the free radicals produced were investigated by electron spin resonance. The eleven esters studied were diethyl adipate and the methyl, ethyl, hexyl, and octyl esters of monocarboxylic acids. The long-lived free radicals observed in all of these compounds are of the type $RCH_2\dot{C}HCOOR'$. These

---

* Supported by the National Science Foundation under Grant No. GP-930.

† National Science Foundation Predoctoral Fellow.

†† Contribution No. 3095

are π-electron radicals with the unpaired electron largely localized on one carbon 2p orbital. The coupling constants of the alcohol protons (R') were resolved in the spectra of several radicals and the values ranged from 3 to 6 Mc/sec. The ester radicals undergo motion in the tubular cavities formed by the urea molecules of the crystal, and this affects the magnitudes of the proton coupling constants. The dependence of the α- and β-proton coupling constants on this motion is briefly considered. From the ethyl heptanoate radical ESR data, recorded over the range of 352°K to 7°K ± 3°K, and from the room-temperature ESR data of all eleven ester radicals, information is obtained regarding the motions and orientations of the ester radicals. In addition, two carboxylic acid-urea inclusion compounds were investigated and the orientations and motions of the well-known radicals produced in these systems ($RCH_2\dot{C}HCOOH$) are compared to those of the ester radicals. Approximate equations are given which relate the observed α-proton coupling constants and spectroscopic splitting factors to the diagonal elements of the α-proton tensors and g-tensors of all radicals investigated.

A. INTRODUCTION

The inclusion compounds formed between urea and the n-hydrocarbons or their derivatives have been extensively studied.[1-4] Crystallographic data have been reported on the crystals formed between urea and acids, alcohols, halides, ethers, and several n-hydrocarbons. By comparing X-ray powder diffraction patterns, it has been concluded that all of these systems have similar hexagonal crystal structures.[5,6] Furthermore, Smith[7] has completed a detailed crystallographic investigation of the n-hexadecane-urea compound. Long crystals, hexagonal in cross section, were formed by the addition of hexadecane to a solution containing urea and isopropyl alcohol. The unit cell is hexagonal (a_o = 8.230 Å and c_o = 11.005 Å), and there are six urea molecules per unit cell. The hexadecane molecules are in an extended planar zigzag configuration with their long axes parallel to the c axis, and are enclosed in tubular cavities formed by spirals of hydrogen-bonded urea molecules. The time average positions of the plane of the hydrocarbon molecules are either perpendicular to the a axis, or are at multiples of 60° to this position. The view along the c axis of a long-chain hydrocarbon- urea compound is given in Fig. 1.

In addition to the crystallographic work, dielectric absorption[8] and nuclear magnetic resonance[9] investigations of several urea inclusion compounds have been reported. Results from all of

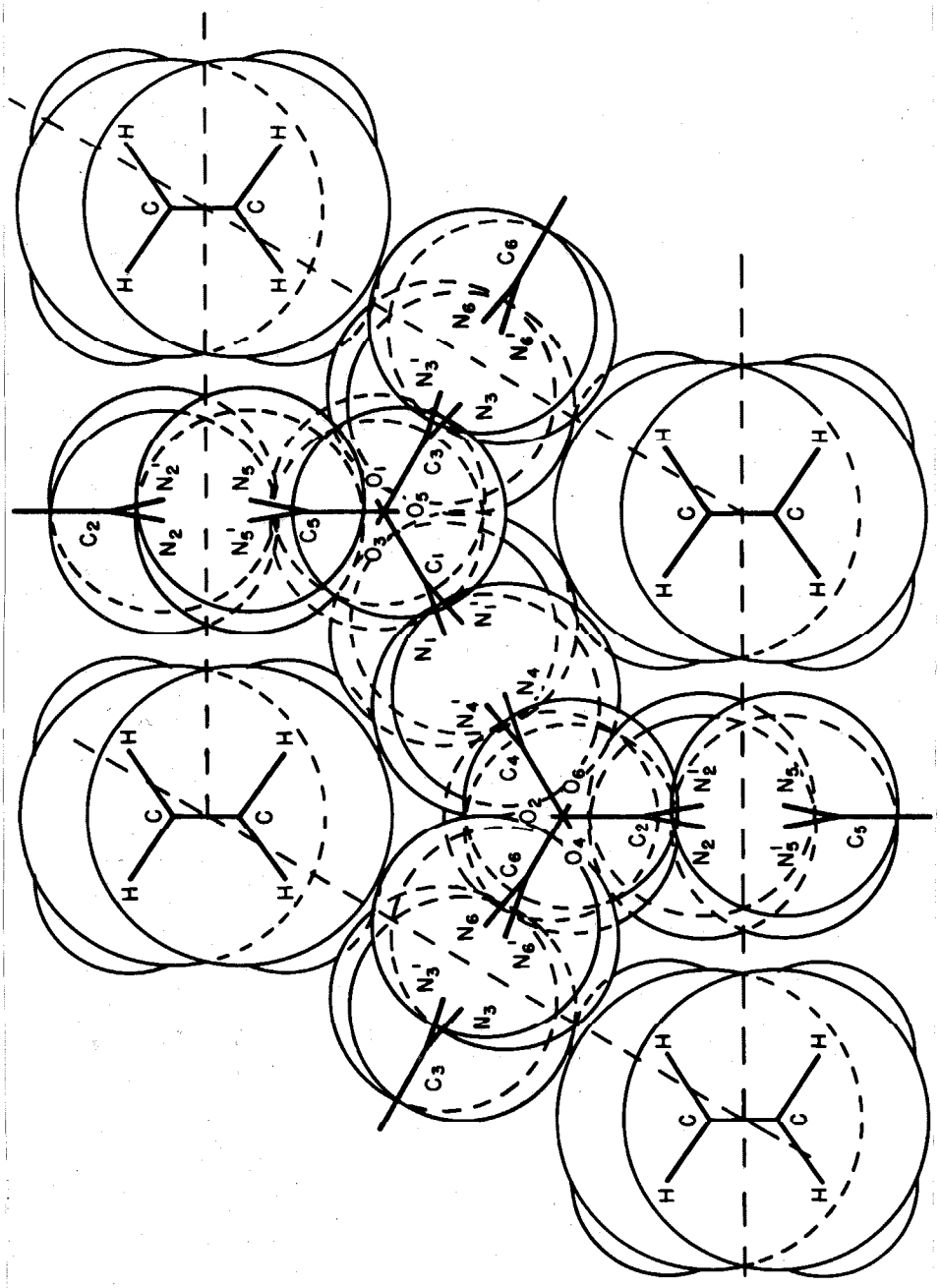

Figure 1
A long-chain hydrocarbon (n-hexadecane)--urea inclusion compound. The contents of the unit cell are projected onto the (001) plane and show the packing arrangement. This figure was reproduced from the crystal structure work (6) of A. E. Smith with his kind permission.

these investigations support the conclusion that the hydrocarbon molecules (or their derivatives) fit only loosely in the tubular cavities, and thus may undergo a large degree of molecular motion.

Because of the simplifying effects of ordered structure and molecular motion, these compounds provide a convenient medium for electron spin resonance (ESR) studies of certain X-ray-produced free radicals. A preliminary account of this technique has been published.[10] In this paper we are concerned with the identification, orientation, and molecular motion of the free radicals produced by the X-irradiation of the ester-urea crystals.

B. PROTON COUPLING CONSTANTS

No crystal structure data have been published on the compounds formed between urea and the straight-chain ester molecules. However, considering the data reported above, it is highly plausible that these compounds have hexagonal crystal structures. Here we will assume this to be the case, and will later provide ESR data supporting this assumption. Anticipating the experimental results, we assume that the only stable radical formed is the one obtained by removal of one of the α-protons[11] from the ester molecule. Therefore we have a model in which there are six orientations of one radical. As in the case of the hexadecane-urea crystal, the esters are taken to be in an extended all-trans configuration with the time average position of the plane containing the carbon atoms perpendicular to the tubular axis. The six orientations

are related by the six-fold symmetry axis of the tubular cavity.[12]

The ester radical is expected to be very similar in electronic structure to the extensively studied radical, $RCH_2\dot{C}HCO_2H$, formed by the X-irradiation of aliphatic dicarboxylic acids.[13-15] Therefore, as in the acid case, the spin density is largely localized on the π-orbital of carbon atom 2 and the problem becomes primarily one involving two isotropic β- protons and one anisotropic α- proton. The coupling constants of both α-and β-protons have been investigated in detail by McConnell and co-workers,[13,16-18] and by others.[14,15] We briefly consider here the aspects of the dependence of the α- and β-proton coupling constants on the motion and orientations encountered in the experimental work reported below (as represented by the above model). The six possible orientations of the radical have a negligible effect on the coupling constants of the β- protons, but are important to the discussion of the α proton coupling constants.

a. <u>The β-Proton Coupling Constants</u> -- Theoretical studies[19-21] suggest that the isotropic coupling constants of the β- protons, a^{β}, are related to the spin density in the p_x, orbital on carbon atom 2, ρ_C^{π}, by the linear equation

$$a^{\beta} = R_{(\theta)}\, \rho_C^{\pi} \qquad (1)$$

Heller and McConnell[13, 22] have suggested that $R(\theta)$ be approximated by the relation

$$R_{(\theta)} = B^0 \cos^2 \theta \tag{2}$$

where θ is the angle between the axis of the $p_{x'}$ orbital on C_2 and the projection of the C_3-H_β bond onto a plane which is perpendicular to the C_2-C_3 bond.

For radicals containing two β-protons attached to the same carbon atom, the two values of θ_0 are $30° \mp \gamma$ or $60° \mp \gamma$, depending on the conformation of the molecule. Eq. (2) then becomes

$$R_{1,2}(\theta) = B^0 \cos^2(30 \mp \gamma) \tag{3ab}$$

or

$$R_{1,2}(\theta) = B^0 \cos^2(60 \mp \gamma) \tag{4ab}$$

The upper and lower signs refer to the positions of protons 1 and 2 respectively, and γ is called the angle of twist (Fig. 2). In the special case that $\gamma = 0$, the two protons will have identical coupling constants. Eq. (2) has been justified by valence-bond theory,[21] and Eqs. (2) and (3ab) have been used in numerous experimental studies of free radicals containing β-protons.[13-15]

If the β-protons undergo motion with respect to the axis of the

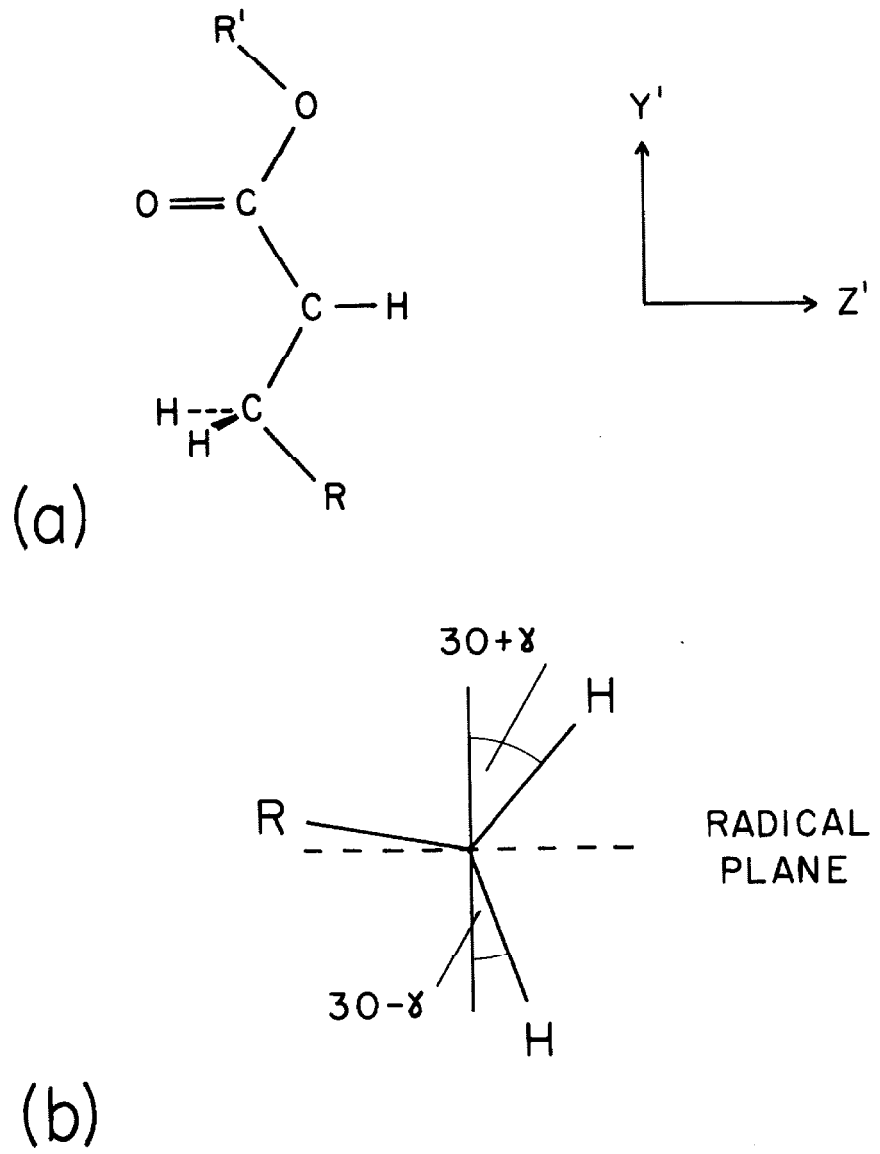

Fig. 2. The definition of the molecular Cartesian coordinate system with respect to the C_2–H_α bond and the $\rho x'$ orbital (perpendicular to plane of paper)on C_2. The origin is at the C_2 nucleus and the positive x′ axis extends into the paper (see footnote 11 for the labeling of protons and carbon atoms). (b) The view along the y′ molecular axis showing one possible geometrical configuration of the free radical β-protons. The solid line and dashed line represent the axis of the $2\rho x'$ orbital and the radical plane, respectively.

$p_{x'}$ orbital, $R(\theta)$ must be replaced by an average value, $\langle R(\theta) \rangle$. For example, if all values of θ are equally likely (e.g., free rotation about the C_2-C_3 bond) and the frequency associated with the motion is large compared to the hyperfine frequency,[24] then

$$\langle R(\theta) \rangle / B^0 = 1/2 \tag{5}$$

In general the values of θ will not all be equally likely, and the probability density function describing the motion must be determined in order to evaluate $\langle R(\theta) \rangle$. Stone and Maki[26] have used the harmonic oscillator and free rotor approximations to evaluate $\langle R(\theta) \rangle$. Several other authors have also considered the effects of molecular motion on β-proton coupling constants.[27-29]

In the case of the ester-urea crystals, the urea molecules restrict the internal motion of the ester molecules and create an essentially infinite barrier to complete rotation about the C_2-C_3 bonds. However, restricted motion about the C_2-C_3 bond is allowed. It is reasonable to assume this motion occurs about some equilibrium position described by the angle $\theta = \theta_0$. The effects of motion may then be readily estimated assuming various probability distribution functions.

If the motion is taken to be constrained between the extreme values of $\theta_0 \pm \alpha$, and all angles between the extreme values are

assumed to be equally probable, then by direct integration of Eq. (2) one obtains

$$\langle R(\theta)\rangle / B^0 = 1/2 + (\cos^2\theta_0 - 1/2)\frac{\sin 2\alpha}{2\alpha} \tag{6}$$

Or, if the motion is described as a simple harmonic oscillation between $\theta_0 + \alpha$ and $\theta_0 - \alpha$, then from Eq. (2) and the probability distribution function for a classical harmonic oscillator one obtains

$$\langle R(\theta)\rangle / B^0 = 1/2 + (\cos^2\theta_0 - 1/2)\, J_0(2\alpha) \tag{7}$$

where $J_0(2\alpha)$ is a Bessel's function of the first kind.

Finally, the motion could be approximated by a quantum mechanical harmonic oscillator. Assuming Boltzman statistics one obtains

$$\langle R(\theta)\rangle / B^0 = 1/2 + (\cos^2\theta_0 - 1/2)[1 - \exp(-E/kt)] \sum_{n=0}^{\infty} \sum_{\nu=0}^{n} \frac{(-2)^{\nu} n!}{(\nu!)^2 b^{\nu} (n-\nu)!} \exp(-nE/kt - 1/b) \tag{8}$$

where $E = \hbar(V_0/I)^{\frac{1}{2}}$ and $b = (IV_0)^{\frac{1}{2}}/\hbar$

$\alpha^2 V_0/2$ is the potential energy term of the harmonic oscillator Hamiltonian and I is the reduced moment of inertia for motion about the

C_2-C_3 bond. Eq. (8) may, in principle, be used to obtain a value for V_0 providing I is known and the torsional motion about the C_2-C_3 bond is not coupled to the other motions of the molecule. Of course, all three equations (5-7) assume that the frequency associated with the motion is large compared to the β proton hyperfine frequency.

The limiting behavior (for small α or low temperatures) of Eqs. (5-7) are qualitatively the same. The dependence of $\langle R(\theta) \rangle$ on the motion in all three of these equations is of the form

$$\langle R(\theta) \rangle / B^0 = 1/2 + (\cos^2 \theta_0 - 1/2)F \qquad (9)$$

where F depends on the motion. This same algebraic form is obtained with any potential function which is symmetric about the equilibrium position θ_0. For example, if one includes the anharmonic potential $V_1 = c_1\alpha^4 + c_2\alpha^6 + \cdots$ as a first-order perturbation of the harmonic oscillator, Eq. (9) is modified only by a change in F. The form of Eq. (9) is also retained if the motion is harmonic and is coupled to other harmonic oscillations. We have omitted from Eq. (9) a correction term of the form G sin $2\theta_0$ resulting from antisymmetric potential terms. This correction could arise, for example, from the perturbation of the harmonic oscillator by an anharmonic potential of the form $V_1 = d_1\alpha^3 + d_2\alpha^5 + \cdots$ the motions of the ester radicals in the urea inclusion compounds are expected to be complex. Therefore, we will only attempt to compare

qualitatively the degree of motion of the β-protons in the different radicals, and we will neglect the correction term, G sin $2\theta_0$.[30]

Rewriting θ_0 as $30 \pm \gamma$. Eqs. (5-9) may be written in the form

$$\langle R_{1,2}(\theta) \rangle = A + B \cos^2(30 \mp \gamma) \qquad (10ab)$$

where $$A = (B^0 - B)/2 \qquad (10c)$$

and A and B depend on the motion and do not contain γ. As the motion decreases B approaches B^0 and A approaches zero. As the motion becomes large Eqs. (7, 8) would not apply but the B and A obtained from Eq. (6) approaches 0 and $B^0/2$ respectively, and therefore Eqs. (10ab) for this angular dependence approach Eq. (5) (as expected). The ester and acid radicals reported below cover the complete range of possible values of A and B.

If the presence of motion is ignored, then one value of B' and one value of γ' may still be found from Eqs. (3ab) which yield the experimental values of the two β proton coupling constants (throughout this section we will denote by primes the values of B and γ obtained from Eqs. (3ab) and the ESR data of a radical undergoing motion). However, the values of B' and γ' will be lower than B^0 and γ. In general, to obtain B^0 the system must be cooled to a temperature at which motion about the C_2—C_3 bond becomes negligible.

The value of γ obtained with B^0 from the low-temperature is not necessarily the same as the room-temperature value of γ since θ_0 may be a function of temperature.

b. The α-Proton Coupling Constant -- The approximate spin Hamiltonian for a system of one proton ($\underset{\sim}{I}$) interacting with one electron ($\underset{\sim}{S}$) in a magnetic field ($\underset{\sim}{H}$) is[16]

$$\mathcal{H} = \mathcal{H}_Z + \mathcal{H}_{hF} \tag{11}$$

where

$$\mathcal{H} = |\beta| \underset{\sim}{S} \cdot \underset{\sim}{g} \cdot \underset{\sim}{H} \tag{12}$$

and

$$\mathcal{H}_{hF} = hAS_{z'}I_{z'} + hBS_{x'}I_{x'} + hCS_{y'}I_{y'} \tag{13}$$

β is the electronic Bohr magneton, $\underset{\sim}{g}$ is the spectroscopic splitting factor tensor, and A, B, C are the diagonal elements of the α proton nuclear hyperfine coupling constant tensor. The nuclear Zeeman term has been neglected. In Eq. (11) the molecular Cartesian coordinate system (x', y', z') is used in which the α proton hyperfine tensor is diagonal. This right-handed coordinate system is assumed to bear the same relation to the geometry of the ester radical as it does to that of the corresponding carboxylic acid radical[16] (Fig. 2).

In our model, the molecular y' axis is approximately parallel to the c axis (tubular axis) of the urea compound. If we consider frequencies of motion in a plane perpendicular to the c axis

sufficiently large to produce an isotropic α-proton splitting in that plane, and assume further that all orientations of x′ and z′ in that plane are equally likely, then Eq. (13) reduces to the axially symmetric form

$$\mathcal{H}_{hf} = hDS_{z'}I_{z'} + hDS_{x'}I_{x'} + hCS_{y'}I_{y'} \tag{14}$$

where $D = (A + B)/2$

Using Eq. (14) in place of Eq. (13) and assuming that the anisotropy of g is small, the α-proton coupling constant, a^{α}, as a function of the angle, Φ, between the magnetic field vector and the crystalline c axis is[16]

$$a^{\alpha} = [D^2 + (C^2 - D^2)\cos^2\Phi]^{\frac{1}{2}} \tag{15}$$

Furthermore, the isotropic value, $a_0{}^{\alpha}$, is

$$a_0^{\alpha} = 1/3\ (A + B + C) = 1/3\ (2D + C) \tag{16}$$

If the motion is not of sufficient amplitude or frequency to justify the use of Eq. (12), then the ESR spectra perpendicular to the c axis will be anisotropic and asymmetric. However, because of the crystal symmetry, the ESR spectra recorded with the

magnetic field parallel to the crystalline c axis will remain symmetric even in the absence of molecular motion. It may be noted that since the β-proton coupling constant is a function of the motion about the C_2–C_3 bond and the α-proton coupling constant is a function of the orientation of the C_2–H_α bond with respect to the crystal coordinate system, the ESR data gives information regarding both the internal motion of the radical and motion of the radical with respect to the laboratory coordinate system.

C. EXPERIMENTAL

During the preliminary identification of radicals the chemicals used were purified by distillation or recrystallization. For the majority of the work standard commercial grade chemicals were used. Crystals of all of the acid and ester urea inclusion compounds used to obtain the data of Table I and Fig. 5 were grown from methanol by slow evaporation. A few crystals of some of the compounds were also grown from ethyl alcohol and from isopropyl alcohol, and yielded the same ESR spectra as the crystals grown from methanol. Thus, although the possibility that solvent molecules are present in the crystals has not been eliminated, if present, their effects on the ESR spectra appear to be negligible.

The crystals were obtained in the form of hexagonal needles (angles measured to $\pm 15'$). The z axis of the crystalline coordinate

system is defined to lie along the needle axis of the urea compound. It will not be necessary to specify the x and y axes other than that they lie in a plane perpendicular to the z axis, and hence perpendicular to the basal plane. The morphology of these compounds is the same as that of the hexagonal hexadecane-urea adduct and this fact suggests that all of these compounds have hexagonal crystal structures and that the z axis lies along the crystalline c axis. This point is considered later in connection with the low-temperature ESR data for the X-irradiated ethyl heptanoate-urea crystal.

The crystals were subjected to 30 kv X-rays from a Machlett AEG-50S X-ray tube for two to ten hours at room temperature. A Varian X-band spectrometer was used to obtain the ESR data, and the modulation amplitude was approximately one megacycle/sec (Mc/sec is abbreviated as Mc in the following sections). Crystals studied at room temperature were mounted on a teflon plug in the microwave cavity with the aid of a microscope. An average of several spectra of three or more crystals was used to obtain each value reported in Table I. The crystals were mounted in a metal dewar system to obtain spectra recorded below room temperature and they were placed in a heated gas-flow system for temperatures above room temperature. The uncertainty in temperature measurements decreased from $\pm 3^\circ$K near liquid helium temperatures to $\pm 1^\circ$K above 30°K, and all temperatures listed without an uncertainty may be taken to be $\pm 1^\circ$K. Peroxylamine disulphonate and diphenylpicrylhydrazyl

(solvent free DPPH; Eastman Co.) were used for the scan calibration and g-value standard, respectively. The total width of the peroxylamine disulphonate spectrum was taken to be 72.9 Mc [31] (26.0 gauss) and the g value of DPPH as 2.0036. [32] For any given urea compound, the major features of the ESR spectra were independent of the source and purity of the chemicals, the ratio of the hydrocarbon derivative to urea in the alcohol solution, and the length of time the crystals were X-irradiated. The resolution of the proton splittings depended slightly on the history of the crystal but this variation was not given any further study.

For each of the urea inclusion compounds reported in Table I, the room-temperature spectrum recorded with the magnetic field in the crystalline xy plane remained unchanged as the crystal was rotated about the z axis. Otherwise, the ESR spectra were anisotropic with respect to arbitrary rotations of the crystal.

D. IDENTIFICATION OF THE ESTER RADICALS

The room-temperature (298°K) ESR spectra of the X-irradiated ethyl hyptanoate-urea crystal are shown in Fig. 3, where xy and z indicate that the magnetic field is perpendicular or parallel, respectively, to the z axis of the crystal. The proton coupling constants obtained from these and other room-temperature spectra are given in Table I. The room-temperature ethyl heptanoate-urea spectrum for the xy orientation clearly consists of six lines of relative intensities 1:1:2:2:1:1, and is due to the interaction of two

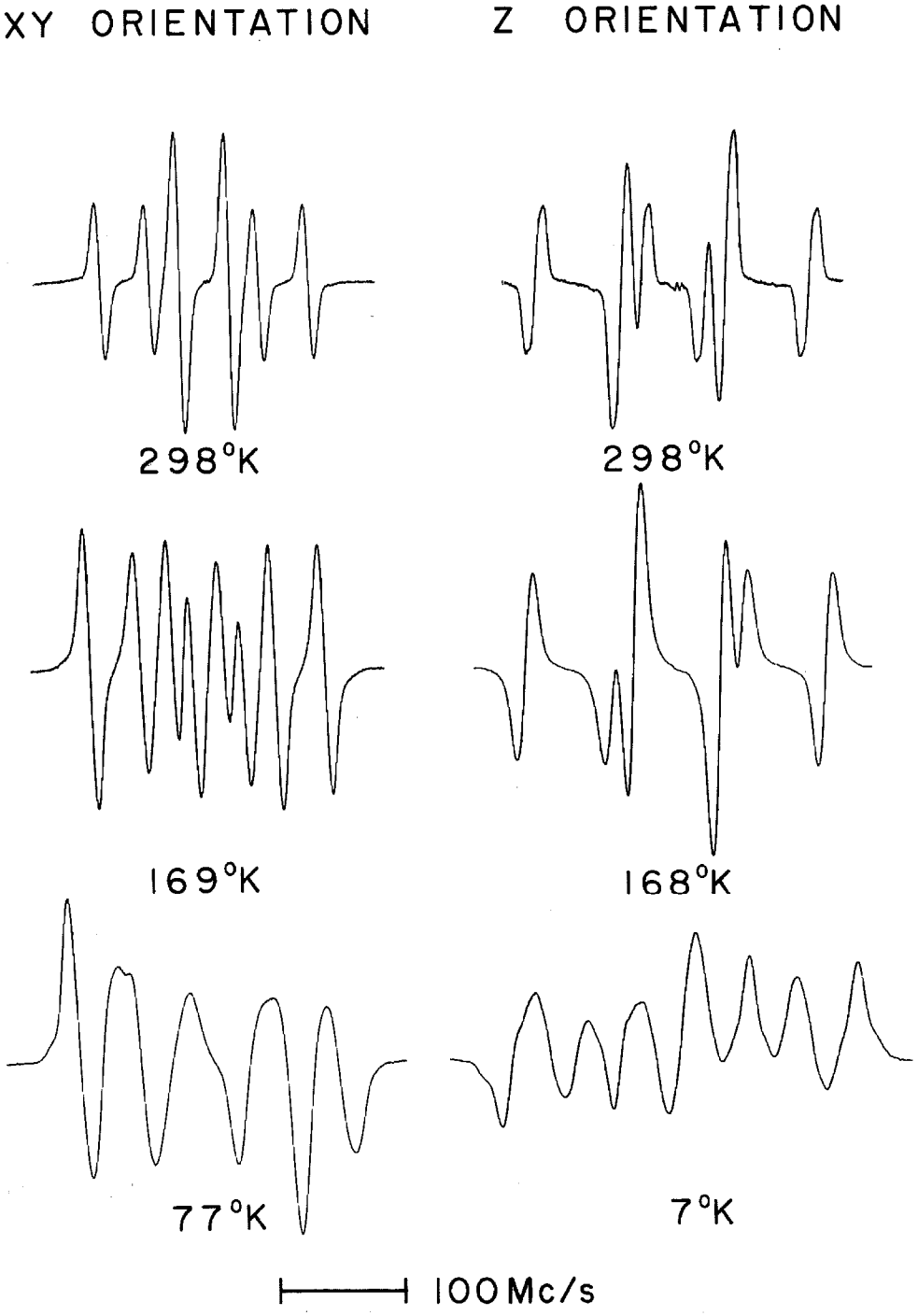

Figure 3
The ESR spectra of the ethyl heptanoate radical as a function of temperature. (The extremely small lines in the center of the z orientation, 298°K spectra, are due to an exciton impurity in the microwave cavity.)

equivalent protons (a = 65 Mc) and a third proton (a = 41 Mc). The z-spectrum of ethyl heptanoate-urea consists of six lines of relative intensities 1:2:1:1:2:1, and results from the interaction of two equivalent protons (a = 84 Mc) and a third proton (a = 68 Mc). Furthermore, a small splitting of each line of the outside doublet into three lines is barely visible. This splitting, and similar splittings of the inner lines, were slightly better resolved in some of the ESR spectra.

Spectra of the radicals formed in the systems methyl octanoate-urea and octyl propionate-urea are shown in Fig. 4. The eight-line equal-intensity spectrum for the xy orientation of the methyl octanoate-urea crystal arises from the interaction of three nonequivalent protons (a = 41 Mc, 64 Mc, 87 Mc). The z spectrum of the methyl octanoate-urea crystal is approximately a six-line spectrum (1:1:2:2:1:1) split further by three approximately equally-coupled protons. The spectrum is adequately reconstructed if the four proton coupling constants are chosen to be 89 Mc, 83 Mc, 66 Mc, and 3 Mc. The xy spectrum of the octyl propionate-urea crystal consists of eight lines of relative intensities 1:1:3:3:3:3:1:1, and is due to three equivalent protons (a = 65 Mc) and a fourth proton (a = 42 Mc). On closer examination it is seen that each line is further split by the interaction of two approximately equivalent protons (a ~ 1-3 Mc). Finally, the z spectrum of the octyl propionate-urea crystal consists of approximately five lines split further by two

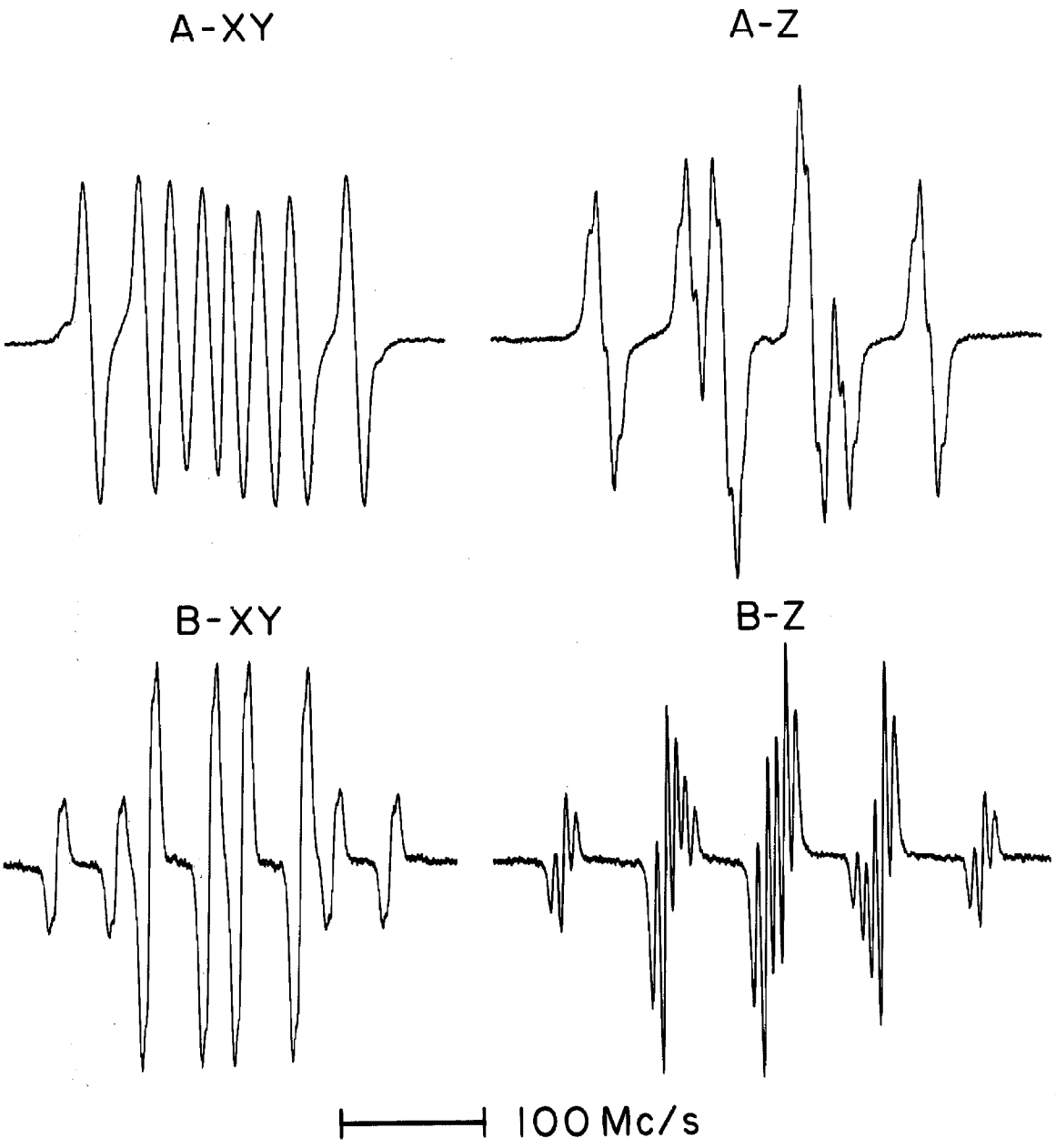

Figure 4

The room-temperature ESR spectra recorded with the magnetic field in the xy plane and along the z axis of two ester-urea crystals. The spectra A and B are of the methyl octanoate radical and the octyl propionate radical, respectively.

protons (a = 6 Mc). The approximately five-line spectrum is due to three equivalent protons (a = 72 Mc) and one proton (a = 84 Mc).

In view of these data, the only reasonable choices for the radicals produced in ethyl heptanoate-urea, methyl octanoate-urea, and octyl propionate-urea crystals, are, respectively,

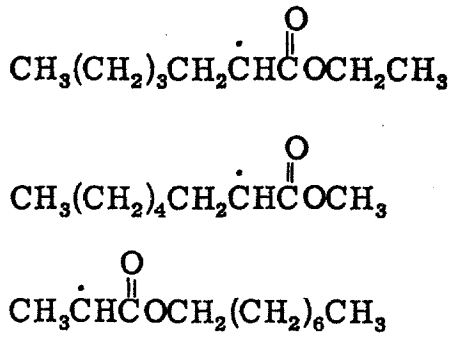

The α- and β-proton coupling constant assignments are given in Table I. The small coupling constants are due to the ζ-protons,[33] and splittings due to the γ-protons are not observed.

As expected, the α-proton coupling constants exhibit large anisotropies. These anisotropies were examined in detail for the systems ethyl heptanoate-urea and octyl propionate-urea at room temperature. If D is taken to be a^{α}_{xy} and C is taken to be a^{α}_{z}, Eq. (15) reproduces the anisotropy within experimental error for all values of the angle Φ (for the limits of experimental errors see Table I). In contrast, and again as expected, the β-proton coupling constants are very nearly isotropic. The maximum and minimum values of a^{β} occur in the z and xy directions respectively, and the two values differ by only a few megacycles.

TABLE I. Summary of proton hyperfine coupling constants for acid and ester radicals.[a-d]

Parent Compound	a^{α}_{z}	a^{β}_{1z}	a^{β}_{2z}	a^{α}_{xy}	a^{β}_{1xy}	a^{β}_{2xy}
Ethyl Hexanoate	82	75	63	40.7	72.6	61.5
Ethyl Heptanoate	84.8	68.3	68.3	40.6	65.4	65.4
Ethyl Octanoate	82	78	69	40.6	74.7	67.2
Ethyl Nonanoate	....	....	....	40.6	$\sim\frac{1}{2}$(136)	$\sim\frac{1}{2}$(136)
Ethyl Decanoate	....	....	....	41.0	$\sim\frac{1}{2}$(146)	$\sim\frac{1}{2}$(146)
Ethyl Undecanoate	83	79	66	41.3	78.0	65.3
Ethyl Dodecanoate	....	....	....	40.8	$\sim\frac{1}{2}$(148)	$\sim\frac{1}{2}$(148)
Methyl Octanoate	83	89	66.5	41.1	87.4	64.4
Hexyl Octanoate	82	76	59	41.0	72.4	57.2
Octyl Propionate[e]	84.4	71.7	71.7	41.9	65.1	65.1
Diethyl Adipate	84	67	67	41.0	64.5	64.5
Decanoic Acid	....	....	....	42.4	$\sim\frac{1}{2}$(178)	$\sim\frac{1}{2}$(178)
Sebacic Acid	81.8	90.4	90.4	42.4	87.2	87.2

FOOTNOTES FOR TABLE I

[a] All values are reported in Mc/sec.

[b] The radicals are those formed by the removal of one α-proton from the parent compound.

[c] $a^{\alpha}, a_1^{\beta}, a_2^{\beta}$ are the coupling constants for the α-proton and the two β-protons, respectively, and xy and z denote the spectra recorded with the magnetic field in the crystalline xy or z directions.

[d] The limits of experimental error varied with the orientation of the crystals and the extent of overlap of the individual lines. Numbers reported to two and three digits are accurate to ± 1.5 Mc/sec and ± 3 Mc/sec, respectively. The β-proton coupling constants listed as approximately one-half a given number indicate that the sum of the two coupling constants is known to ± 2 Mc/sec and their difference is only a few Mc/sec, but the two individual values are not accurately known. Some values are omitted (. . .) due to poor accuracy caused by the extensive overlapping of lines. There was nothing unusual about these overlapped spectra and the α- and β-proton coupling constants were in the same range as those reported in Table I. The decanoic acid radical, for example, gave a four-line z-spectrum of approximate (but not exact) intensity ratio 1:3:3:1 which is due to three nearly equivalent protons ($a \sim \frac{1}{3}(252)$ Mc/sec).

[e] The radical derived from octyl propionate exhibits three magnetically-equivalent β protons ($a_3^{\beta} = a_2^{\beta} = a_1^{\beta}$).

The three β-protons of the octyl propionate radical have equal coupling constants, which indicates that the methyl group is rotating (or undergoing large amplitude oscillations) at room temperature. From Eqs. (1, 5) the values of $\rho_C^\pi B^0(CH_3)$ are

$$\rho_C^\pi B^0 (CH_3)_{xy} = 2a_{xy}^\beta = 130\,\text{Mc}$$

$$\rho_C^\pi B^0 (CH_3)_z = 2a_z^\beta = 143\,\text{Mc}$$

The two values differ because of the anisotropy of the β-proton coupling constants. Only the product and not the individual values of ρ_C^π and $B^0(CH_3)$ are determined from these data. (To avoid unnecessary subscripts, the spin densities on carbon atom 2 of all radicals are written simply as ρ_C^π. This does not imply that all of the spin densities are equal, although evidence for this equality is presented later, and each value of ρ_C^π is to be identified with the particular radical being considered.)

In the case of the ethyl heptanoate radical, the two β-protons are also equivalent, but it is not possible to determine from the room-temperature data whether this is due to stationary equivalent 30° or 60° positions, small oscillations about one of these positions, or a complete averaging of the angle θ as given by Eq. (5). If one assumes that the last explanation is correct, the values of $\rho_C^\pi B^0(CH_2)$ are

$$\beta_C^{\pi} B^0 (CH_2)_{xy} = 2a_{xy}^{\beta} = 131\,Mc$$

$$\beta_C^{\pi} B^0 (CH_2)_z = 2a_z^{\beta} = 137\,Mc$$

These values are approximately the same as those for $\rho_C^{\pi} B^0 (CH_3)$, and this provides partial verification of the assumption of complete averaging of the angle θ. A further discussion of the ethyl heptanoate-urea crystal is given in the following section.

The two β–protons of the methyl octanoate radical are not equivalent. Using the two a_{xy}^{β} values and Eqs. (1, 3) (or Eqs. (10 a, b) with A = 0), the values of $\rho_C^{\pi} B'(CH_2)_{xy}$ and γ' are found to be 102 Mc and 7.5°, whereas using Eqs. (1, 4), the values are 302 Mc and 2.5°. Any set of two β-proton coupling constants must satisfy both Eq. (3) and Eq. (4), and further data are needed to decide which conformation is correct. By arguments given above

$$B \geqslant B' \geqslant B/2$$

where the prime indicates motion about the C_2—C_3 bond. Noting that for the very similar octyl propionate radical $\rho_C^{\pi} B(CH_3)$ = 130 Mc, the second set of values for $\rho_C^{\pi} B'(CH_2)$ and γ may be discarded. It is, therefore, concluded that the β-protons of the methyl octanoate radical are undergoing oscillations with respect to the α-proton about positions shifted from the 30° symmetry positions (Fig. 2). The β-proton coupling constants of these radicals are discussed further below.

E. TEMPERATURE VARIATIONS OF THE ETHYL HEPTANOATE RADICAL SPECTRA

X-irradiated single crystals of the ethyl heptanoate-urea compound were investigated at temperatures above and below room temperature. The spectra at elevated temperatures for both the xy and z orientations were similar to the room-temperature spectra. The intensities of the spectra decreased markedly above 345°K, and the highest temperature for which spectra were recorded was 352°K. Below room temperature, spectra were recorded down to 7°K ± 3°K and a few of these spectra are given in Fig. 3. The xy spectrum gradually changed from a six-line to an eight-line spectrum and the eight lines became unsymmetrical at lower temperatures (~150°K) due to incomplete averaging of the six orientations of the radical. Rotation of the crystal about the z axis, while maintaining the magnetic field in the xy plane, produced marked changes in the spectra at 77°K. The features of the spectra were reproducible at intervals of about 60° and at no other angles. This data supports the assumption that the crystal structure is hexagonal and that the c axis lies along the z direction of the crystal.

Spectra recorded with the magnetic field along the z axis also changed gradually with decreasing temperature, and all temperature effects at all orientations were reversible. Due to the overlap of lines in both the xy and z orientations, values of the coupling constants were obtained only over certain temperature regions.

Fortunately, these regions were complementary, and either the xy or z coupling constants were obtained for most temperatures.

The a^{α}_{xy} coupling constant of the ethyl heptanoate radical was measured down to 150°K, and the a^{α}_{z} coupling constant was measured from 298°K to 220°K and from 135°K to 7°K ± 3°K. The values of the α-proton coupling constant for both orientations were found to be approximately independent of temperature. The value of a^{α}_{z} decreased approximately 3 Mc in going from 7°K ± 3°K to 298°K, and a^{α}_{xy} remained unchanged over the range 298°K to 150°K. Three effects which in principle could change the value of a^{α} with a change in temperature are: (1) a change in the value of ρ^{π}_{C} due to motion about the C_1—C_2 bond, (2) motion of the α-proton in the xz or yz planes, and (3) reorientation of the molecule with respect to the crystalline z axis. Barring the highly unlikely cancellation of these effects, one may conclude that ρ^{π}_{C} is independent of temperature, that the molecular motion (at frequencies greater than the hyperfine frequency) of the α-proton occurs primarily in the xy plane, and that there are no major reorientations of the molecular axes with respect to the crystalline z axis over the temperature range investigated. Since the unpaired spin density is largely localized on carbon atom 2, motion about the C_1—C_2 bond would not be expected to have a large effect on ρ^{π}_{C} and therefore no conclusions about this motion may be drawn from the above data.

The β-proton coupling constant data over the range 7°K ± 3°K to 250°K is presented in Fig. 5. Above 250°K the values of a^{β}_{xy} and

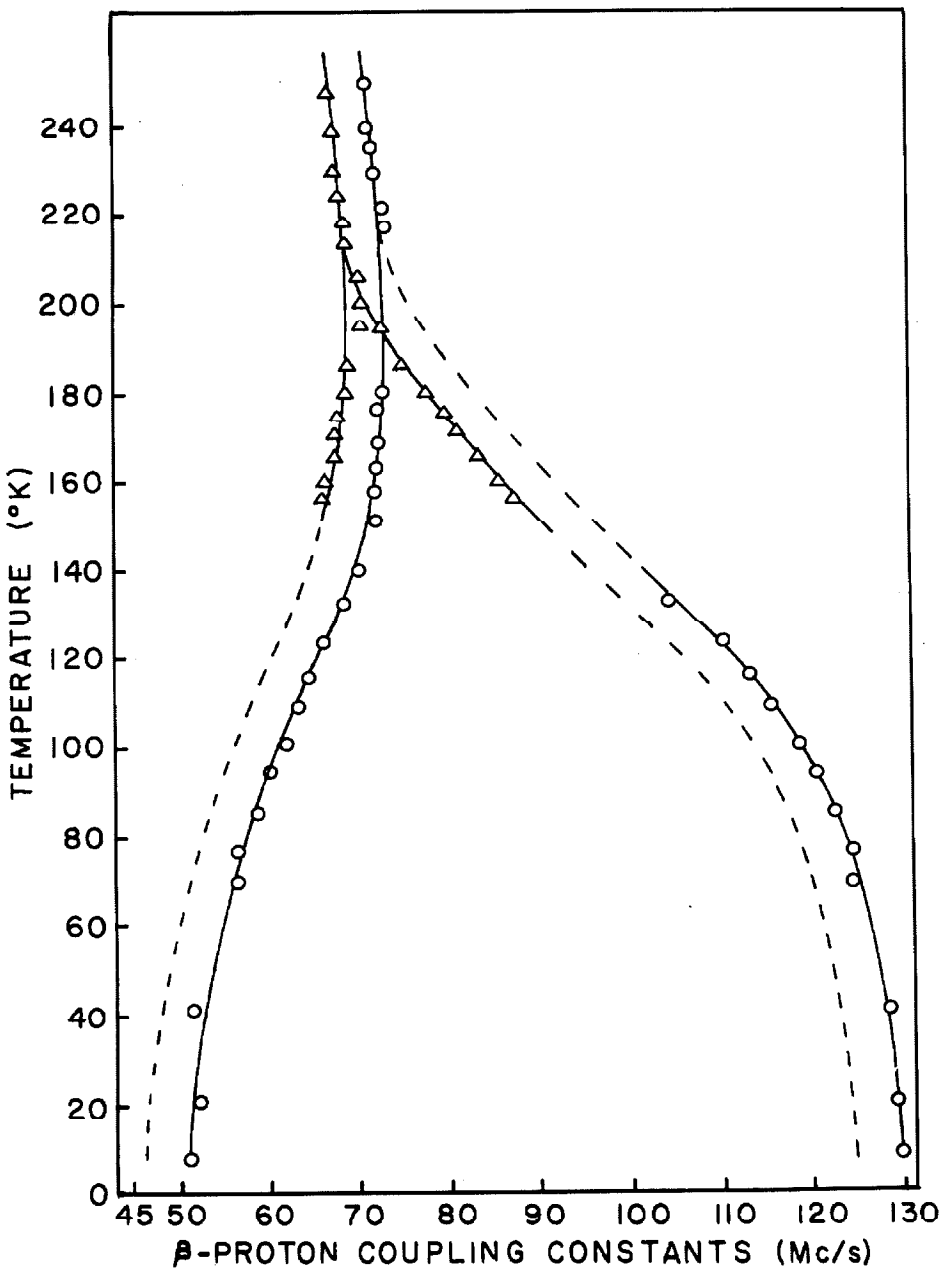

Figure 5

The two β-proton coupling constants of the ethyl heptanoate radical as a function of temperature.

a_z^β decreased gradually to the room-temperature values, a change of approximately 1 to 3 Mc in 50°K. The two sets of curves in Fig. 5 would, of course, coincide if the β-proton hyperfine interaction were completely isotropic. Below 250°K the β-protons became magnetically nonequivalent, causing the gradual transition from a six- to an eight-line spectrum. Using the same arguments as for the methyl octanoate radical room-temperature data, it is found that Eqs. (3ab) and not (4ab) lead to acceptable values of $\rho_C^\pi B'(CH_2)$ for all data derived from the eight-line spectra.

The values of γ' and $\rho_C^\pi B'$ obtained from Eqs. (3ab) increase with decreasing temperature. Taking 131 Mc and 50 Mc as the low-temperature limiting values of a_{1z}^β and a_{2z}^β, the values of γ and $\rho_C^\pi B^0(CH_2)_z$ are found to be 22° and 133 Mc. The low-temperature limiting value of $\rho_C^\pi B^0(CH_2)_z$ may be compared to the values 143 Mc for $\rho_C^\pi B^0(CH_3)_z$ and 137 Mc for $\rho_C^\pi B^0(CH_2)_z$ obtained from Eq. (5) and the room-temperature octyl propionate radical data and ethyl heptanoate radical data, respectively. The experimental uncertainties in these values are roughly ± 6 Mc, and are large due to the doubling of the experimentally-observed values of the room-temperature data to obtain $\rho_C^\pi B^0(CH_2)$ and $\rho_C^\pi B^0(CH_3)$, and due to uncertainties in the measurements of the broader lines of the low-temperature spectra. Within the limits of experimental error these three values of $\rho_C^\pi B$ are approximately equal. And since the values of B and the values of ρ_C^π are expected to be nearly equal, this again supports the assumption of complete averaging of the β-proton

positions in the ethyl heptanoate radical at room temperature.

Further qualitative information about the β-proton motion may be obtained from Eqs. (8, 10ab) and the data of Fig. 5. By combining Eqs. (1, 10ab) one obtains

$$\frac{2a_1^{\beta} - \rho_C^{\pi} B^0}{2a_2^{\beta} - \rho_C^{\pi} B^0} = \frac{\cos^2(30-\gamma)-1/2}{\cos^2(30+\gamma)-1/2} \qquad (17)$$

With a known value of B^0 this equation may be used to estimate γ. Eq. (17) is double-valued in the sense that if γ_1 is a solution so is the angle $90-\gamma_1$.[34] However, only one of these angles yields the experimental coupling constants by Eqs. (10ab), and the choice of angles is made by comparing the low-temperature results of Eqs. (10ab) and Eq. (17). Over the temperature range 7°K ± 3°K to 130°K, γ for the ethyl heptanoate radical is found to be approximately constant and equal to 22° ± 4°. Above 130°K the values of γ obtained from Eq. (17) decrease slowly with increasing temperature, but this change may not be significant. Once γ (hence θ_0) has been shown to be constant, Eq. (8) may in principle be used to estimate V_0. Ignoring anharmonicities, Eq. (8) would be applicable providing at the temperatures of interest all motions which might couple with the torsional motion about the C_2—C_3 bond are negligible. This is equivalent to requiring that V_0 be much less than the potential barriers associated with motion about other bonds in the radical. If, as a gross approximation, the groups attached to C_2 and C_3 are allowed to undergo motion and the radical is assumed to be in a planar zigzag conformation,

then $I \sim 1.7\ (10)^{-38}$ gm cm^2 for the ethyl heptanoate radical. From Eq. (8) and the β-proton coupling constant data in the temperature range 7°K ± 3°K to 40°K, V_0 is found to be in the neighborhood of 1-3 Kcal/mole. Other reasonable values of I yield similar values of V_0, and these values of V_0 are of course merely order-of-magnitude estimates of V_0. Since potential barriers associated with other bonds in the ester radical cannot be assumed to be much less than 1 Kcal/mole,[35,36] and since the exact value of I is not known, a reliable value of V_0 cannot be obtained from the ESR data of Fig. 5.

Preliminary spectra of the octyl propionate radical have also been recorded over the temperature range 298°K to 7°K ± 3°K. As in the case of the ethyl heptanoate radical, a_z^α is independent of temperature. However, the methyl group of the octyl propionate radical is apparently still undergoing rotation or large amplitude oscillations at 7°K ± 3°K. This behavior is similar to that reported for the $CH_3\dot{C}(COOH)_2$ radical, which is formed by the X-irradiation of methylmalonic acid.[28]

F. DISCUSSION OF THE ROOM-TEMPERATURE ESTER RADICAL SPECTRA

In addition to ethyl heptanoate, octyl propionate, and methyl octanoate, several other esters were investigated at room temperature. After X-irradiation, each of these systems exhibited the radical formed by the removal of one α proton from the ester

molecule. The ζ-proton coupling constants were resolved in the z-spectra of several ester radicals, and they ranged from 3Mc to 6Mc. The α-and β-proton coupling constant data are summarized in Table I. Within the limits of experimental accuracy, all of the ester radicals have the same values of a_z^{α} and a_{xy}^{α}. This suggests that all of the ester radicals have the same spin density, ρ_C^{π}, and the same orientation of the α-proton with respect to the crystalline z axis.

Of the ester radicals reported in Table I, only those derived from ethyl heptanoate, octyl propionate, and diethyl adipate exhibit magnetically-equivalent β-protons, and the coupling constants are the same for all three radicals. Therefore, as in the case of the ethyl heptanoate and octyl propionate radicals, the β-protons of the diethyl adipate radical are undergoing complete averaging as given by Eq. (5). The radicals derived from either ethyl nonanoate, ethyl decanoate, or ethyl dodecanoate have two β-proton coupling constants that differ by only a few megacycles, and therefore the spectra are not completely resolved. However, the sum of the two coupling constants, a_{xy1}^{β} and a_{xy2}^{β}, is easily measured to within 2 Mc, and in Table I the values of these coupling constants are listed as approximately one-half of this sum. The fact that the β-proton coupling constants are nearly equal to those of the ethyl heptanoate radical implies that oscillations about the C_2–C_3 bonds in these three radicals are of nearly the same amplitude as in the ethyl heptanoate radical.

For the remainder of the ester radicals listed in Table I, the two β-proton coupling constants differ sufficiently to produce well-resolved eight-line spectra, and it is again found that Eqs. (3ab) and

not (4ab) lead to acceptable values of B′. From Eq. (17) and the data of Table I, values of γ_1 and γ_1-90° are readily obtained. In the absence of low-temperature data, A and B must be evaluated in order to determine which of the two angles is correct. By subtracting Eq. (10a) from Eq. (10b) and simplifying the resulting equation, one obtains

$$\rho_C^{\pi}B = \frac{2(a_1^{\beta}-a_2^{\beta})}{(3)^{\frac{1}{2}}|\sin 2\gamma|} \qquad (18)$$

In Eq. (18), both angles yield the same value of $\rho_C^{\pi}B$. The value of $\rho_C^{\pi}A$ is determined from Eq. (10c), $\rho_C^{\pi}B$, and a known value of $\rho_C^{\pi}B^0$ (CH_2). Since ρ_C^{π} is apparently a constant, the value of $\rho_C^{\pi}B^0$ (CH_2) is the same for all ester radicals having two β-protons, and is approximately the same as that of $\rho_C^{\pi}B^0$ (CH_3). Here we will take the value of $\rho_C^{\pi}B_{xy}^0$ to be 131 Mc. Upon substituting $\rho_C^{\pi}A$, $\rho_C^{\pi}B$, and the two angles into Eqs.(10ab), only one of the two angles yields the experimentally observed β–proton coupling constants and the other angle is discarded. By this procedure, the values of γ for ethyl hexanoate, ethyl octanoate, ethyl undecanoate, methyl octanoate, and hexyl octanoate are determined to be 30°, 10°, 15°, 15°, and 45°, respectively (all angles ± 8°). These angles may be compared to the values of γ', 4°, 3°, 4°, 7°, and 6°, respectively, obtained for the same radicals from Eqs. (3ab).

The amplitudes of oscillation about the C_2–C_3 bonds may be estimated with the above values of γ and Eq. (6) or Eq. (7). Since the oscillations are large, Eq. (6) and not Eq. (7) is used here, although it may be noted that the equations give the same result for small angles. For instance, taking B^0 and γ to be 131 Mc and 22°, the two values of

$\langle R_1(\theta)\rangle$ and of $\langle R_2(\theta)\rangle$ obtained from Eqs. (6) and (7) differ by only 5% and 2.5%, respectively, for an oscillation amplitude of 30°. Using Eq. (6) the amplitudes of oscillation for the above six radicals fall in the range of 70 to 80 degrees. By the same equation, the values of α of the other ester radicals are at least 80° to 90°, and therefore there exists large amplitudes of oscillation about the C_2–C_3 bonds of all ester radicals reported in Table I.

By this point it is obvious that the assumption of a time average planar zigzag conformation of the ester radicals is an approximation. For such a conformation, γ would be zero and the equilibrium angle, θ_0, of the two β-protons would be 30°. The angles of twist for the radicals exhibiting magnetically equivalent (or nearly equivalent) β-protons cannot be obtained from the ESR data. However, the room-temperature values of γ for the six ester radicals exhibiting eight resolved lines, and the low-temperature value of γ for the ethyl heptanoate radical are significant. Considering the constraints imposed by the van der Waals radius of the tubular cavity, this implies twisting about other bonds besides the C_2–C_3 bond. From Fig. 1, or by use of molecular models, it is seen that a molecule with an angle of twist about the C_2–C_3 bond is most easily accommodated by the tubular cavity if there exist also similar out-of-plane adjustments in adjacent bonds of the ester molecule (This same argument applies to oscillations about the C_2–C_3 bond since a cooperative motion is required in order to achieve the large amplitude oscillations of the β-protons.) It is clear, however, that all radicals in a given ester-urea compound have approximately the same angle of twist, γ, and the same degree of molecular motion.

Otherwise, the ESR spectra would be a superposition of lines from each nonequivalent radical and the spectra would be complex.[37] Of course, whether or not the undamaged molecules exist in a time-average planar zigzag configuration cannot be determined from the ESR data.

G. THE CARBOXYLIC ACID-UREA INCLUSION COMPOUNDS

Of the two acids investigated, one (decanoic acid) is a mono-carboxylic acid, and the other (sebacic acid) is a dicarboxylic acid. The radicals produced by X-irradiation of these acid-urea crystals are

$$CH_3(CH_2)_6CH_2\dot{C}H\overset{O}{\overset{\|}{C}}OH$$

$$HO\overset{O}{\overset{\|}{C}}CH_2(CH_2)_5CH_2\dot{C}H\overset{O}{\overset{\|}{C}}OH$$

and are formed by removal of one α-proton from the corresponding acid molecule (Fig. 6). The above sebacic acid radical has also been found in X-irradiated single crystals of sebacic acid,[38] and this general type of radical has been observed in many other crystalline dicarboxylic acids.[13-16] The above two carboxylic acid radicals are briefly investigated here primarily as a test of the model chosen to represent the radicals in the urea inclusion compounds. The α-proton coupling constants of the acid radicals are given in Table I, and are approximately the same as those of the ester radicals. As with the esters, taking D to be a^{α}_{xy} and C to be a^{α}_{z}, Eq. (15) reproduces the a^{α}

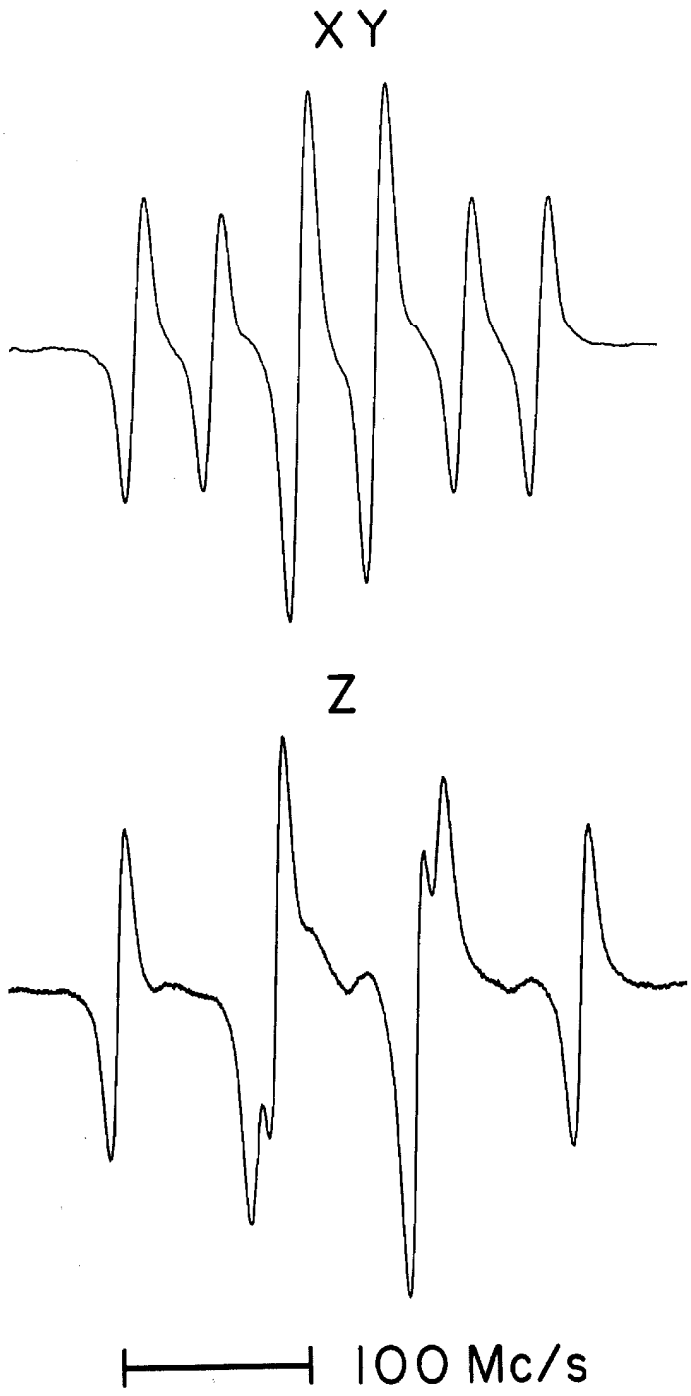

Figure 6
The room-temperature ESR spectra recorded with the magnetic field in the xy and z directions of an X-irradiated sebacic acid-urea crystal.

anisotropy to within ± 2Mc for both the sebacic acid radical and the decanoic acid radical. The values, in Mc, of C, D, a_0^α are 82, 42, 56 and 84, 42, 56 for the sebacic acid radical and the decanoic acid radical, respectively.

To compare these results, the diagonal a^α tensor elements for the radicals in pure dicarboxylic acids are needed, and there are differences in the values reported for these tensor elements. Two examples are the values for the succinic acid radical[14] and the sebacic acid radical.[38] The diagonal values of the a^α tensor, C, B, A, for these two radicals are 92, 59, 30 and 88, 56, 27 Mc, respectively. From these tensor elements, the values of C, D, a_0 are 92, 44, 60 and 88, 41, 57, respectively. The agreement between these values and those for the acid-urea crystals is satisfactory. The values of D and a_0^α for all four systems are essentially identical, and the C values of the radicals in the urea adducts are slightly below those of the radicals in the pure acid crystals. The difference in C values may be caused by the molecular y′ axis being tilted away from the crystalline z axis. Besides decreasing the apparent value of C, this shift would of course also increase the value of D obtained from a_{xy}^α over the one derived from the average of the diagonal tensor elements.

The a_z^α and a_{xy}^α of the acid radicals are approximately equal to those of the ester radicals (Table I). This is an indication that the spin densities, ρ_C^π, and the orientations of the radicals with respect to the molecular z axis are approximately the same for the acid and ester radicals. The value of ρ_C^π is nearly unity, as may be seen by

comparison of the above values of a_o^α with the range of a_o^α values, 59 Mc to 64 Mc, recently reported for transient alkyl radicals[29] (note: $a_o^\alpha = Q\rho_C^\pi$, where Q is a constant.[19, 20] The fact that ρ_C^π is nearly unity in the case of the carboxyl radicals has already been established.[16]) Although no detailed temperature investigations of the acid spectra were undertaken, the spectra of both acid radicals changed gradually and reversibly with temperature. Splittings due to the carboxyl proton or the γ-protons were not resolved in any spectrum of either acid radical.

The two β protons of the sebacic radical are magnetically equivalent and a^β for these two protons is found to be equal to 87 Mc. The two β-protons of the decanoic acid radical are nearly equivalent ($\pm$ 1-3 Mc) and the values of the two β-proton coupling constants are approximately the same as those of the sebacic acid radical. From Eqs. (3, 4), and using the more accurate a^β of the sebacic acid radical, the values of $\rho_C^\pi B'_{xy}$ are 116 Mc and 349 Mc for equilibrium angles of 30 and 60 degrees respectively, and again the value 349Mc is discarded. The value of 116 $\pm$ 2 Mc is slightly below the $\rho_C^\pi B_{xy}^0$ values for the octyl propionate radical (130 $\pm$ 3 Mc) and the ethyl heptanoate radical (131 $\pm$ 3 Mc), suggesting that the β-protons of the acid radicals are undergoing limited motion about the 30° equilibrium position. Taking B^0 to be 130 Mc, the angle of oscillation, γ, for the sebacic acid radical lies in the range 30° to 45°. It should be stressed here that Eq. (6) is being used only to compare, qualitatively, motion about the C_2–C_3 bond. However, it is clear that the degree of motion about the C_2–C_3 bond is much larger in the ester radicals than it is in the acid

radicals.

One major difference between the ester and the acid radicals is the possibility of forming hydrogen bonds involving the carboxylic protons. X-ray diffraction studies of several pure crystalline dicarboxylic acids have established that the acid molecules are bonded end to end by intermolecular hydrogen bonds.[39,40] It has been suggested that the acid molecules in the acid-urea crystals are bonded together in the same manner.[41] The hydrogen bonding in either the monocarboxylic or dicarboxylic acids would effectively hinder oscillations about the C_2–C_3 bond (as is readily seen by use of molecular models). Another possible, although less likely, explanation of the reduced motion in the acids is hydrogen bonding between the acid molecules and the urea molecules. The O—H$\cdots$N bond is known,[42] and hydrogen bonding is observed between molecules of urea and oxalic acid in the monoclinic urea-oxalic acid crystals.[43] Hydrogen bonding involving the urea protons may also occur in both the acid and ester molecules, but this bonding would not easily explain the difference in molecular motion in the two cases.

The above discussion is relevant to the question of possible complete rotation (or rapid reorientation among the six radical positions) of the hydrocarbon derivatives in the tubular cavities. The room-temperature ESR spectra of both the acid and ester radicals could result from large amplitude oscillations of the α-proton in the xy plane or from rotation of the entire molecule about the crystalline z axis. The gradual and continuous changes of the spectra with temperature

require the presence of large oscillations of the α-proton but do not rule out entirely the possibility of complete rotation at room temperature. However, because of the formation of the C—O···X hydrogen bonds mentioned above it is very unlikely that the dicarboxylic acids undergo rotation at room temperature. Hydrogen bonding between the dicarboxylic acid molecules would create molecular units of essentially infinite length, and hydrogen bonding between the acid molecules and the urea molecules would create a barrier to rotation of the carboxyl groups.

An estimation of the lower limits of the frequency and amplitude associated with the α-proton motion may be obtained from Eqs. (11-13) and the acid radical tensor elements quoted above. If the radicals are freely rotating in the tubular cavities, then the only condition necessary to obtain an isotropic splitting in the xy plane is that the rotational frequency be large compared to the hyperfine frequency (motional frequency $\gg$ 60Mc/sec for the acid and ester radicals). If instead of rotating freely, the α-proton is oscillating in the xy plane with an amplitude, δ, about some equilibrium position, then the amplitude of oscillation is also important. From Eqs. (11-13) one may obtain the very approximate relation

$$\Delta a^{\alpha}_{xy} \sim (A-B)[(\cos^2\phi_0)-\tfrac{1}{2}]\frac{\sin 2\delta}{2\delta} \qquad (19)$$

where Δa^{α}_{xy} is a measure of the α-proton anisotropy in the xy plane, and ϕ_0 is the angle between the magnetic field (in the xy plane) and either the x' or z' molecular axes. For the ester and acid radicals

the difference between A and B is evidently ~29 Mc and if δ is taken to be greater than 80°, then $:0 \geq \Delta a^{\alpha}_{xy} \geq 3$ Mc. Since there are six radical orientations (in general, three different values of φ_0) that contribute to the ESR spectra, an anisotropy of a few Mc would only contribute to the broadening of the ESR lines, and would not produce a measurable effect on the splittings in the xy plane.

H. SPECTROSCOPIC SPLITTING FACTOR DATA

The g-values of the ester radicals reported in Table I are identical within experimental error. The averages of the values measured with the magnetic field in the crystalline xy and z directions are g(xy) = 2.0031 and g(z) = 2.0036, respectively. The values of the two acid radicals are also the same and are given by g(xy) = 2.0025 and g(z) = 2.0041. The experimental uncertainty in all g-value measurements is ±.0003 (relative to the g-value assumed for DPPH). As in the case of most organic free radicals, the anisotropy of the g-value is small, and therefore the electron spin vector is aligned along the magnetic field direction. This was assumed in calculating the proton coupling constants from the ESR data.

It is desirable to relate the measured g-value data to the isotropic g-value, g_0. It cannot be assumed that the principal elements of the g-tensor correspond to the molecular x', y', z' directions. (The minimum element evidently lies along the z' direction[14,44].) However, we have shown that the large amplitude motions of the molecular x' and z' axes occur in the crystalline xy plane. For this situation the isotropic g-value is given to a good approximation by the

relation $g_0 \simeq \frac{1}{3}(2g(xy) + g(z))$, regardless of the orientations of the principal values of the g-tensor in the molecular coordinate system. From this formula and the above data, g_0 for the ester and acid radicals are 2.0033 and 2.0030, respectively. These values of g_0 are essentially identical to those reported for the adipic acid radical (2.0031) and the succinic acid radical (2.0030). (g-Value data have not been reported for the sebacic acid radical produced in crystalline sebacic acid.)

I. SUMMARY

The long-lived free radicals observed in all of the aliphatic ester-urea crystals investigated were of the type $RCH_2\dot{C}HCOOR'$. These radicals are similar to the well-known free radicals produced in X-irradiated dicarboxylic acids, except that the splittings due to the alcohol protons (of R′) are present in the ESR spectra of the ester radicals. These previously unobserved splittings provide evidence that a small fraction of the unpaired spin density is distributed on the carboxyl group of the ester radical. The room-temperature study of the ester radicals shows that (a) the orientation of the axis of the 2p orbital on C_2 with respect to the crystalline c axis (tubular axis) is the same for all radicals studied; (b) there exist motions of the α- and β-protons at frequencies greater than 10-100 Mc/sec; (c) the amplitude of the α-proton motion in a plane perpendicular to the c axis is greater than ~80°, and the anisotropy of the α-proton coupling constant is adequately described by an axially-symmetric spin Hamiltonian; (d) the amplitudes of oscillation of the β-protons with

respect to the α-protons are large for all ester radicals, but the β-proton positions are completely averaged only for a few of the radicals studied; (e) there exist significant deviations from time-average planar zigzag configurations in many ester radicals (causing non-equivalence of the β-protons); and (f) all radicals of a given ester-urea crystal have the same time-average configuration and approximately the same degree of molecular motion (indicating a high degree of order in the ester-urea crystals).

In addition to the room-temperature study of the eleven ester radicals, the ethyl heptanoate radical was also investigated over the temperature range 352°K to 7°K ± 3°K and it was found that: (a) Over this range there is no significant reorientation of the axis of the 2p orbital on C_2 with respect to the crystalline c axis; (b) the α-proton motion occurs primarily in a plane perpendicular to the c axis; (c) the β-proton angle of twist is approximately independent of temperature over the range 130°K to 7°K ± 3°K; (d) the large amplitude oscillations about the C_2–C_3 bonds decrease continuously with decreasing temperature; and (e) both the anisotropy of the low-temperature ESR spectra and the morphology of the crystals suggest that the ester-urea crystals have hexagonal structures. All temperature effects are reversible. Considering the constraints imposed by the tubular cavities, the large amplitude oscillations about the C_2–C_3 bonds strongly suggest that the intramolecular motions of the ester radicals are cooperative.

Two acid-urea crystals, decanoic acid-urea and sebacic acid-urea were also studied and the ESR data showed that: (a) The long-

lived radicals are of the type $RCH_2\dot{C}HCOOH$; (b) the acid radical α-proton motion and orientation are similar to the ester radical motion and orientation; and (c) there exists motion of the β-protons of similar frequency (i. e., above 10-100 Mc/sec) but much lower amplitude than in the ester radicals. This decrease in motion is evidently caused by hydrogen bonds involving the carboxyl protons of the acid radicals. For both the acid and ester radicals one may obtain the approximate values for one α-proton hyperfine (principal) tensor element, the average of the other two elements, the isotropic α-proton coupling constant, and the isotropic g value, g_0.

J. ACKNOWLEDGEMENTS

We are especially indebted to Professor Harden M. McConnell for helpful discussions and for generous use of his laboratory facilities.

We are also greatly indebted to Dr. Albert E. Smith for providing photographs of the crystallographic work on the urea inclusion compounds, and for permission to reproduce these photographs.

K. REFERENCES

[1]O. Redlich, C. M. Gable, A. K. Dunlop, and R. W. Millar, J. Am. Chem. Soc. 72, 4153 (1950).

[2]K. A. Kobe and W. G. Domask, Petroleum Refiner 31, No. 3, 106 (1952).

[3]W. Schlenk, Jr., Fortsch. Chem. Forsch. 2, 92 (1951).

[4]Other terms often used to describe these crystals are occlusion compounds, adducts, complexes, and canal complexes. The nomenclature is somewhat unfortunate as these systems are neither compounds nor complexes. They are simply crystalline structures in which one of the components fits into cavities formed by the other. There exist no chemical bonds between the two components (other than perhaps hydrogen bonds).

[5]W. Schlenk, Jr., Ann. 565, 204 (1949).

[6]A. E. Smith, J. Chem. Phys. 18, 150 (1950).

[7]A. E. Smith, Acta Cryst. 5, 224 (1952).

[8]R. J. Meakins, Trans. Faraday Soc. 51, 953 (1955).

[9]D. F. R. Gilson and C. A. McDowell, Mol. Phys. 4, 125 (1961).

[10]O. H. Griffith and H. M. McConnell, Proc. Natl. Acad. Sci. U. S. 48, 1877 (1962).

[11]The convention for the labeling of protons (α, β, γ, ζ) and carbon atoms (C_1, C_2, C_3) used here is the following

$$\underset{}{\overset{\gamma \quad \beta \quad \alpha \quad O \qquad \zeta}{R\text{–}CH_2\text{–}CH_2\text{–}CH_2\text{–}C\text{–}O\text{–}CH_2\text{–}R'}}$$
$$\underset{C_3 \quad C_2 \quad C_1}{}$$

[12]The choice of the number of orientations of the ester radicals needs to be qualified. For the purpose of this footnote, the carbon nuclei are assumed to be in a planar zigzag conformation. Therefore, there are presumably twelve orientations; the six mentioned above, and six more related to the first six by two-fold rotations about the c axis. Even more orientations may exist if the ester molecules stack in a head-to-head fashion in the tubular cavities, rather than in a head-to-tail fashion. In any case, if we assume that the molecular x′ and z′ axes lie in the crystalline xy plane there are only three magnetically distinguishable orientations (see Fig. 2 for the definitions of the axes). We will refer to the

existence of six orientations rather than to three (or some other number) to emphasize the hexagonal structure of the crystal. Of course, the lengths of the hydrocarbon derivatives are not integral multiples of the urea spiral repeat distance (except by accident). As pointed out by Smith,[7] this causes a one-dimensional disorder along the c axis of the crystal. However, all orientations may be obtained from the above-mentioned orientations by simple translations along the c axis, and therefore the disorder does not affect the ESR spectra proving the carbon nuclei are in a planar zigzag configuration.

[13]C. Heller and H. M. McConnell, J. Chem. Phys. 32, 1535 (1960).

[14]D. Pooley and D. H. Whiffen, Mol. Phys. 4, 81 (1961).

[15]J. R. Morton and A. Horsfield, Mol. Phys. 4, 219 (1961).

[16]H. M. McConnell, C. Heller, T. Cole, and R. W. Fessenden, J. Am. Chem. Soc. 82, 766 (1960).

[17]H. M. McConnell and R. W. Fessenden, J. Chem. Phys. 31, 1688 (1959).

[18]H. M. McConnell and J. Strathdee, Mol. Phys. 2, 129 (1959).

[19]H. M. McConnell and D. B. Chesnut, J. Chem. Phys. 28, 107 (1958).

[20]A. D. McLachlan, H. Dearman, and R. Lefebvre, J. Chem. Phys. 33, 65 (1960).

[21]A. D. McLachlan, Mol. Phys. 1, 233 (1958).

[22]The actual relation suggested by Heller and McConnell is $R(\theta) = A^0 + B^0 \cos^2 \theta$. As noted by these authors, the constant A^0 is expected to be zero on theoretical grounds.[21, 23] A^0 is found to be negligible within the limits of experimental error for the radicals discussed here. (For example, assume that either $B^0(CH_2) = B^0(CH_3)$ or that the ethyl heptanoate radical at 298°K is undergoing complete averaging of the β-proton positions with respect to the α-proton. One may then solve the three equations involving the completely averaged room-temperature β-proton data and the 7°K ± 3°K ethyl heptanoate radical data for the three unknowns A^0, B^0, and γ. A^0 is found to be zero within the limits of ± 5 Mc.) It may be noted that all proton coupling constants are listed as their absolute values. The α-and β-proton coupling constants of very similar radicals have been found to be negative[16] and positive,[23] respectively.

[23]P. G. Lykos, J. Chem. Phys. 32, 625 (1960).

[24]This is perhaps too stringent a requirement on the frequency of the motion. Arguments based on rapidly fluctuating magnetic environments[25] suggest that the criterion is that the frequency of the motion should be large compared to the difference in the hyperfine frequencies considered. This argument applies to the α-as well as to the β-proton hyperfine interactions. This distinction does not affect significantly our qualitative arguments involving the motion of the protons.

[25]P. W. Anderson and P. R. Weiss, Rev. Mod. Phys. 25, 269 (1953).

[26]E. W. Stone and A. H. Maki, J. Chem. Phys. 37, 1326 (1962).

[27]S. Ohnishi, S. Sugimoto, and I. Nitta, J. Chem. Phys. 37, 1283 (1962).

[28]C. Heller, J. Chem. Phys. 36, 175 (1962).

[29]R. W. Fessenden and R. H. Schuler, J. Chem. Phys. 39, 2147 (1963).

[30]It is difficult to estimate the correction term. However, the quantity G must approach zero as the amplitudes of oscillation become small. For large-amplitude oscillations the motion will be complex and one must decide to what extent the resultant motion may be described as a symmetric movement about an equilibrium position. For very large oscillations (e. g., $\geq 90°$) one expects qualitatively that the values of the β-proton coupling constants would be nearly independent of the angle of twist. In other words, the effect of the B and G terms of Eqs. (10ab) are expected to become negligible with respect to $B^0/2$, and thus Eqs. (10ab) should approach Eq. (5). This is experimentally observed to be the case for the ethyl heptanoate radical motion. We will proceed to use equations based on Eqs. (10ab), but it should be remembered that we are only attempting to estimate the effects of complex motion on the β-proton coupling constants qualitatively.

[31]J. J. Windle and A. K. Wiersema, J. Chem. Phys. 39, 1139 (1963).

[32]R. T. Weidner and C. A. Whitmer, Phys. Rev. 91, 1279 (1953).

[33]We have observed radicals formed by the removal of one α-proton from several other hydrocarbon derivatives. For example, many alkyl ketones and ethers yielded radicals of the form

$$R\text{–}\dot{C}H\text{–}\overset{\overset{O}{\|}}{C}\text{–}R' \quad \text{and} \quad R\text{–}\dot{C}H\text{–}O\text{–}R'$$

respectively. Other examples are the radicals formed from sulfides and unsaturated compounds (both alkenes and alkynes). The ξ-proton splittings of the ester radicals are being considered further in connection with the current work on these and other radicals formed by the X-irradiation of urea inclusion compounds. Similar studies are also in progress using X-ray techniques and the inclusion compounds of trans-anti-trans-anti-trans-perhydrotriphenylene, which were recently reported by Farina, Allegra, and Natta (M. Farina, G. Allegra, and G. Natta, J. Am. Chem. Soc. 86, 517 (1964)).

[34]Actually, of course, if γ_1 is a solution to Eq. (17), so are the angles $\gamma = \gamma_1 \pm n\,90°$ ($n = 0, 1, 2\ldots$). These angles fall into two sets, those corresponding to even values of n and those corresponding to odd values of n. Only one set yields the correct values of the coupling constants by Eqs. (10ab), and all of the members of each set are magnetically equivalent. Similar arguments hold for Eqs. (3ab). If α is a solution to 3ab, so are the angles $\alpha = \pm\ \alpha_1 \pm n\,180°$. These angles correspond to magnetically-equivalent orientations of the β-protons and for our purposes are considered to be the same.

[35]D. J. Millen, Progr. Stereochem. 3, 138 (1962).

[36]E. B. Wilson, Adv. Chem. Phys. 2, 367 (1959).

[37]Although there is no obvious trend in the ester radical conformations of the series beginning with the ethyl hexanoate radical and ending with the ethyl dodecanoate radical, there are differences in the conformations of these and the other radicals reported in Table I. The van der Waals radius of the tubular cavity is necessarily nonuniform and it is tempting to suggest that this is related to the differences in the angles of twist of the ester radicals. However, the lengths of the ester molecules are not, in general, integral multiples of the urea spiral repeat distance and therefore the positions of the urea molecules relative to the C_2–C_3 bonds would not be expected to be identical for all ester radicals of a given crystal. Thus, one might expect that if the nonuniformity of the van der Waals radii caused the variations in the angles of twist, then the radicals of a given crystal would not all have the same angle of twist. This argument assumes that there do not exist unoccupied spaces in the tubular cavities. If there are spaces between the ester molecules, then the nonuniformity of the cavities, hydrogen bonding of the ester group with the urea molecules, or distortions of the lattice caused by the ester functional groups would readily explain the above observations. Another possible explanation is the existence of a cooperative effect among the ester molecules. In any case the structures appear to be highly ordered, since the radicals of a given inclusion compound do have the same angle of twist. (This also suggests that the ester radicals are not rotating in the tubular cavities.) In all of these arguments we are, of course, ignoring the remote possibility that although all stable radicals in one crystal have a given conformation, there exist other

conformations corresponding to radicals which are unstable and are therefore not observed.

Others have observed deviations from planar zigzag conformations. Smith[7] has found that in the n-hexadecane-urea crystal the hydrocarbon chain length is slightly shorter than that calculated for an extended planar configuration. This is supported by the observation that the urea/hydrocarbon ratio for this crystal is lower than expected for an extended planar configuration.[1,3,7] However, Smith[7] found that two other compounds, n-dodecane and decamethylene dibromide, do exist in planar extended zigzag configurations in the urea inclusion compounds.

[38]F. B. Booth, Ph. D. Thesis, California Institute of Technology (1963).

[39]J. D. Morrison and J. M. Robertson, J. Chem. Soc. 1949, 980.

[40]J. M. Robertson and J. D. Morrison, J. Chem. Soc. 1949, 993.

[41]L. C. Fetterley, Ph. D. Thesis, University of Washington (1950).

[42]J. Donohue, J. Phys. Chem. 56, 502 (1952).

[43]J. H. Sturdivant, private communication.

[44]H. M. McConnell and R. E. Robertson, J. Phys. Chem. 61, 1018 (1957).

II. ELECTRON SPIN RESONANCE OF RĊHCOR' RADICALS IN X-IRRADIATED KETONE-UREA INCLUSION COMPOUNDS*

O. Hayes Griffith†

Gates and Crellin Laboratories of Chemistry‡
California Institute of Technology
Pasadena, California

Single crystals of six inclusion compounds formed between aliphatic ketones and urea were X-irradiated at room temperature and the free radicals produced were investigated by electron spin resonance. The six ketones investigated were 2-nonanone, 6-undecanone, 3-tetradecanone, 2-undecanone, 2-dodecanone, and 3-undecanone. The long-lived free radicals observed in all of these compounds ($RCH_2\dot{C}HCOR'$) are formed by the removal of one α proton from the parent ketone. The unpaired spin density in the 2p orbital adjacent to

---

* Supported by the National Science Foundation under Grant. No. GP-930.

† National Science Foundation Predoctoral Fellow.

‡ Contribution No. 3177.

the carbonyl group is 0.81 ± .04. A contour plot of the spin density as a function of the molecular orbital parameters is given. In qualitative agreement with the ESR results, the molecular orbital methods predict the position of maximum spin density to be adjacent to the carbonyl group.

A. INTRODUCTION

The free radicals produced in a series of X-irradiated aliphatic ester-urea inclusion compounds have recently been investigated by electron spin resonance (ESR).[1] The use of an inclusion compound has the distinct advantage over a low temperature glass or powder in that all of the guest molecules of the compound are magnetically equivalent at one or more crystalline directions. Only one ester radical ($R\dot{C}HCOOR'$) and no urea radicals were detected after X-irradiation. The ester-urea single crystals were investigated as a function of temperature and of orientation in the magnetic field, and information regarding the structure and motion of the ester radical was obtained. It is of interest to investigate other aliphatic molecules by this method. In particular, the aliphatic ketone molecules are of interest because of the presence of only one oxygen atom. This simplification in structure makes possible a more quantitative investigation of the X-ray produced ketone radicals. In this paper the radicals in a series of X-irradiated ketone-urea inclusion compounds are identified, the coupling constants are given, and the experimental and theoretical positions of maximum spin density

are determined.[2]

B. EXPERIMENTAL

Single crystals of the inclusion compounds formed between urea and the aliphatic straight-chain ketones were grown from a methanol solution by either slow evaporation or by slow cooling. In all cases ketones were chosen which gave the best quality of urea inclusion crystals and, therefore, the lengths of the ketone molecules studied are somewhat arbitrary. The crystals obtained were either hexagonal needles or flat hexagonal plates and were stable for several months in air at room temperature. The z axis of the cartesian crystalline coordinate system is defined to lie along the needle axis of the urea compound and therefore the z axis is parallel to the six faces of the hexagonal prism. The x and y axes are not specified other than that they lie in a plane perpendicular to the needle axis of the crystal. The morphology of the ketone-urea crystals is typical of the morphology of crystals formed between urea and a variety of long straight chain molecules.[3] The ketone molecules are therefore expected to exist in an extended zigzag conformation in the hollow (hexagonal) cavities formed by the urea molecules.[4] We will assume this to be the case throughout the following discussion, although no crystallographic data has been reported for the ketone-urea compounds studied in this paper.

The X-ray apparatus, X-band ESR spectrometer, modulation amplitude, and calibration standards were the same as employed in I.

A conventional small dewar connected by means of a transfer tube to a liquid helium dewar was used to cool the crystals below room temperature. The rate of cold helium gas flow was controlled by varying the power dissipated in a resistor located inside the liquid helium dewar. A heated nitrogen gas flow system was used to obtain temperatures above room temperature. Crystals of the 6-undecanone-urea compound were heated to ~ 325°K for a few minutes prior to recording the final ESR spectra to remove small quantities of additional radicals. The lines due to these radicals were not sufficiently resolved to allow identification of the radicals. The other X-irradiated ketone-urea inclusion compounds listed in Table I were not heated before obtaining the ESR spectra. For any given inclusion compound, the major lines of the ESR spectra were independent of the ratio of the ketone to urea in the methanol solution and to the length of time the crystals were X-irradiated.

C. RADICAL IDENTIFICATION

The ESR spectra obtained for the X-irradiated 2-nonanone, 6-undecanone, and 3-tetradecanone urea inclusion compounds are given in Figs. 1-3. The ESR hyperfine pattern of the 2-nonanone-urea crystal results from two nonequivalent but nearly isotropic proton coupling constants and one anisotropic proton coupling constant. The lines are further split by three small proton coupling constants which are resolved only at certain orientations of the magnetic field. The ESR

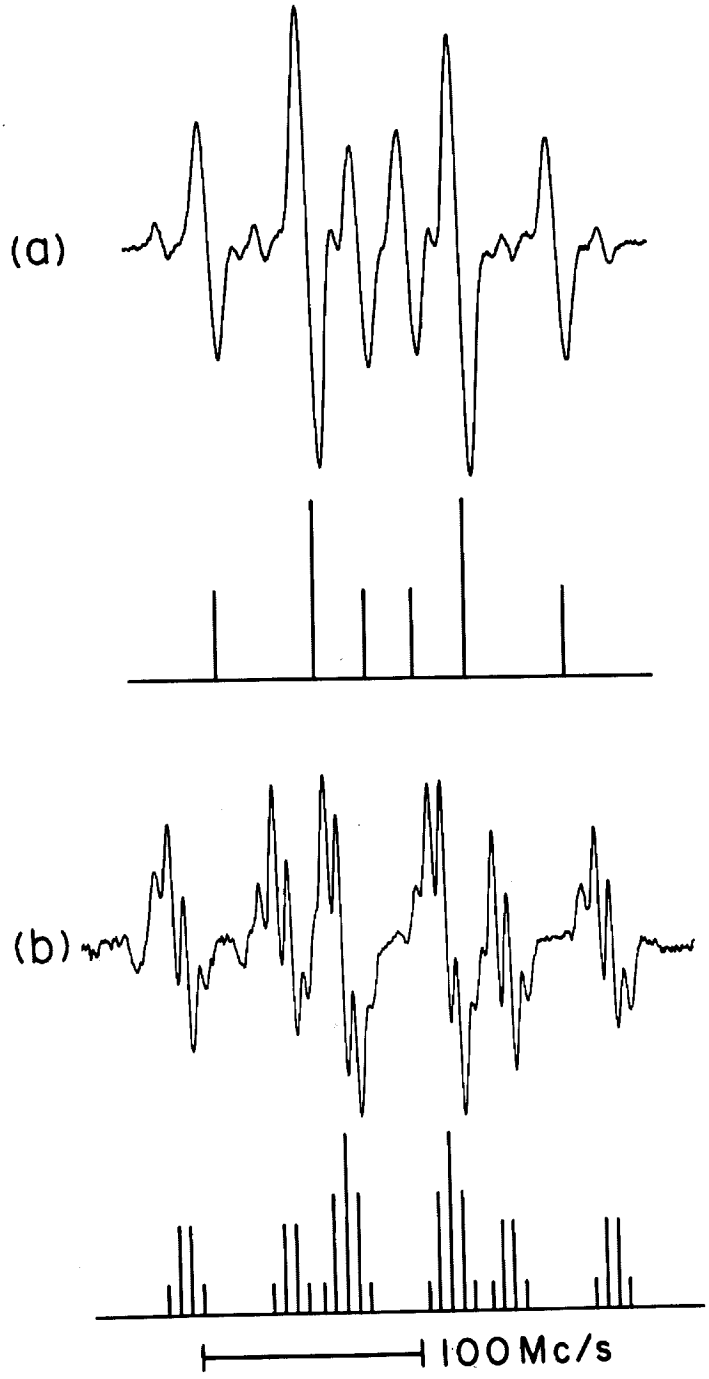

Figure 1
The room-temperature ESR spectra of an X-irradiated 2-nonanone-urea crystal with the magnetic field vector (a) 70° from the z axis and (b) parallel to the z axis. The reconstructed "stick" spectra of the $CH_3COCH(CH_2)_5CH_3$ radical for these two orientations are given below the observed spectra.

spectra obtained for the 6-undecanone-urea crystal are similar except that the small splittings arise from two equivalent proton coupling constants. Finally, the ESR spectra obtained for the 3-tetradecanone-urea crystal may be constructed from three equal and nearly isotropic proton coupling constants, one anisotropic coupling constant, and two approximately equivalent coupling constants of much smaller magnitude than the other four. Therefore, the only logical choices for the radicals produced in the 2-nonanone, 6-undecanone, and 3-tetradecanone urea inclusion compounds are, respectively,

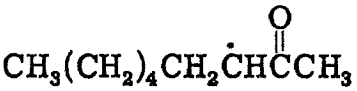

(1)

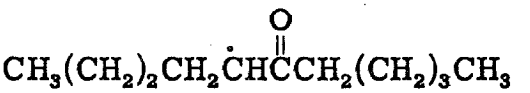

(2)

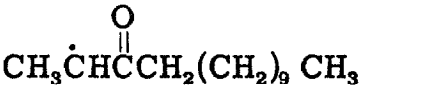

(3)

and the magnitudes and assignments of the proton coupling constants are given in Table I.[5] In agreement with results obtained for other radicals, the β-proton coupling constants are very nearly isotropic and the α-proton coupling constants are anisotropic. The small splittings result from the previously unresolved ζ-proton coupling constants. Splittings due to the γ-protons are not resolved.

Three other ketones, 2-undecanone, 2-dodecanone, and 3-undecanone, were also investigated and the results are summarized in Table I. The radicals observed in all ketone-urea inclusion compounds may be

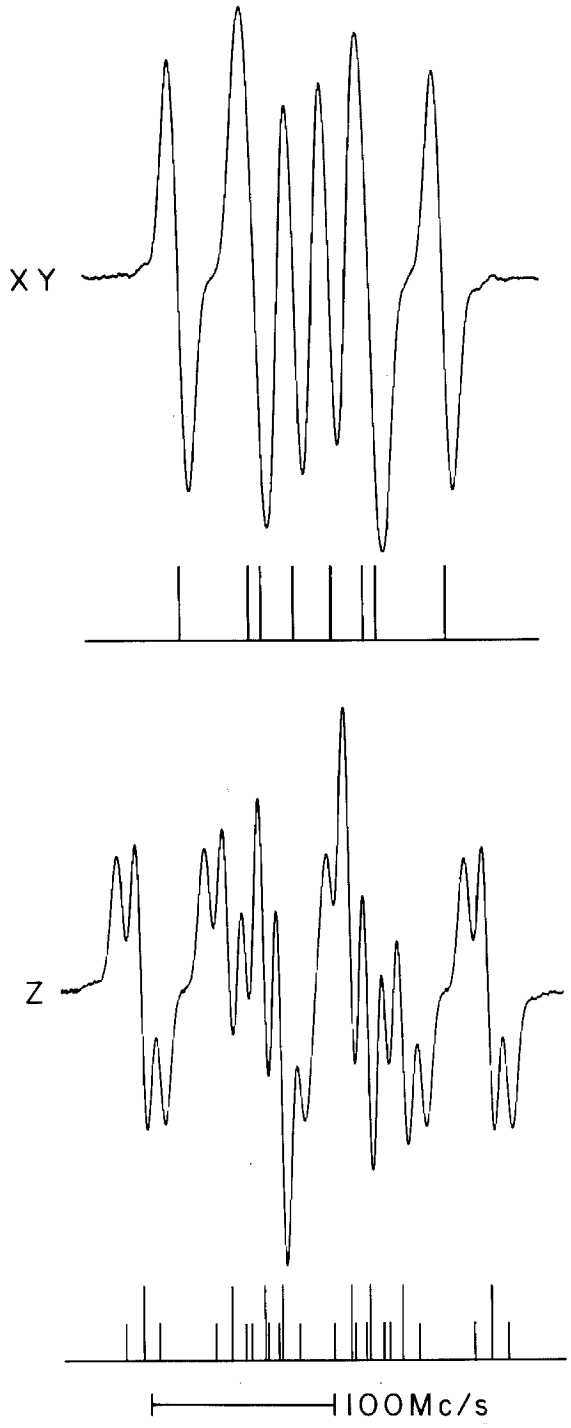

Figure 2
The room-temperature ESR spectra of an X-irradiated 6-undecanone-urea crystal with the magnetic field parallel to the xy plane and along the z axis, respectively. The reconstructed spectra of the CH_3CH_2-$\dot{C}OCHCH_2CH_3$ radical are given below the observed spectra.

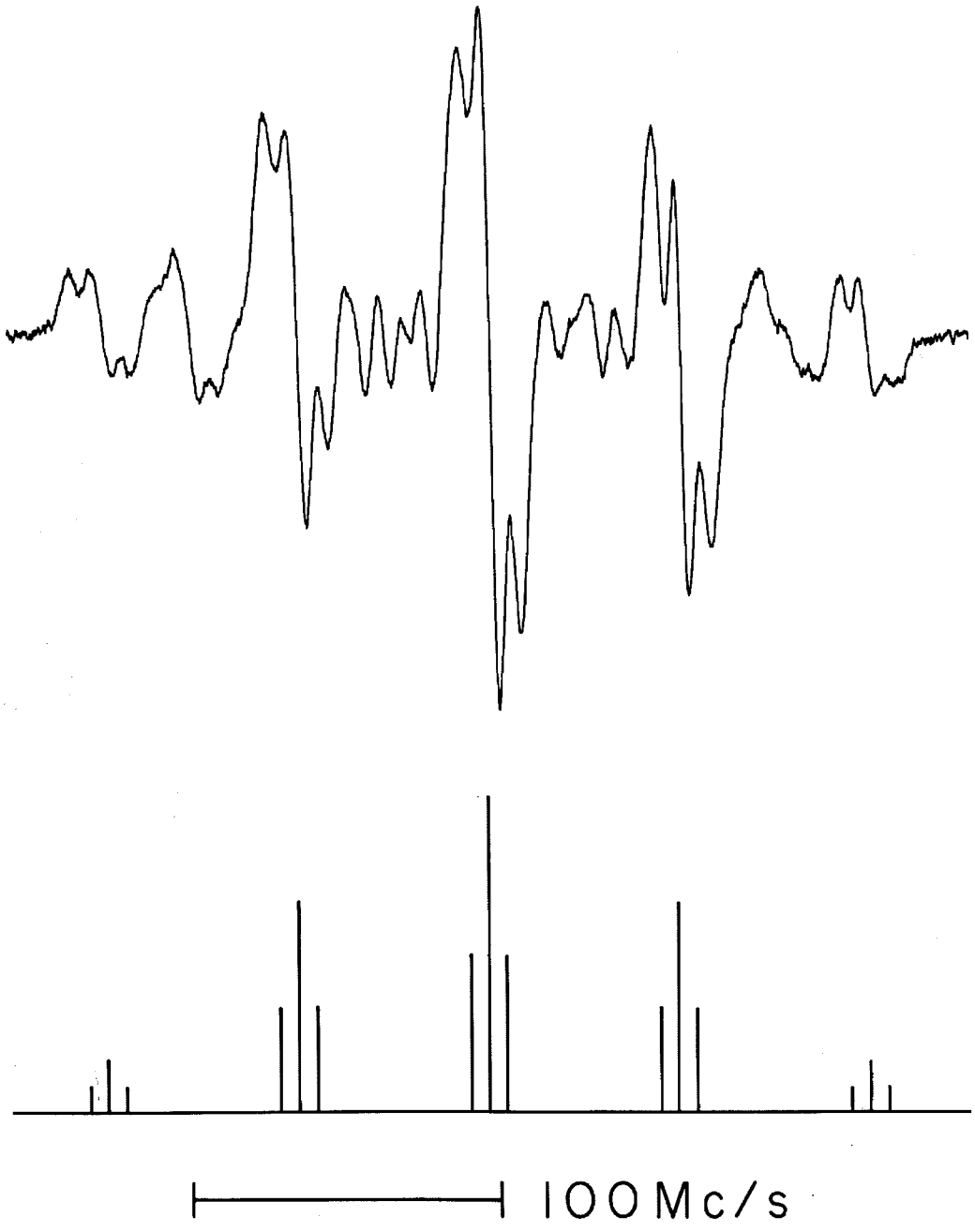

Figure 3
The ESR spectra of an X-irradiated 3-tetradecanone-urea crystal at 310°K. The magnetic field is approximately 40° from the crystalline z axis. The reconstructed spectra is that of the $CH_3\dot{C}HCOCH_2(CH_2)_9$-$CH_3$ radical and the remaining (major) lines are apparently due to the $CH_3C_{\lambda}HCO\dot{C}H(CH_2)_4CH_3$ radical.

TABLE I. PROTON HYPERFINE COUPLING CONSTANTS OF KETONE RADICALS[a, b]

RADICAL[c]	T (°K)	a_z^α	a_{1z}^β	a_{2z}^β	a_z^ζ	a_{xy}^α	a_{1xy}^β	a_{2xy}^β
$CH_3\overset{O}{\overset{\|}{C}}\dot{C}H(CH_2)_5CH_3$	298	76	71	47	5.4	38	68	45
$CH_3(CH_2)_4\overset{O}{\overset{\|}{C}}\dot{C}H(CH_2)_3CH_3$	298	76	66	48	9.1	38	63	45
$CH_3(CH_2)_{10}\overset{O}{\overset{\|}{C}}\dot{C}HCH_3$[d]	310	~75	64	64	9.0	39	58	58
$CH_3\overset{O}{\overset{\|}{C}}\dot{C}H(CH_2)_7CH_3$	313	77	71	53	5.0	39	68	50
$CH_3\overset{O}{\overset{\|}{C}}\dot{C}H(CH_2)_8CH_3$	322	75	70	52	5.5	38	66	49
$CH_3(CH_2)_7\overset{O}{\overset{\|}{C}}\dot{C}HCH_3$[d]	298	~75	65	65	9.5	38	57	57

FOOTNOTES FOR TABLE I

[a] a^{α}, a^{β}, and a^{ζ} are the coupling constants for the α proton, β protons, and the ζ protons, respectively, and xy and z denote the spectra obtained with the magnetic field in the crystalline xy or z directions. All coupling constants are reported in Mc/sec.

[b] The ESR spectra of three of the radicals were recorded at temperatures above 298°K in order to improve resolution. The temperatures chosen are somewhat arbitrary. The change of resolution with temperature is caused by a slight temperature dependence of the β-proton coupling constants. The accuracy of a_z^{α} (~ 75 Mc/sec) for the third and sixth radicals is decreased to ± 3 Mc/sec by the extensive overlapping of spectral lines. All other a^{α} and a^{β} values are estimated to be accurate to within ± 2 Mc/sec. The small a_z^{ζ} values should be accurate to within ± 0.7 Mc/sec.

[c] These radicals are formed from the parent compound by the removal of one α proton. The parent ketones are, from top to bottom, 2-nonanone, 6-undecanone, 3-tetradecanone, 2-undecanone, 2-dodecanone, and 3-undecanone.

[d] These two radicals each exhibit three magnetically equivalent β protons ($a_3^{\beta} = a_2^{\beta} = a_1^{\beta}$).

thought of as being formed by the removal of one hydrogen atom from the α position of the parent ketone, and there was no evidence for stable paramagnetic sites associated with the urea molecules. The g values of all six radicals were measured at room temperature and were found to be the same within experimental error. The average g value and the estimated error with the magnetic field parallel and perpendicular to the z axis, respectively, are g(z) = 2.0040 ± .0003 and g(xy) = 2.0044 ± .0003. As may be seen from Fig. 3, the ESR spectra of the X-irradiated 3-tetradecanone-urea compound are complicated by the presence of one or more additional radicals. All radicals present have roughly the same thermal stability and it was not possible to greatly change the relative concentrations of the radicals by either heating the crystal or subjecting the crystal to ultraviolet light. However, the outermost unidentified doublet is split by two small and approximately equivalent coupling constants. From further considerations of the magnitudes of the various splittings it appears that all major unidentified lines can be assigned to the radical $CH_3CH_2C\dot{O}CH(CH_2)_9CH_3$. An analogous situation occurs in the case of the X-irradiated 3-undecanone-urea compound. We will not be concerned further with these additional radicals since a well resolved example of a nearly identical radical is present in the 6-undecanone-urea crystal.

All of the above radicals were remarkably stable. The radical concentrations remained approximately constant during the several hours of room temperature experimentation. However, the concentrations of the radicals decreased slowly as the crystals were heated and

the ESR signals disappeared at temperatures well below the melting points of the crystals.

D. EXPERIMENTAL DETERMINATION OF THE SPIN DENSITY ρC_2^{π}

a. From α-Proton Coupling Constant Data

It is apparent from the data of Table I that the ketone radicals are very similar to the previously reported carboxylic acid[6] and ester[1] radicals. That is, there is a large spin density associated with carbon atom 2, a small spin density associated with carbon atom 1, and presumably a small spin density associated with the oxygen atom. These are evidently π-electron spin densities and are referred to as ρC_2^{π}, ρC_1^{π}, and ρO^{π}, respectively. (It will be shown later that the π-electron assumption is supported by all available data.) We will immediately limit the discussion to ρC_2^{π} since this diagonal spin density matrix element is so much larger than the adjacent one, ρC_1^{π}, that the off-diagonal elements of the spin density matrix[7] may well dominate ρC_1^{π}. This means, in effect, that the estimate of ρC_1^{π} obtained from the coupling constant data by the usual methods may be highly unreliable. The value of ρC_2^{π}, on the other hand, may be obtained by two independent methods and, therefore, ρC_2^{π} can be obtained with good accuracy. The procedure followed here is as follows: the value of ρC_2^{π} is estimated from the α-proton coupling constant data and from the β-proton coupling constant data; the theoretical values of ρC_2^{π} are obtained as a function of the molecular orbital parameters and these spin densities are then

compared to the experimental ρC_2^{π}.

The maximum value of the α-proton coupling constant, a^{α}, occurs when the magnetic field is parallel to the z axis and the minimum value of a^{α} occurs with the magnetic field perpendicular to the z axis of the crystal. These two values of a^{α} are referred to as a_z^{α} and a_{xy}^{α}, respectively, and they are the same within experimental error for all ketone radicals studied (Table I). The first step in obtaining the spin density is to extract the isotropic contribution, a_0^{α}, from a_{xy}^{α} and a_z^{α}. This is somewhat more troublesome for included radicals than for radicals rapidly tumbling in solution or rigidly held in a crystal lattice because molecular motion in the urea inclusion compounds averages a portion, but not all, of the anisotropic proton-electron hyperfine interaction.

In I, the equation

$$a_0^{\alpha} = (1/3)\,(2a_{xy}^{\alpha} + a_z^{\alpha}) \qquad (4)$$

was used to obtain a_0^{α} from experimental values of a_{xy}^{α} and a_z^{α}. This simple relation will also be useful in obtaining an approximate value of a_0^{α} for the ketone radicals. In obtaining Eq. (4), the α-proton tensor elements in the xy plane are assumed to be averaged by molecular motion. This averaging can be accomplished by various types of motion. The tensor elements are obviously averaged by rapid rotation of the radicals about the crystalline z axis. They are approximately averaged if the amplitude of the radical motion in the xy plane is greater than ~ 80° and all bond positions in this range are equally probable (the residual few Mc/sec anisotropy would have a negligible effect on the splittings but

could inhomogeneously broaden the ESR lines). The tensor averaging would also be accomplished provided that each radical executes a random walk among the orientations related by an n-fold axis of symmetry parallel to the crystalline z axis ($n \geq 3$). If $n = 6$ this corresponds to a rapid jumping of the radicals between the six positions of minimum energy in the hexagonal tubular cavities of the crystal. All of the above types of motion are, in principle, allowed by the general structure of the inclusion crystals.[8]

For each of the six ketone-urea compounds reported in Table I, the room temperature spectra recorded with the magnetic field perpendicular to the crystalline z axis remained unchanged as the crystal was rotated about the z axis, but were anisotropic with respect to arbitrary rotations of the crystal. This behavior is typical of all included radicals studied thus far and it results from the motional averaging of the tensor elements in the xy plane. As a final check of Eq. (4) for such a radical, the value of a_0, obtained from this equation and the included acid radical ESR data, was compared to a_0 reported for similar radicals in "rigid" dicarboxylic acid crystals.[1] The two values were identical within experimental error and this provides a partial justification of the use of Eq. (4) for other included radicals. Assuming Eq. (4) to be valid for the ketone radicals, $a_0^\alpha = 51 \pm 2$ Mc/sec for all six ketone radicals of Table I. The π-electron spin density on atom 2, ρC_2^π, may now be obtained from McConnell's well known equation,[9] $a_0^\alpha = Q \rho C^\pi$, where Q is a proportionality constant and ρC^π is the π-electron spin density on the carbon atom bonded to the α proton. A good estimate of Q is

62.7 Mc/sec. This number is the value of a_0^{α} reported by Fessenden and Schuler for the ethyl radical ($CH_3\dot{C}H_2$, $\rho C^{\pi} \simeq$ unity).[10] Taking Q to be 62.7 Mc/sec, $\rho C_2^{\pi} = 0.82$.

b. From β-Proton Coupling Constant Data

The value of ρC_2^{π} may also be obtained from the ketone β-proton coupling constants. The β protons undergo motion with respect to the π orbital on C_2 and the value of ρC_2^{π} cannot, in general, be obtained without a knowledge of the nature of the motion. However, the methyl group attached to carbon atom 2 of the 3-tetradecanone radical is rotating (or undergoing large amplitude oscillations) at frequencies large compared to the β-proton hyperfine frequency, as is evidenced by the equivalence of the three β protons. This is also the case for the methyl group of the 3-undecanone radical and for these two radicals the usual expression relating the spin density to the β-proton coupling constants reduces to $a_0^{\beta} = (B/2)\,\rho C_2^{\pi}$, where a_0^{β} is the isotropic component of the β-proton coupling constant and B/2 is a proportionality constant.[11] The experimental value of a^{β} contains an anisotropic component as well as the isotropic component and these two contributions must be separated before this equation can be used to obtain ρC_2^{π}. Fortunately, the anisotropic component is small and, therefore, the method employed to extract a_0^{β} is not critical.

Heller[12] has observed that, for the $CH_3\dot{C}(CO_2H)_2$ radical, the anisotropic components of the β-proton hyperfine coupling constants are

adequately described by the Hamiltonian

$$\mathcal{H}_d = -g|\beta| g_N \beta_N T_\perp (1-3\cos^2\alpha) S_H I_H \qquad (5)$$

In Eq. (5) α is the angle between the magnetic field direction, $\underset{\sim}{H}$, and the $CH_3-\dot{C}H$ carbon-carbon bond, S_H and I_H, are the components of S and I along $\underset{\sim}{H}$, and $-g|\beta| g_N \beta_N h^{-1} T_\perp \rho C^\pi \equiv B_d \rho C_2^\pi = (-)2.2$ Mc/sec. The isotropic value of the three β-proton coupling constants is (+)70.9 Mc/sec for this radical. From the data reported by Morton and Horsfield[13] for the similar radical $CH_3\dot{C}HCO_2H$, a_0^α, a_0^β, and B_d are (-)54.7, (+)70.3, and (-)3.0 Mc/sec, respectively. If we take $\rho C_2^\pi = 0.90 \pm .04$ for these two radicals, then a good estimate of B_d is (-)2.9 ±0.6 Mc/sec.

For the included radicals,[14] the α-proton tensor elements are averaged in the xy plane and this requires a motional averaging of the C_2-C_3 bond positions in the tubular cavities. If the motions of these radicals are again taken to be free rotation, large amplitude (equal probability) motion or a random jumping motion, Eq. (5) yields

$$a_{xy}^\beta = \rho C_2^\pi [B_d(1-\tfrac{3}{2}\sin^2\theta) + R/2] \qquad (6)$$

$$a_z^\beta = \rho C_2^\pi [B_d(1-3\cos^2\theta) + R/2] \qquad (7)$$

$$a_0^\beta = \rho C_2^\pi (R/2) = 1/3\,(2a_{xy}^\beta + a_z^\beta) \qquad (8)$$

where a^{β}_{xy} and a^{β}_{z} are the β-proton coupling constants with the magnetic field perpendicular and parallel to the z axis, respectively, and θ is the angle between the C_2-C_3 bond and the z axis. Using Eq. (8) and the data of Table I, a^{β}_{0} = 59.6 Mc/sec for the 3-tetradecanone and 3-undecanone radicals. For the ethyl radical a^{β}_{0} = 75.4 Mc/sec. If R is assumed to be the same for the ketone and ethyl radicals then ρC_2^{π} (ketone) = 59.6/75.4 = 0.79. This value of ρC_2^{π} is in excellent agreement with the value of 0.82 obtained from the α-proton coupling constant data.

From Eqs. (6) and (7) and a value for θ we may also estimate the anisotropic component of a^{β}. If the $\dot{C}-H_{\alpha}$ bond and the axis of the 2p orbital on C_2 lie in the xy plane and the σ bonds involving C_2 are sp^2 hybridized, then the most probable value of θ is readily seen to be 30°. (These requirements are, of course, more stringent than those used in obtaining ρC_2^{π}.) Taking $\theta = 30°$ and $\rho C_2^{\pi} = 0.79$, Eqs. (6) and (7) give $a^{\beta}_{z} \simeq 62$ Mc/sec and $a^{\beta}_{xy} \simeq 60$ Mc/sec which are in agreement with the data of Table I.[15]

c. Effects of Temperature Changes on the ESR Spectra

The principal question remaining is whether the above experimental value of ρC_2^{π} is a meaningful quantity associated with this class of aliphatic ketone radicals, or whether this spin density is a temperature-dependent function of intramolecular motion about the C_2-C_1 bonds. In the case of two included ester radicals, the ethyl heptanoate radical and the octyl propionate radical, it was possible to obtain well resolved

spectra over the wide temperature range from roughly 340°K to 7°K.[1] The ester α-proton coupling constants, and hence ρC_2^{π}, were observed to be independent of temperature over this entire range within experimental error. The ester β-proton coupling constants changed gradually with temperature due to temperature-dependent motion about the C_2-C_3 bonds. For the ketone radicals it was not possible to completely resolve the ESR spectra over this wide a range of temperatures. However, some data in addition to that presented in Table I were obtained over limited temperature ranges both above and below room temperature. For example, well resolved xy and z ESR spectra were recorded for the 3-tetradecanone-urea crystals at 313, 323, and 333°K. (We refer to spectra obtained with the magnetic field in the xy and z crystalline directions as xy and z spectra, respectively.) Well resolved xy and z spectra were also recorded for the 6-undecanone and 2-dodecanone radicals at approximately 333°K. The α-proton coupling constants derived from these data are the same as those of Table I within the estimated experimental error of ± 2 Mc/sec. At these temperatures the spectra recorded with the magnetic field in the xy plane were isotropic with respect to rotations of the magnetic field in this plane, and spectra for all orientations of the magnetic field were symmetric.

The X-irradiated 6-undecanone-urea crystals were cooled from room temperature to 30°K. Both the xy and z spectra changed gradually with temperature and the xy spectra began showing signs of asymmetry below 270°K. At 77°K the xy spectra were anisotropic with respect to

rotations of the magnetic field in the xy plane. The features of these anisotropic spectra were repeated at intervals of 60° in the xy plane, and at no other orientations of the magnetic field. As with the ester radicals, this observation supports the assumption that the crystals are hexagonal and that the z direction lies along the crystallographic c axis. Although no coupling constant data were obtained from the asymmetric xy ESR spectra, approximate coupling constants were measured from the symmetric 6-undecanone radical z spectra for temperatures down to 190°K. Over this range a_z^α was independent of temperature within an estimated experimental error of ± 4 Mc/sec, which suggests that ρC_2^π is temperature-independent (over this temperature range). Below 190°K the z spectra were sufficiently broadened and unresolved to prevent measurement of the coupling constants. There was, however, no indication of any major changes in the magnitude of a_z^α from 190°K to 30°K. Below 50°K there was very little change in the general features of the spectra obtained with the magnetic field either parallel or perpendicular to the z axis of the 6-undecanone-urea crystal. All of the above temperature effects on all ketone radical spectra were reversible.

The data of Table I provide adequate evidence that the spin density distribution is independent of the length of the ketone molecule and the exact position of the carbonyl group in the chain (and therefore of the precise conformation of these radicals in the tubular cavities). In addition, the above ESR data, recorded over a range of temperatures, strongly suggest that ρC_2^π is independent of temperature. Therefore,

with reasonable certainty, the value 0.81 ± 0.04 representing the average of the values obtained from the α- and β-proton coupling constant data may be taken to be a meaningful property of this general class of aliphatic ketone radicals. The estimated error of ± 0.04 reflects the variations among the possible choice for R and Q as well as the approximations in the formulas used and the limits of experimental accuracy.

Before proceeding to the molecular orbital calculations it is advisable to consider the π-electron assumption in greater detail. McConnell, Heller, Cole, and Fessenden have shown that the radical $\dot{C}H(CO_2H)_2$ is a π-electron radical; the odd electron spin is largely localized in an orbital antisymmetric to reflection in the plane containing three carbon atoms and the α-hydrogen atom.[6] Other dicarboxylic acid radicals and alkyl radicals having both α and β protons interacting with the unpaired spin are also known to be π-electron radicals.[10,11] Since the magnetic properties of the ketone radicals are so similar to those of the acid and alkyl radicals, the ketone radicals are almost certainly π-electron radicals. The g values of the ketone radicals are quite similar to those of the acid and alkyl radicals. The isotropic coupling constants a_0^α and a_0^β are also consistant with the known π-electron proton coupling constants. Turning now to the anisotropic components of the proton coupling constants, we note that if the carbon atom 2 is sp^2 hybridized then the C_2–H_α bond lies in or near the crystalline xy plane. This follows from the fact that the "walls" of the tubular cavities

restrict the possible orientations of the long straight-chain molecules. Smith[4] has found using X-ray crystallographic techniques that the included n-hydrocarbons exist in a time-averaged extended zigzag conformation (this would place the C_2-H_α bond of the corresponding $R\dot{C}HR$ π radical in the xy plane). In I it was shown that the C_2-H_α bonds of the carboxylic acid radicals are approximately in the xy plane by comparing the a^α_{xy} and a^α_z of these radicals with the known principal elements of the α-proton tensor. Extending these arguments to the ketone radicals, the ratio of a^α_{xy} (ketone)/a^α_{xy} (acid or ester) is 0.93 and the ratio of a^α_z (ketone)/a^α_z (acid or ester) is 0.92. These two ratios are the same within experimental error which implies a similar averaging of the tensor elements in all three radical systems. The very small ketone β-proton coupling constant anisotropy has already been shown to be consistant with this radical orientation and hybridization. All of the data are therefore consistant with the π-electron model assumed both in obtaining the experimental value of ρC_2^π and in the following calculations.

E. MOLECULAR ORBITAL CALCULATIONS OF SPIN DENSITY

The spin densities were calculated using the Hückel theory[16] and the method of McLachlan.[17] For these molecular orbital calculations the nuclear framework of the ketone radical is represented by the structure

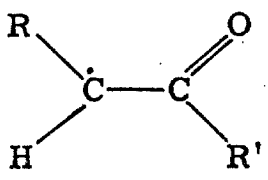

in which all atoms shown are coplanar. The unpaired spin density is extended over C_2, C_1, and the oxygen atom, and each of these three atoms contributes one electron to the π system. In the Hückel molecular orbital method the two parameters relating α_O and β_{CO} to α_C and β_{CC} are defined by the equations $\underline{h} \equiv (\alpha_O - \alpha_C)/\beta_{CC}$ and $\underline{k} \equiv \beta_{CO}/\beta_{CC}$. The one-electron wave functions are obtained by the usual variational procedure and the spin densities are given by the squares of the coefficients of the half-filled molecular orbital. The spin densities are, of course, a function of the two parameters $\underline{h}$ and $\underline{k}$. In order to obtain the best overall view of the method, the range of $\underline{h}$ and $\underline{k}$ values used here is much larger than the usual range employed in Hückel calculations.

The results for ρC_2^{π} are summarized by the solid lines of Fig. 4. It is interesting to note that the spin density is quite insensitive to variations in $\underline{h}$ and it is very sensitive to changes in $\underline{k}$. Even though only one spin density site is being considered (and hence a unique pair of $\underline{h}$ and $\underline{k}$ is not obtained), this insensitivity to $\underline{h}$ makes possible an estimation of $\underline{k}$. If $\underline{h}$ is constrained to the liberal range of $0.7 \leq \underline{h} \leq 2.0$ then $\underline{k} \simeq 2.0 \pm 0.3$. This value compares favorably with $\underline{k} \simeq 1.6$ reported by Vincow and Frankel[18] for a series of semiquinone anion radicals. Both of these values, however, are somewhat higher than the range $0.8 \leq \underline{k} \leq 1.4$ most frequently employed[16] in the determination of properties (other than spin densities) of compounds containing carbonyl groups.

McLachlan has obtained approximate spin density formulas from considerations of the perturbed self-consistent field theory. In the

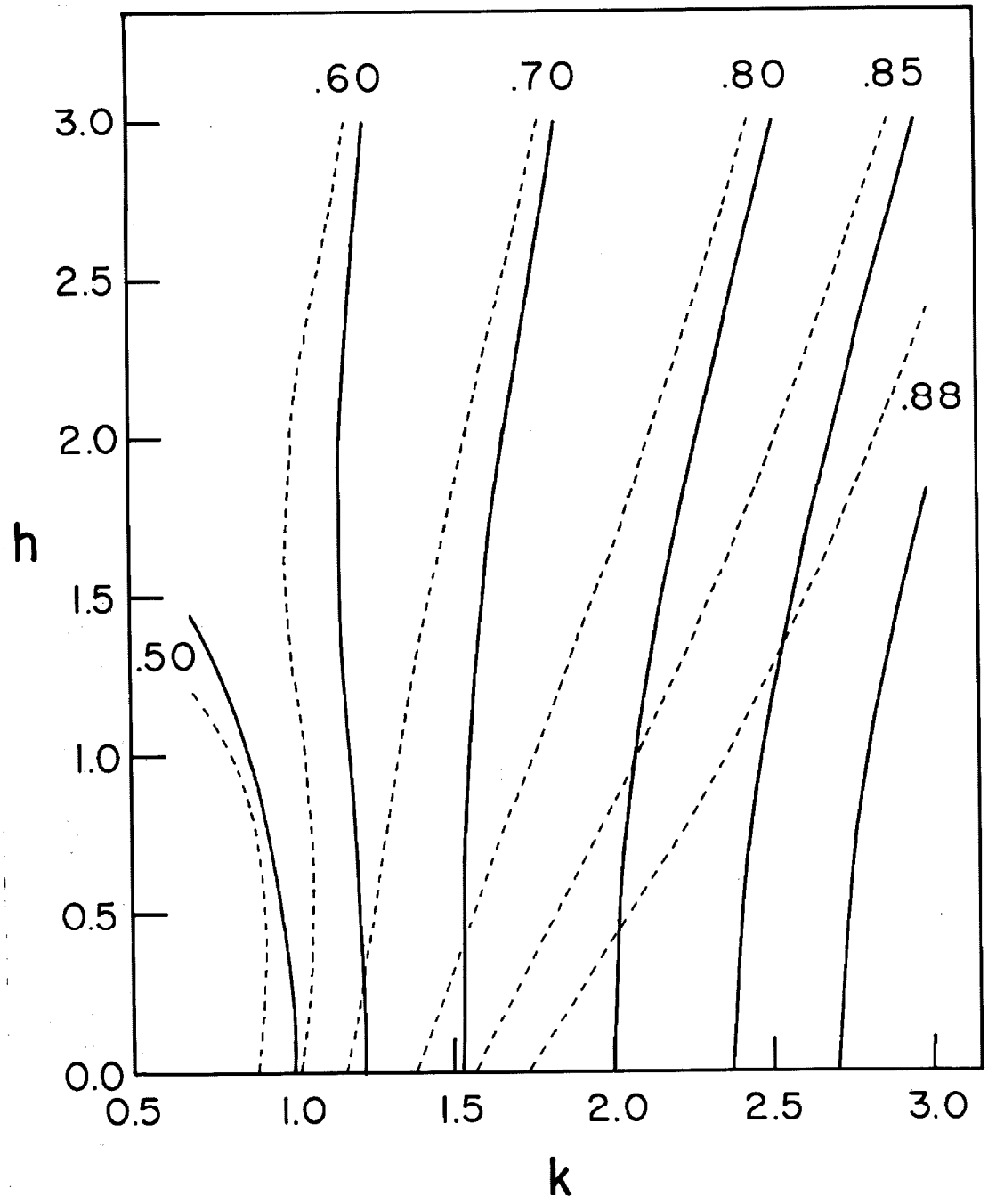

Figure 4
The electron spin density on carbon atom 2 as a function of the molecular orbital parameters h and k. The solid and broken lines represent the Hückel and McLachlan ($\lambda = 1.1$) values, respectively.

simplest form of McLachlan's approximate method the spin density ρ_r^{π} is given by

$$\rho_r^{\pi} = C_{ro}^2 - \lambda \sum_s \pi_{rs} C_{so}^2 \qquad (9)$$

where π_{rs} and C_{ro}^2 are the atom-atom polarizabilities and spin densities, respectively calculated from the Hückel theory and λ is a semiempirical constant which we will take equal to 1.10. The values of ρC_2^{π} obtained by this method are given by the broken lines of Fig. 4. Eq. (9) has the pronounced effect of shifting ρC_2^{π} to lower values of $\underline{k}$. This shift is desirable since now the values of $\underline{h}$ and $\underline{k}$ obtained for other properties of carbonyl compounds yield values of ρC_2^{π} in much better agreement with the experimental value. A unique pair of $\underline{h}$ and $\underline{k}$ values cannot, of course, be obtained from the single experimental quantity ρC_2^{π}.

The ketone radical can be considered as an allyl radical in which the electron distribution is polarized by replacing one terminal carbon atom of the core by an oxygen atom. For the allyl radical, $\underline{h} = 0$, $\underline{k} = 1$ and the Hückel and McLachlan values of ρC_2^{π} are 0.50 and 0.60, respectively. In the ketone radical the π-electron density about the oxygen atom increases and therefore ρC_2^{π} increases.[19] For example, the Hückel <u>charge</u> densities of the ketone radical are 0.10, 0.17, and -0.27 for C_2, C_1, and the oxygen atom, respectively (assuming $\underline{h} = 1.0$ and $\underline{k} = 2.0$). The Hückel <u>spin</u> densities for this choice of parameters are 0.78, 0.03, and 0.18 for C_2, C_1, and the oxygen atom, respectively. The Hückel charge densities on all three carbon atoms of the allyl radical are zero, and the Hückel spin densities are 0.50, 0.00, and 0.50 for the

three carbon atoms, taken consecutively.[20] This polarization effect of oxygen is so strong that the ketone radical is probably better described as an aldehyde group weakly interacting with the adjacent π electron. Further considerations of the electronic structure of this radical are of interest, and self-consistent field and configuration interaction calculations are currently in progress.

F. ACKNOWLEDGEMENTS

We are especially indebted to Professor Harden M. McConnell for enlightening discussions and for the use of his laboratory facilities.

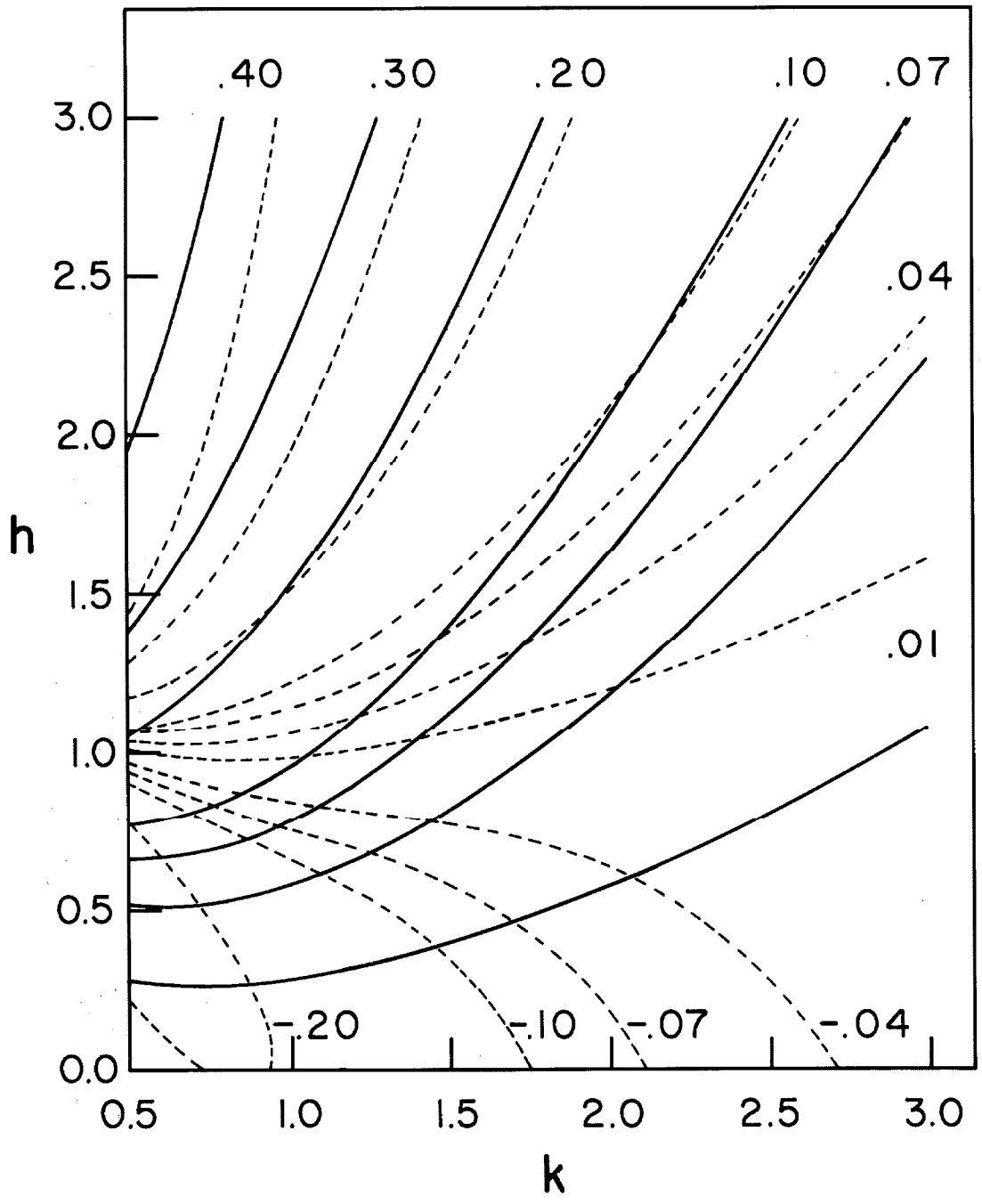

Figure 5
The electron spin density on carbon atom 1 as a function of the molecular orbital parameters h and k. The solid and broken lines represent the Hückel and McLachlan ($\lambda = 1.1$) values, respectively.

G. REFERENCES

[1]O. H. Griffith, J. Chem. Phys., 41, 1093 (1964), in the following referred to as I.

[2]Although the ketone radical ($R\dot{C}HCOR'$) has undoubtedly been mentioned in interpretations of powder or low-temperature glass ESR spectra, we are unaware of any previous systematic investigation of this type of radical in an oriented matrix.

[3]W. Schlenk, Jr., Ann., 565, 204 (1949).

[4]A. E. Smith, Acta Cryst., 5, 224 (1952).

[5]The convention for the labeling of protons ($\alpha, \beta, \gamma, \zeta$) and carbon atoms ($C_1$, C_2, C_3) used here is

$$\underset{C_3}{\overset{\gamma}{}}\ \underset{C_2}{\overset{\beta}{}}\ \underset{C_1}{\overset{\alpha}{}}\ \overset{O}{}\ \underset{C_4}{\overset{\zeta}{}}$$
$$R-CH_2-CH_2-\dot{C}H-C-CH_2-R'$$

[6]H. M. McConnell, C. Heller, T. Cole, and R. W. Fessenden, J. Am. Chem. Soc., 82, 766 (1960).

[7]H. M. McConnell, J. Chem. Phys., 28, 1188 (1958).

[8]Eq. (4) is actually more general than suggested by these arguments. Limited motion out of the xy plane is certain to occur in these crystals and Eq. (4) is still applicable for this situation. Eq. (4) would also be applicable in the limiting case of spherical averaging of the C_2-H_α bonds in the crystal since for this case $a^\alpha_{xy} = a^\alpha_z$ (this extremely large freedom of motion has not occurred in any system investigated

thus far). Returning to the random walk argument, the walk need not be over the full 360°. For example, a random jump between two positions in the xy plane 90° apart leads to Eq. (4). Regardless of the argument, it should be kept in mind that this equation is only an approximation; as indeed must be the case for motion as complex as that occurring in the inclusion crystals. The information regarding this motion obtained from the α-proton coupling constant is obviously restricted. The fact that the lines are broadened when the magnetic field is in the xy plane suggests that the amplitude of the C_2-H_α bond is large but does not correspond precisely to the case of free rotation.

[9]See, for example, H. M. McConnell and D. B. Chesnut, J. Chem. Phys., 28, 107 (1958).

[10]R. W. Fessenden and R. H. Schuler, J. Chem. Phys., 39, 2147 (1963).

[11]C. Heller and H. M. McConnell, J. Chem. Phys., 32, 1535 (1960).

[12]C. Heller, J. Chem. Phys., 36, 175 (1962).

[13]J. R. Morton and A. Horsfield, J. Chem. Phys., 35, 1142 (1961).

[14]The signs of the coupling constants are not determined from the experiments reported here and all proton coupling constants are listed as their absolute values. The isotropic components of the α- and β-proton coupling constants of very similar radicals are known to be negative and positive, respectively.

[15]The spin density on carbon atom one may be estimated by a

similar procedure providing one assumes that $a^{\zeta} = (R/2)\,\rho C_1^{\pi}$ where R is the same for the β and ζ protons. As before, only radicals having rotating (ζ proton) methyl groups and known orientations will be useful for this purpose. From the data of Table I, the three radicals derived from 2-nonanone, 2-undecanone, and 2-dodecanone are all seen to have the three equivalent ζ-proton coupling constants characteristic of a rotating methyl group. For the most probable conformations of these radicals, the orientation of the C_1-C_4 bonds are inclined at approximately the same angle from the crystalline z axis (tubular axis) as are the C_2-C_3 bonds of all six ketone radicals. The relative isotropic and anisotropic components of the three ζ-proton coupling constants obtained from the 2-nonanone, 2-undecanone, and 2-dodecanone radicals will, therefore, be approximately the same as those of the three β-proton coupling constants obtained from the 3-tetradecanone and 3-undecanone radicals. Assuming this to be the case, ρC_1^{π} (ketone) $\simeq \rho C_2^{\pi}$ (ketone) $\times\, a_Z^{\zeta}$ (ketone)$/a_Z^{\beta}$ (ketone) $= \pm\, 0.07$. Or, from similar geometrical considerations of the previously investigated octyl propionate ester radical (for which $\rho = 0.90 \pm .04$), ρC_1^{π} (ketone) $\simeq \rho C_2^{\pi}$ (ester) $\times\, a_Z^{\zeta}$ (ketone)$/a_Z^{\beta}$ (ester) $\simeq \pm\, 0.07$. The agreement in these two values of ρC_1^{π} is encouraging. A detailed knowledge of the orientations of these radicals is not necessary because the anisotropy of a^{β} (and a^{ζ} in this approximation) is small. The sign of ρC_1^{π} relative to ρC_2^{π} cannot be determined from these experiments. The value of $\pm\, 0.07$ may be subject to revision when the effect of the

off-diagonal elements of the spin-density matrix are considered.

[16]A. Streitwieser, Jr., Molecular Orbital Theory for Organic Chemists (John Wiley & Sons, New York, 1961).

[17]A. D. McLachlan, Mol. Phys., 3, 233 (1960).

[18]G. Vincow and G. K. Fraenkel, J. Chem. Phys., 34, 1333 (1961). See also: P. H. Rieger and G. K. Fraenkel, ibid., 37, 2811 (1962); R. Dehl and G. K. Fraenkel, ibid., 39, 1793 (1963).

[19]This effect is easily seen by considering the two structures $\dot{C}-C=X$ and $C=C-\dot{X}$. These two structures contribute equally in the case of the allyl radical. For the ketone radical, however, the first structure contributes to a greater extent. This increases the electron density about the oxygen atom and increases the spin density on carbon atom 2.

[20]For this choice of parameters, the McLachlan C_2, C_1, and oxygen spin densities for the ketone are + 0.839, - 0.008, and + 0.170, respectively. The McLachlan spin densities are + 0.597, - 0.194, and + 0.597 for the three allyl carbon atoms, taken consecutively (see also Fig. 5).

III. ELECTRON SPIN RESONANCE AND ELECTRONIC STRUCTURE OF THE RĊHOR' ETHER RADICALS*

O. Hayes Griffith

Gates and Crellin Laboratories of Chemistry†
California Institute of Technology
Pasadena, California

Single crystals of inclusion compounds formed between urea and a series of aliphatic ethers were X-irradiated and studied by electron spin resonance. The stable, X-ray-produced free radicals were all of the general type RĊHOR'. The approximate value for the spin density on the carbon atom is 0.70 ± 0.08. The unpaired spin distribution is discussed in terms of the Hückel and approximate configuration interaction π-electron molecular orbital models and the valence-bond method. The theoretical spin distributions are found to be in qualitative agreement with the experimental spin distribution.

A. INTRODUCTION

In the preceding paper,[1] the radical $RH\dot{C}-\overset{O}{\overset{\|}{C}}R'$ was investigated by electron spin resonance (ESR). This ketone radical is of special

* Work supported in part by the National Science Foundation (Grant No. GP-930), and in part by a grant from the Shell Companies Foundation.

† Contribution No. 3179.

interest because it is one of the simplest hetero-atom radicals in which each atom contributes one electron to the π-system. Radicals in which one atom contributes two electrons to the π-system are also of interest and one of the simplest examples of this type of radical is RHC—OR'. Here the spin density is primarily localized on only two atoms: the oxygen atom and an adjacent carbon atom. In this paper a positive identification of the radical RĊHOR' is reported in a series of ether-urea inclusion compounds.[2] Approximate values of the carbon and oxygen spin densities are determined from the coupling constant data and the spin distribution is discussed in terms of the π-electron molecular orbital and valence bond methods.

B. EXPERIMENTAL

To prepare single crystals of each inclusion compound investigated, the ether was added slowly to a urea-saturated methanol solution until the inclusion compound began to precipitate out of solution. The precipitate was then redissolved by the addition of a slight excess of methanol and the solution was cooled slowly from 298°K to 273°K over a period of from 36 to 48 hours. The resulting crystals were long hexagonal needles. The z axis of each crystal is defined as lying along the needle axis and the plane perpendicular to the needle axis is referred to as the xy plane. Apparently no crystallographic data has been reported for these ether-urea crystals. The general hexagonal structure of urea inclusion compounds has, however, been shown to be independent of the exact nature of the linear host

molecule.[4] We may safely assume, therefore, that the ether-urea crystals have the tubular structure characteristic of organic urea inclusion compounds.[5]

The ether-urea inclusion compounds are relatively unstable, decomposing in 1-3 hours in air at room temperature. To avoid this problem the crystals were X-irradiated at liquid nitrogen temperatures and the majority of the ESR spectra were taken with the sample at ~ 273°K, rather than at room temperature. Below 273°K the crystals were stable for at least one or two days. A few crystals X-irradiated at 273°K had 273°K ESR spectra identical to those obtained from crystals X-irradiated at 77°K. It appears, therefore, that the 273°K ESR spectra are independent of the temperature at which the crystals were X-irradiated. The other experimental details, including the X-ray tube, X-band ESR spectrometer, and cooling apparatus were the same as employed in II.

C. RADICAL IDENTIFICATION

To obtain a positive identification of the X-ray produced free radicals it was necessary to investigate more than one aliphatic ether. The walls of the tubular cavities hinder intermolecular radical reactions but do not prevent intramolecular radical rearrangements and therefore there are several possible structures for the final radicals produced. Furthermore, the relative magnitudes of the ζ and γ proton coupling constants were not known.[6] However, it sufficed to investigate examples of two types of ether molecules;

RCH_2OCH_2R and RCH_2OCH_3. As examples of the first type, several of the symmetrical ethers were investigated briefly. Single crystals of the inclusion compounds formed between urea and dibutyl ether (di-n-butyl ether), di-n-pentyl ether, di-n-hexyl ether, di-n-octyl ether, or di-n-decyl ether were prepared and X-irradiated. The ESR spectra were qualitatively the same for all five systems. The spectra of dibutyl ether, however, was much more nearly symmetric (suggesting the presence of only one radical), therefore this compound was chosen for further study. The spectra obtained with the magnetic field along the needle axis and perpendicular to the needle axis of the dibutyl ether-urea crystal are given in Fig. 1.

The methyl octyl ether (methyl n-octyl ether) urea inclusion compound was chosen as an example of a long-chain methyl ether, RCH_2OCH_3. The spectra obtained from these crystals at $\sim 273°K$ are shown in Fig. 2. These spectra result from one anisotropic coupling constant, two equal and nearly isotropic coupling constants, and three small coupling constants. The small splittings are only resolved when the angle between the magnetic field vector and the z axis is less than $\sim 75°$. The dibutyl ether-urea spectra, on the other hand, result from one anisotropic proton coupling constant, two equal and nearly isotropic coupling constants, and two much smaller coupling constants. Again the two small coupling constants are not resolved when the magnetic field vector is within 15° of the xy plane. From the consideration of both sets of data it is easily seen that the radicals produced from dibutyl ether and methyl octyl ether are,

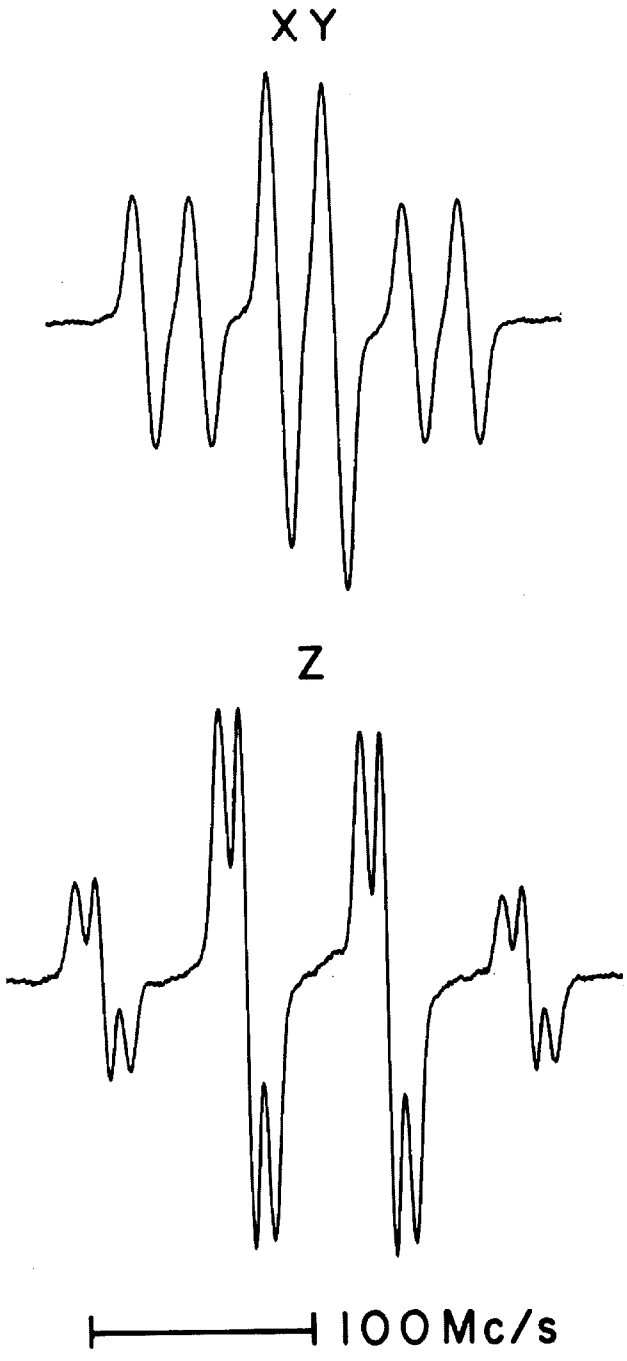

Figure 1

The 273°K ESR spectra of an X-irradiated dibutyl ether-urea crystal with the magnetic field in the xy plane and parallel to the z axis, respectively.

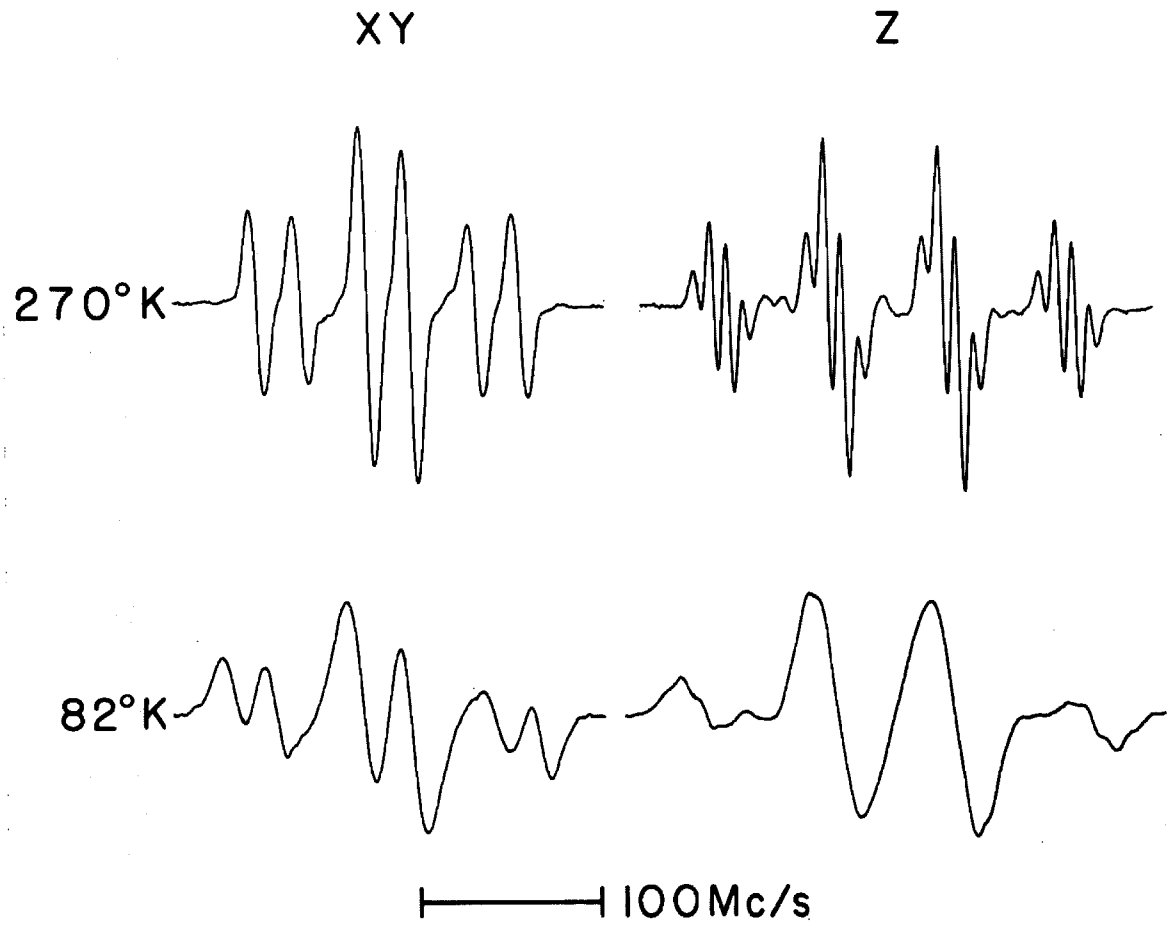

Figure 2

The ESR spectra of an X-irradiated methyl octyl ether-urea crystal.

respectively,

$$CH_3CH_2CH_2\dot{C}HOCH_2(CH_2)_2CH_3 \qquad (1)$$

and

$$CH_3(CH_2)_5CH_2\dot{C}HOCH_3 \qquad (2)$$

The anisotropic proton coupling constant and the large isotropic coupling constants are the familiar α and β proton coupling constants, a^{α} and a^{β}, respectively. The small splittings are caused by the ζ proton coupling constants, a^{ζ}, and splittings resulting from the γ protons are not observed.

In addition to the above inclusion compounds, one other compound, 1,4-diethoxybutane-urea, was investigated in order to obtain the value of a^{β} for a rotating methyl group. The radical of interest for this purpose is

$$CH_3CH_2OCH_2CH_2CH_2CH_2O\dot{C}HCH_3 \qquad (3)$$

The reconstructed stick spectra for this radical along with the observed ESR spectra are shown in Fig. 3. It is clear from Fig. 3 that radical (3) and at least one other radical are present in the X-irradiated 1,4-diethoxybutane-urea compound. From the magnitude of the splittings of the z orientation spectrum, the second radical is evidently

$$CH_3CH_2OCH_2CH_2CH_2\dot{C}HOCH_2CH_3 \qquad (4)$$

No further investigation of radical (4) was undertaken because, for our purposes, it is essentially equivalent to radical (2).

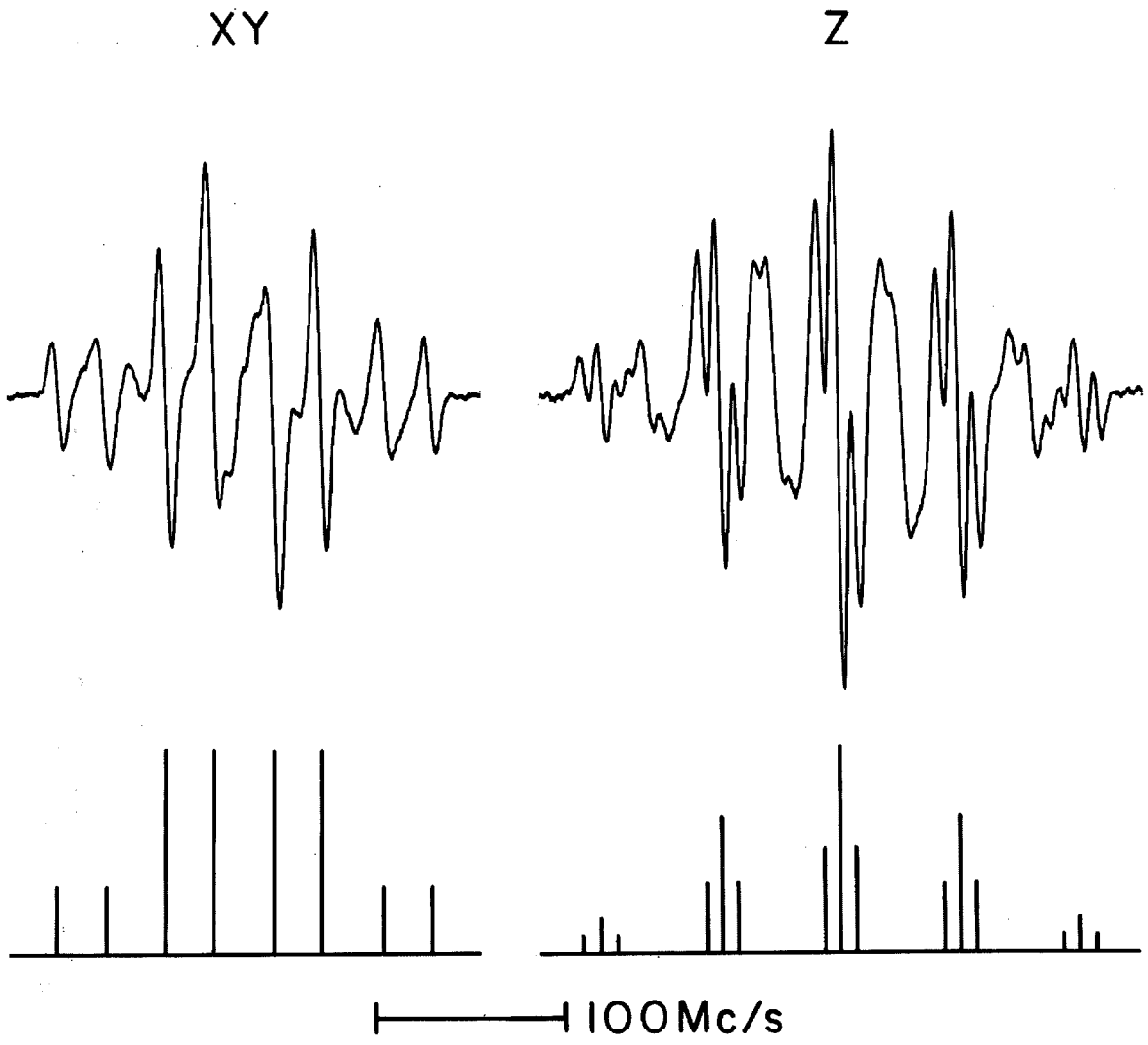

Figure 3

The 273°k ESR spectra of an X-irradiated 1,4-diethoxybutane-urea crystal with the magnetic field along the xy and z crystalline directions, respectively. Below the observed spectra are the reconstructed "stick" spectra for the xy and z orientations of the radical $CH_3CH_2O(CH_2)_4\dot{O}CHCH_3$.

The 273°K ESR spectra for all of the above ether radicals are isotropic with respect to rotations of the magnetic field in the xy plane and are anisotropic with respect to other rotations of the magnetic field (this is characteristic of included radicals). The g value is also very nearly isotropic. The g values measured with the magnetic field parallel and perpendicular to the z axis of radicals (1-3) are 2.0040 ± 0.0004 and 2.0030 ± 0.0003, respectively. All of the radicals observed were stable for several hours at 273°K. If the crystals were allowed to warm up to room temperature, however, the ESR signal disappeared in 15 to 30 minutes. The coupling constant data for radicals (1), (2), and (3) are summarized in Table I.

In addition to the ESR data obtained at 270°K, the methyl octyl ether-urea crystals were investigated over the temperature range from 290°K to 40°K. There were no changes in either the line widths or the splittings over the range 290°K to 240°K. Around 240°K the spectra began to show signs of broadening and the 82°K ESR lines are significantly broadened (Fig. 2). Below 80°K the spectral lines appeared to broaden slightly as the temperature was lowered, but the effect was not as pronounced. The overall width of the 40°K ESR spectra increased ~10% over the 270°K value; this is consistent with a decrease in the amplitude of motion about the C_2—C_1 bonds as the temperature was lowered from 240°K to 40°K. There were no rapid changes in the ESR spectra as the temperature was lowered (such as might be caused by a reorientation of the ether

TABLE I. Proton Hyperfine Coupling Constants.[a, b, c]

Ether	Radical	a_z^{α}	a_z^{β}	a_z^{ζ}	a_{xy}^{α}	a_{xy}^{β}
Dibutyl ether	$CH_3(CH_2)_3O\dot{C}H(CH_2)_2CH_3$	64	63	8.2	23.6	60.4
Methyl octyl ether	$CH_3(CH_2)_6\dot{C}HOCH_3$	63	63	8.5	24.3	60.4
1,4-diethoxy butane	$CH_3CH_2O(CH_2)_4O\dot{C}HCH_3$	63	62	8.5	24.3	56.6

[a] a^{α}, a^{β}, and a^{ζ} are the α, β, and ζ proton coupling constants, respectively, and xy and z denote the spectra recorded with the magnetic field in the crystalline xy and z directions. The two β protons of the dibutyl ether radical or the methyl octyl ether radical are magnetically equivalent and the three β protons of the 1,4-diethoxybutane radical are magnetically equivalent.

[b] The coupling constants reported here are the average values obtained from a minimum of three groups of four spectra, each group being obtained from a different crystal. All values are in units of megacycles per second. The limits of experimental error varied with the orientations of the crystal in the magnetic field and the accuracy was greatest in

the xy orientation (where the differences between the a^{α} and a^{β} are the largest). The estimated errors in a^{α}_{xy} and a^{β}_{xy} for the first two radicals are ± 1.5 Mc/sec. a^{α}_{xy} and a^{β}_{xy} of the 1,4-diethoxybutane radical are accurate to ± 2.0 Mc/sec and the a^{α}_{z} and a^{β}_{z} for all three radicals are accurate to within ± 2.5 Mc/sec. The accuracy of the small ζ proton coupling constants are estimated to be ± 0.8 Mc/sec.

[c] The temperature of the inclusion crystals was maintained at approximately 273°K, while obtaining the data reported in Table I. However, the spectra are relatively insensitive to changes in temperature and variations as great as ± 15°K produced no measurable change in the coupling constants.

radicals) and all temperature effects were reversible.

D. EXPERIMENTAL SPIN DENSITY DISTRIBUTION

a. From α Proton Coupling Constant Data

It is immediately apparent from Table I that the values of the α proton coupling constants for all three radicals are the same. Therefore, in addition to identifying the radicals produced, some general conclusions may be reached regarding the unpaired spin distribution of this class of aliphatic ether radicals. Equation (4) of II will be useful in obtaining the isotropic component, a_o^α, from the experimental values of a_{xy}^α and a_z^α. First, however, the effect of the dipolar interaction between the α proton and the spin density on the oxygen atom must be estimated. To accomplish this the unpaired spin density on carbon atom two, ρC^π , and the unpaired spin density on the oxygen atom, ρO^π , are assumed to be associated with the 2p orbitals of the carbon and oxygen atoms, respectively. The α proton is sp^2 hybridized and the oxygen atom, carbon atoms one and two, and the α proton are coplanar. All of the dipolar matrix elements obtained using the above assumptions may be evaluated according to the method of McConnell and Strathdee.[7] In the present work, only the α proton-ρO^π interaction was estimated by this method and the α proton-ρC^π dipolar tensor elements were taken from the experimental data on the malonic acid radical ($\rho C^\pi \simeq 0.90$) obtained at zero magnetic field.[8]

For the numerical calculations the $\dot{C}$—H and the $\dot{C}$—O bond

distances were assumed to be 1.08 Å and 1.35 Å, respectively. The oxygen 2p orbital was approximated by a Slater orbital with z = 4.55 and the nondiagonal elements of the spin density matrix were neglected (so that $\rho O^{\pi} + \rho C^{\pi} = 1.0$).[9] Using these approximations the α proton $-\rho O^{\pi}$ dipolar tensor elements were calculated, the tensor was transformed to the usual α proton-ρC^{π} coordinate system, and the total contributions to a^{α} were calculated by standard methods.[12] The value of a_z^{α} and a_{xy}^{α} were obtained by assuming motional averaging in the xy plane and integrating over the angular variables in the general expression for a^{α}. The resulting equations are not given here because they are space-consuming and will not be useful in later discussions. Values of ρC^{π} ranging from 0.5 to 0.9 were substituted into these equations and in each case the estimate of a_o^{α} obtained using Eq. (4) of II and the computed a_{xy}^{α} and a_z^{α} was compared with a_o^{α} obtained directly from the initial ρC^{π}. The net result is that the difference between the value of a_o^{α} obtained from Eq. (4) of II and the correct value of a_o^{α} is quite small for the large ρC^{π} encountered in the ether radicals. For example, from the data obtained from radicals (1-3) and using Eq. (4) of II, $a_o = 37.2$ Mc/sec. If the proportionality constant relating a_o^{α} and ρC^{π} is assumed to be the same for the ether radicals and the ethyl radical (CH_3CH_2, $\rho C^{\pi} \simeq 1.0$, $a_o^{\alpha} = 62.7$ Mc/sec)[13], then ρC^{π} (ether) = $37.2/62.7 \simeq 0.60$. The correction for the α proton-ρO^{π} dipolar interaction lowers this value negligibly, 0.7%. Therefore, the value predicted for ρC^{π} from the above simple model is ~ 0.60.

b. From β Proton Coupling Constant Data

The isotropic component of the β proton coupling constant estimated from Eq. (II-8) and the data of the 1,4-diethoxybutane radical (3) is 58.4 Mc/sec. The value of R/2 for the ethyl radical is 75.4 Mc/sec and if radical (3) is assumed to have this same R/2, then ρC^{π} (ether) = 58.4/75.4 = 0.77. This value of ρC^{π} is in qualitative agreement with the value obtained from the α proton data. Quantitatively, however, one might hope for better agreement. In this connection, it is of interest to compare these results with the α and β proton coupling constant data for the chemically generated ethanol radical, $CH_3\dot{C}HOH$, recently reported by Dixon and Norman.[3] The solution ESR spectra for this radical directly yield a_o^{α} = 42.1 Mc/sec and a_o^{β} = 61.8 Mc/sec. If the coupling constant data of the ethyl radical are again used to determine the proportionality constants, the values of ρC^{π} obtained from a_o^{α} and from a_o^{β} are 0.67 and 0.81, respectively. These values are in good agreement with the corresponding ether radical values of 0.61 and 0.77. The discrepancy between the values obtained from the α and β proton coupling constant data is apparently caused by a poor choice of the proportionality constants. In other words, the differences in the σ bonds of the two radicals apparently is reflected in the values of the proportionality constants. However, we will tentatively assign the approximate values of 0.70 ± 0.08 and 0.30 ± 0.08 for the experimental spin densities on the ether carbon and oxygen atoms,

respectively. These values and the estimated errors may be subject to change as better values of the proportionality constants become available.[14]

To what extent this spin distribution is effected by molecular motion is difficult to determine quantitatively because of the broadened lines of the low-temperature spectra (Fig. 2). It is clear that there are no major changes in the width of the spectra over a wide temperature range. As the temperature is lowered the small changes that do occur are in a direction consistent with a decrease in β proton motion and inconsistent with an increase in the contribution of the structure $RH\ddot{C}—\dot{O}R'$ (see valence-bond section). That is, the small temperature dependence of the splittings is readily explained in terms of the β proton motion, but is much more difficult to explain in terms of a temperature-dependent spin distribution. This does not provide a complete answer to the question of motion about the $\dot{C}$—O bond, but does strongly suggest that the spin distribution measured is a meaningful approximation to the maximum π-overlap spin distribution.

E. THEORETICAL SPIN DENSITY DISTRIBUTION

a. Hückel MO Method

In view of the experimental results, the natural starting point for a discussion of the $R\dot{C}HOR'$ radical is the π-electron approximation. The two π-molecular orbitals are approximated as linear combinations of the $2p_x$ atomic orbitals of carbon atom 2 (χ_c) and the oxygen atom (χ_o). The three σ MOs of carbon atom 2 are taken

to be sp^2 hybrids and the oxygen atom is assumed to be unhybridized.[15] Therefore, of the eight oxygen electrons, four are associated with the oxygen 1s and 2s AOs, one with a $2P_y$ σ MO, another with a $2P_z$ σ MO, and the remaining two with the π-electron system. The σ (or σ and n) electrons will not be considered explicitly. With these assumptions the ether radical becomes a three-electron problem. In this respect the ether radical is formally similar (except for symmetry) to the ethylene negative ion. The ether radical will first be considered in the framework of the Hückel MO approximation and then as a configuration interaction (CI) problem. Finally the CI results are interpreted in terms of the valence bond formalism in order to obtain a better physical description of the unpaired spin distribution.

The single configuration wave function appropriate for the ether radical in the Hückel approximation is

$$\psi = (6)^{-\frac{1}{2}} (-1)^{P} P \phi_1 \alpha \phi_1 \beta \phi_2 \alpha \tag{5}$$

where

$$\phi_i = C_{i1}\chi_C + C_{i2}\chi_O \tag{6}$$

and P is the π-electron permutation operator. The C_{ij}s are determined by the variational method using a one-electron Hamiltonian and the usual Hückel approximations[18] for the matrix elements of the 2×2 secular determinant. The spin densities are the squares of the AO coefficients of ϕ_2 and are a function of the two parameters

h and k. A partial contour plot of ρC^{π} is given in Fig. 4 (and ρO^{π} is just $1 - \rho C^{\pi}$). The Hückel spin densities are in qualitative agreement with the experimental spin densities. That is, the range of generally accepted values of h and k ($1 \leq h \leq 2$ and $0.8 \leq k \leq 1.6$)[18] predict a large spin density on the carbon atom and a much smaller spin density on the oxygen atom. It is obvious from Fig. 4 that the problem is overdetermined. A given spin density may be obtained using any value of h provided the proper k is chosen. In other words the spin density is determined only by the ratio h/k and not by the individual h and k values. The ratio of h to k corresponding to $\rho C^{\pi} = 0.70 \pm 0.08$ is 0.9 ± 0.4 and this overlaps well with the generally accepted range, $0.6 \leq h/k \leq 2.5$.

The ether charge densities may also be obtained from Fig. (4). In the Hückel theory the carbon atom charge density of the ether radical is $\rho C^{\pi} - 1$ and the oxygen charge density is equal to the oxygen spin density (ρC^{π} and ρO^{π} are chosen to be positive). If the ratio h/k is positive then $-0.5 < (\rho C^{\pi} - 1) < 0.0$ and $0.0 < \rho O^{\pi} < +0.5$ (Fig. 4). For $\rho C^{\pi} = 0.70 \pm 0.08$, the π-electron carbon and oxygen charge densities are -0.30 ± 0.08 and $+0.03 \pm 0.08$, respectively. This rather large polarization of the π-electron distribution corresponds to a π-electron dipole moment of 1.9 ± 0.5 D.

b. Configuration Interaction

The ether radical represents one of the simplest possible

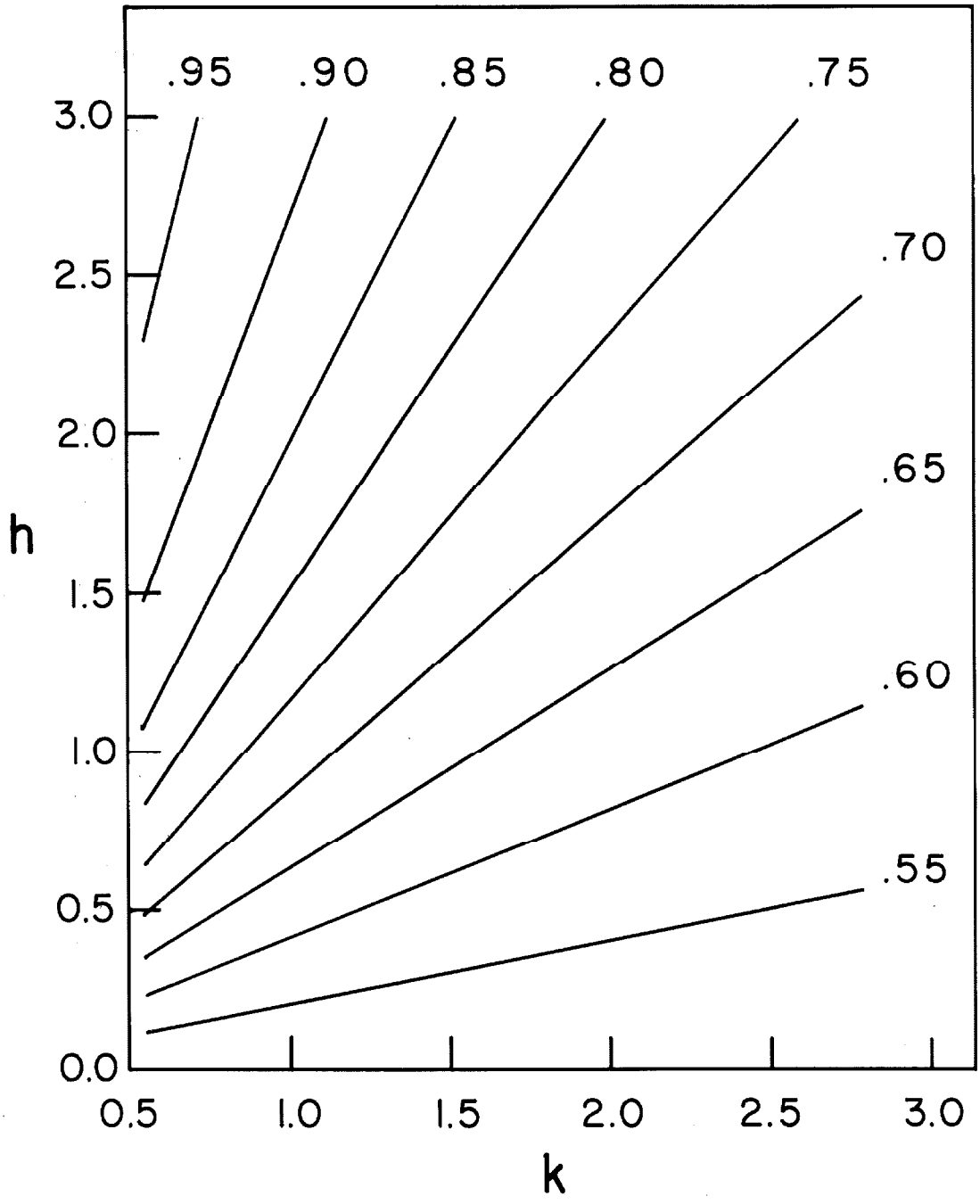

Figure 4

The electron spin density on carbon atom 2 as a function of the two Hückel molecular orbital parameters, h and k.

heteronuclear configuration interaction (CI) problems since there are only two π-electron configurations. The two configuration wave functions and the two configurations are

$$\psi_1 = (6)^{-\frac{1}{2}}(-1)^P P\,\phi_1\alpha\phi_1\beta\,\phi_2\alpha \qquad \phi_2 \;\underline{\uparrow} \qquad (7)$$

$$\phi_1 \;\underline{\uparrow\downarrow}$$

and

$$\psi_2 = (6)^{-\frac{1}{2}}(-1)^P P\,\phi_1\alpha\phi_2\alpha\phi_2\beta \qquad \phi_2 \;\underline{\uparrow\downarrow} \qquad (8)$$

$$\phi_1 \;\underline{\uparrow}$$

ψ_1 is similar to Eq. (5) except that in the CI case the wave functions ϕ_1 and ϕ_2 are taken to have the full ethylenic symmetry.[19] That is

$$\phi_1 = (2)^{-\frac{1}{2}}(1+S)^{-\frac{1}{2}}(\chi_C + \chi_O) \qquad (9)$$

and

$$\phi_2 = (2)^{-\frac{1}{2}}(1-S)^{-\frac{1}{2}}(\chi_C - \chi_O) \qquad (10)$$

where S is the atomic orbital overlap integral. The functions ψ_1 and ψ_2 are normalized and are rigorously orthogonal. The CI wave function, Ψ_{MO}, and Hamiltonian, $\mathcal{H}_\pi$, in this approximation are

$$\Psi_{MO} = C_1\psi_1 + C_2\psi_2 \qquad (11)$$

and

$$\mathcal{H}_\pi = \mathcal{H}_{core(1)} + \mathcal{H}_{core(2)} + \mathcal{H}_{core(3)} + 1/r_{12} + 1/r_{13} + 1/r_{23} \qquad (12)$$

Using McConnell's definition of the spin-density operator,[20] the elements of the atomic orbital spin-density matrix may be determined from Ψ. In terms of C_1 and C_2 these elements are

$$\rho C^{\pi} = \tfrac{1}{2} C_2^2 (1+S)^{-1} + \tfrac{1}{2} C_1^2 (1-S)^{-1} + C_1 C_2 (1-S^2)^{-\frac{1}{2}} \quad (13)$$

$$\rho O^{\pi} = \tfrac{1}{2} C_2^2 (1+S)^{-1} + \tfrac{1}{2} C_1^2 (1-S)^{-1} - C_1 C_2 (1-S^2)^{-\frac{1}{2}} \quad (14)$$

$$\rho CO^{\pi} = \rho OC^{\pi} = \tfrac{1}{2} C_2^2 (1+S)^{-1} - \tfrac{1}{2} C_1^2 (1-S)^{-1} \quad (15)$$

and the spin density function $\rho^{\pi}(x, y, z)$ is

$$\rho^{\pi}(x, y, z) = \rho C^{\pi} |\chi_C|^2 + \rho CO^{\pi} (\chi_C^* \chi_O + \chi_O^* \chi_C) + \rho O^{\pi} |\chi_O|^2 \quad (16)$$

The coefficients C_1 and C_2 are determined by the usual variational procedure. The matrix elements of the resulting 2×2 secular determinant may be expanded in terms of the AOs in much the same way as for ethylene.[19] The estimation of the core integrals of the ether radical deserves some elaboration. The core Hamiltonian is

$$\mathcal{H}_{core(i)} = -\tfrac{1}{2} \nabla^2_{(i)} + U^{+}_{C_2(i)} + U^{++}_{O(i)} + U^{O}_{C_1(i)} + U^{O}_{C_3(i)} + U^{O}_{H\alpha(i)} \quad (17)$$

where U^{+} (or U^{++}) and U^{O} denote the potentials due to charged and neutral atoms of the core. The approximate eigenvalue equation[21]

$$[-\tfrac{1}{2} \nabla^2_{(i)} + U^{+}_{O(i)}] \chi_{O(i)} = U_{OO} \chi_{O(i)} \quad (18)$$

can be used to eliminate the kinetic energy integral providing one assumes that[22]

$$U^{++}_{o(i)} = U^{+}_{o(i)} - \int \chi^2_{o(j)} 1/r_{ij}\, dv_j \qquad (19)$$

In Eq. (18) U_{oo} is the usual valence state orbital energy. There is, of course, a similar eigenvalue equation involving χ_c and U_{cc}. In other aspects, the treatment of the ether core parallels that of the ethylene molecule. The expressions obtained for the oxygen core integral α_o^{core} and the carbon core integral α_c^{core} are

$$\alpha_o^{core} = U_{oo} - (CC|OO) - (OO|OO) - (C_2{:}OO) - (C_3{:}OO) \qquad (20)$$

$$\alpha_c^{core} = U_{cc} - 2(CC|OO) - (O{:}C_2C_2) - (C_1{:}C_2C_2) - (H_\alpha{:}C_2C_2) \qquad (21)$$

and the parameter, β, introduced by Pariser and Parr[23] is

$$\beta \equiv \frac{\beta^{core} - (S/2)(\alpha_c^{core} + \alpha_o^{core})}{(1 - S^2)} \qquad (22)$$

Fortunately the spin-density distribution depends only on the difference between α_o^{core} and α_c^{core} and not on the individual core integrals. This tends to reduce the errors involved in the values of U_{oo} and U_{cc} and renders the method of evaluating the coulomb and neutral penetration integrals less critical. Initially, we will take the orbital energies to be the negative of the valence state ionization potentials; $U_{oo} = -I_o = -17.3$ ev and $U_{cc} = -I_c = -11.4$ ev.[16,24] The coulomb integrals obtained by the method of Pariser and Parr with $Z_c = 3.25$, $Z_o = 4.55$, and $R_{co} = 1.35$ Å, are $(CC|CC) = 10.8$ ev, $(OO|OO) = 14.7$ ev, and $(CC|OO) = 8.2$ ev.[16] The neutral penetration integrals $(p{:}qq)$ were calculated by standard

methods[21, 25] using Slater orbitals. The contributions of these penetration integrals to α_O^{core} and α_C^{core} were found to be the same within ~0.3 ev,[26] and therefore they were not included in the spin-density calculations. If differential overlap is neglected, these are all of the quantities (other than β) entering into the expressions for the spin-density matrix elements. The appropriate value of β for this radical is not available, but the values -1.5, -2.5, and -3.5 ev span what might be considered a reasonable range. From Eqs. (13), (14), and (15), (ρC^{π}, ρCO^{π}, ρO^{π}) are (0.97, 0.16, 0.03), (0.93, 0.25, 0.07), and (0.89, 0.32, 0.11) for β = -1.5, -2.5, and -3.5 ev, respectively.

The calculated values for ρC^{π} are somewhat larger than the experimental value. This is due, in part, to the neglect of the effect of bonding on U_{OO} and U_{CC}. For example, in benzene and other hydrocarbons Hush and Pople[27] found that the value of U_{CC} is ~-9.5 ev, which is significantly less negative than the valence state value, -11.4 ev. The effect of bonding of the hydrocarbon σ electrons is apparently to decrease the stability of the π electrons.[16] For the ether radical the large dipole moments present an added complication. The π-electron dipole moment is apparently ~1.9 ± 0.5 D and is in the direction $C^{-}—O^{+}$. There is also present a large σ-electron moment. In ether molecules this moment is 1-2 D[28, 29] and is almost certainly in the direction $C^{+}—O^{-}$. The π and σ dipole moments therefore have opposite polarity. The π-electron moment of the ether radical increases the electronegativity

of the oxygen atom and this should increase the σ-dipole moment over the value obtained for the ether molecule. The sum of the σ and π contributions may therefore be a moment in the direction $C^{+}\!-\!O^{-}$, and this would increase the stability of the electrons on carbon while decreasing the stability of the electrons on oxygen (through changes in electron repulsion). If this is the case, the net effect is a suppression of the quantity $U_{OO} - U_{CC}$ below the valence state value of -5.9 ev. An arbitrary, but not unreasonable, choice of $U_{OO} - U_{CC}$ is -2.5 ev. For this choice (ρC^{π}, ρCO^{π}, ρO^{π}) become (0.93, 0.25, 0.07), (0.86, 0.34, 0.14), and (0.79, 0.40, 0.21) for β = -1.5, -2.5, and -3.5 ev, respectively. These spin densities are in much better agreement with the experimental values. (The agreement could be further improved if the differences between the coulomb integrals were also suppressed.)

The approximations employed to obtain these spin distributions are obviously not free from criticism. Nevertheless, the simplified CI theory does predict the correct order of magnitude for the unpaired spin densities (for either choice of $U_{OO} - U_{CC}$). Furthermore, if overlap is retained and the Mulliken approximation,[19] $pq = \frac{1}{2}S(pp + qq)$, is employed then the calculated spin densities are not significantly altered from the above values. No major change occurs because the overlap integral is small (S = 0.165) and because all terms appearing in C_1 and C_2 which depend linearly on S, vanish.

c. Valence Bond Model

The two valence-bond or spin-state wave functions and corresponding structures are

$$\psi_{NE} = 6^{-\frac{1}{2}}(1-S^2)^{-\frac{1}{2}}(-1)^P P\chi_c\alpha\chi_o\alpha\chi_o\beta \qquad RH\dot{C}—\underline{\ddot{O}}R' \qquad (23)$$

$$\psi_{CH} = 6^{-\frac{1}{2}}(1-S^2)^{-\frac{1}{2}}(-1)^P P\chi_c\alpha\chi_c\beta\chi_o\alpha \qquad RH\overset{\ominus}{\ddot{C}}—\underline{\overset{\oplus}{O}}R' \qquad (24)$$

where ψ_{NE} and ψ_{CH} designate the functions corresponding to the neutral structure and the structure with charge separation, respectively. The appropriate linear combination of these two functions, Ψ_{VB}, would normally be obtained from the Hamiltonian, $\mathcal{H}_\pi$, by the variational method. However, in this case Ψ_{VB} is entirely equivalent to Ψ_{MO}. By expanding ψ_1 and ψ_2 in terms of ψ_{NE} and ψ_{CH}, Ψ_{MO} becomes

$$\Psi_{MO} = \left[\frac{C_1}{\sqrt{2(1+S)}} + \frac{C_2}{\sqrt{2(1-S)}}\right]\psi_{NE} + \left[\frac{C_2}{\sqrt{2(1-S)}} - \frac{C_1}{\sqrt{2(1+S)}}\right]\psi_{CH} \qquad (25)$$

If overlap is neglected, ρC^π is just the square of the coefficient of ψ_{NE} and this is identical to Eq. (13). In other words ρC^π is a measure of the contribution of the valence bond structure $RH\dot{C}—\ddot{O}R'$ to the total wave function. The CI theory predicts the contribution of this structure to be 95-80%, which compares favorably with the experimental value of $70 \pm 8\%$. Similarly, the π-electron charge is directly related to the contribution of the structure $RH\ddot{C}—\dot{O}R'$. By comparing Eq. (25) with Eqs. (13) and (14) the charge densities associated with oxygen and carbon are $|\rho O^\pi|$ and $1-|\rho C^\pi|$,

respectively (which are of the same form as the Hückel MO results). The CI (or VB) theory predicts a π-electron polarization of $C^{\delta-}—O^{\delta+}$ where $.05 < \delta < 0.2$. The valence-bond method is perhaps the easiest to visualize; one readily predicts that the neutral structure (23) contributes to a larger extent than does the polar structure (24). However, the simple Hückel, CI, and VB predictions are all in agreement with the experimental results.

F. ACKNOWLEDGEMENTS

It is a pleasure to acknowledge several helpful discussions with Professor Harden M. McConnell, Dr. Russell M. Pitzer, and Martin S. Itzkowitz. We are especially indebted to Professor McConnell for the use of his magnetic resonance instruments and to Dr. Marjorie C. Caserio for a generous sample of methyl octyl ether.

G. REFERENCES

[1]O. H. Griffith, to be published (referred to as II).

[2]We are unaware of any previous investigation of this aliphatic ether radical. However, an ESR investigation of the alcohol radical reported by Dixon and Norman[3] is closely related to this work and we will have occasion to compare the results obtained for the two systems.

[3]W. T. Dixon and R. O. C. Norman, J. Chem. Soc. 1963, 3119.

[4]W. Schlenk, Jr., Ann. 565, 204 (1949).

[5]A. E. Smith, Acta Cryst. 5, 224 (1952).

[6]The convention for the labeling of protons ($\alpha, \beta, \gamma, \zeta$) and carbon atoms ($C_1, C_2, C_3$) used here is

$$\overset{\gamma}{\text{R}}\text{—}\overset{\beta}{\text{CH}_2}\text{—}\overset{\alpha}{\text{CH}_2}\text{—}\overset{\cdot}{\text{CH}}\text{—O—}\overset{\zeta}{\text{CH}_2}\text{—R'}$$

$$C_1 \quad C_2 \quad C_3$$

[7]H. M. McConnell and J. Strathdee, Mol. Phys. 2, 129 (1959).

[8]T. Cole, T. Kushida, and H. C. Heller, J. Chem. Phys. 38, 2915 (1963).

[9]The actual $\dot{C}$—O bond length of the ether radical is not known. The distance 1.35 Å represents a bond with two-thirds single and one-third double bond character. (This, for example, is a reasonable length for a three-electron bond[10] between a carbon and an oxygen atom.) The double and single bond lengths were obtained using the formula of Schomaker and Stevenson.[10] The effective nuclear

charge of oxygen and of carbon were obtained from Slater's rules.[11] These values of Z_O, Z_C, and the internuclear distance, R_{CO}, were employed in all calculations of this paper.

[10]L. Pauling, The Nature of the Chemical Bond (Cornell University Press, New York, 1960).

[11]C. A. Coulson, Valence (Clarendon Press, Oxford, 1952) p. 41.

[12]H. M. McConnell, C. Heller, T. Cole, and R. W. Fessenden, J. Am. Chem. Soc. 82, 766 (1960).

[13]R. W. Fessenden and R. H. Schuler, J. Chem. Phys. 39, 2147 (1963).

[14]Preliminary data from X-irradiated sulfide-urea inclusion compounds suggest that a similar problem may exist for the RHĊSR' radicals.

[15]These assumptions do not enter into the Hückel calculation explicitly but they do, of course, affect the magnitudes of the core integrals in the configuration interaction calculation. The oxygen atom is undoubtedly hybridized to some extent and Sidman[16] has discussed this question for the case of formaldehyde. However, the ionization potential, coulomb integrals, and neutral penetration integral apparently do not depend critically on the degree of core hybridization.[16,17] Hybridization of the carbon atom may be more troublesome. In the contributing structure RHC̈—ȮR' (see valence-bond section), there is an unshared electron pair on the carbon atom and this is reminiscent of the nonplanar ammonia molecule. If the

carbon atom has a tendency to hybridize in a similar fashion, then the a^{α}_{xy}, a^{α}_{z} and a^{β} coupling constants might well appear anomalous. Nevertheless, a large nonplanarity of the carbon core would greatly increase the magnitude of the proton coupling constants and this is not observed.

[16]J. W. Sidman, J. Chem. Phys. 27, 429 (1957).

[17]R. D. Brown and M. L. Heffernan, Trans. Faraday Soc. 54, 757 (1958).

[18]A. Streitwieser, Jr., Molecular Orbital Theory for Organic Chemists (John Wiley & Sons, Inc., New York, 1961).

[19]R. G. Parr, Quantum Theory of Molecular Electronic Structure (W. A. Benjamin, New York, 1963).

[20]H. M. McConnell, J. Chem. Phys. 28, 1188 (1958).

[21]M. Goeppert-Mayer and A. L. Sklar, J. Chem. Phys. 6, 645 (1938).

[22]Alternatively, one may consider an eigenvalue equation involving the second ionization potential of oxygen. The spin density distribution obtained by the two approaches is essentially the same if the appropriate valence-state ionization potentials are employed.

[23]R. Pariser and R. G. Parr, J. Chem. Phys. 21, 466 (1953); 21, 767 (1963).

[24]J. Parks and R. G. Parr, J. Chem. Phys. 32, 1657 (1960).

[25]K. Ruedenberg, J. Chem. Phys. 34, 1861 (1961).

[26]To obtain the penetration integrals the $\dot{C}$—H_{α} was taken to be 1.08 Å. The C_1—C_2 and C_3—O bonds were assumed to have

normal single bond lengths; 1.54 Å and 1.42 Å, respectively. Equally complete cancellation of the penetration integrals occurs if a Slater Z value of 4.90 is used.

[27]N. S. Hush and J. A. Pople, Trans. Faraday Soc. 51, 600 (1955).

[28]C. P. Smyth, Dielectric Behavior and Structure (McGraw-Hill, New York, 1955).

[29]L. G. Wesson, Tables of Electric Dipole Moments (The Technology Press, Cambridge, Mass., 1948).

IV. AN ELECTRON SPIN RESONANCE STUDY OF X-IRRADIATED FUMARIC ACID-UREA CRYSTALS[1a, b]

By O. Hayes Griffith,[1c] and Alvin L. Kwiram

Gates and Crellin Laboratories of Chemistry
California Institute of Technology
Pasadena, California

Single crystals of the monoclinic fumaric acid-urea crystals were X-irradiated at room temperature and investigated by electron spin resonance. The urea molecules of this previously unreported crystal minimize polymerization of fumaric acid and permit an investigation of X-ray-produced monomer radicals. The dominant radical observed is the well-known $HO_2CCH_2\dot{C}HCO_2H$ radical. The α-proton tensor is obtained and the major orientations of this radical are related to the crystal morphology. Single crystals of succinic acid-urea

were also briefly investigated and the orientations of the X-ray produced carboxylic acid radicals ($R\dot{C}HCO_2H$) in all three "molecular compounds" were the same with respect to the three very similar crystal morphologies. The degree of radical motion in the fumaric acid-urea, succinic acid-urea, and adipic acid-urea crystals is much less than that of similar radicals in the hexagonal urea inclusion compounds.

A. INTRODUCTION

The electron spin resonance (ESR) study of X- or γ-irradiated saturated crystalline dicarboxylic acids has provided useful information regarding the electronic structure, magnetic properties, and orientations of free radicals of the type $R\dot{C}HCO_2H$[2], and it is of interest to investigate X- or γ-ray damage in the unsaturated dicarboxylic acid, fumaric acid. However, γ-rays have been shown to polymerize acrylamide, methacrylamide, vinyl stearate, acrylic acid, methacrylic acid, and related compounds in the solid state[3, 4]. More recently several derivatives of maleic and fumaric acid have been found to dimerize in the solid state under the action of u.v. light[5]. For example, fumaronitrile and dimethyl fumarate photodimerize to yield tetracyanocyclobutane[6] and tetracarbomethoxycyclobutane[7], respectively. It is therefore reasonable to expect that γ-irradiation of fumaric acid might cause

polymerization in the solid state. Cook, Rowlands, and Whiffen[8] have shown that polymerization does occur in γ-irradiated fumaric acid by observing that the dominant radical present after irradiation is of the form $HO_2CCH(R)\dot{C}HCO_2H$. In addition, some of the minor lines of the spectra were tentatively assigned to the radical $HO_2CCH_2\dot{C}HCO_2H$[9]. Simultaneously with this work, single crystals of fumaric acid-urea were prepared and studied by ESR in this laboratory[10]. These mixed crystals, although apparently not previously reported, were expected to be stable by analogy with the crystals formed between saturated dicarboxylic acids and urea reported by Schlenk[11]. These mixed crystals effectively "dilute" the fumaric acid and suppress polymerization, thereby making feasible a study of the X-ray-produced monomer radicals. The identification and orientations of the major free radical ($HCO_2CH_2\dot{C}HCO_2H$) observed in the fumaric acid-urea crystals is discussed below and the orientations of this radical are compared to those of the free radicals in other dicarboxylic acid-urea crystals.

B. EXPERIMENTAL

The crystals of fumaric acid-urea were grown from a methanol solution containing mole ratios of fumaric acid-urea of from 1:3 to 1:10. The habit of the fumaric acid-urea crystals obtained from the methanol solution by slow evaporation is illustrated in Fig. 1, and the exterior angles are given in Table I. Defining the crystal faces as shown in Fig. 1, the crystals grew with face h in contact with the crystallizing dish. By titration with potassium permanganate the mole ratio of fumaric acid to urea in the crystal was

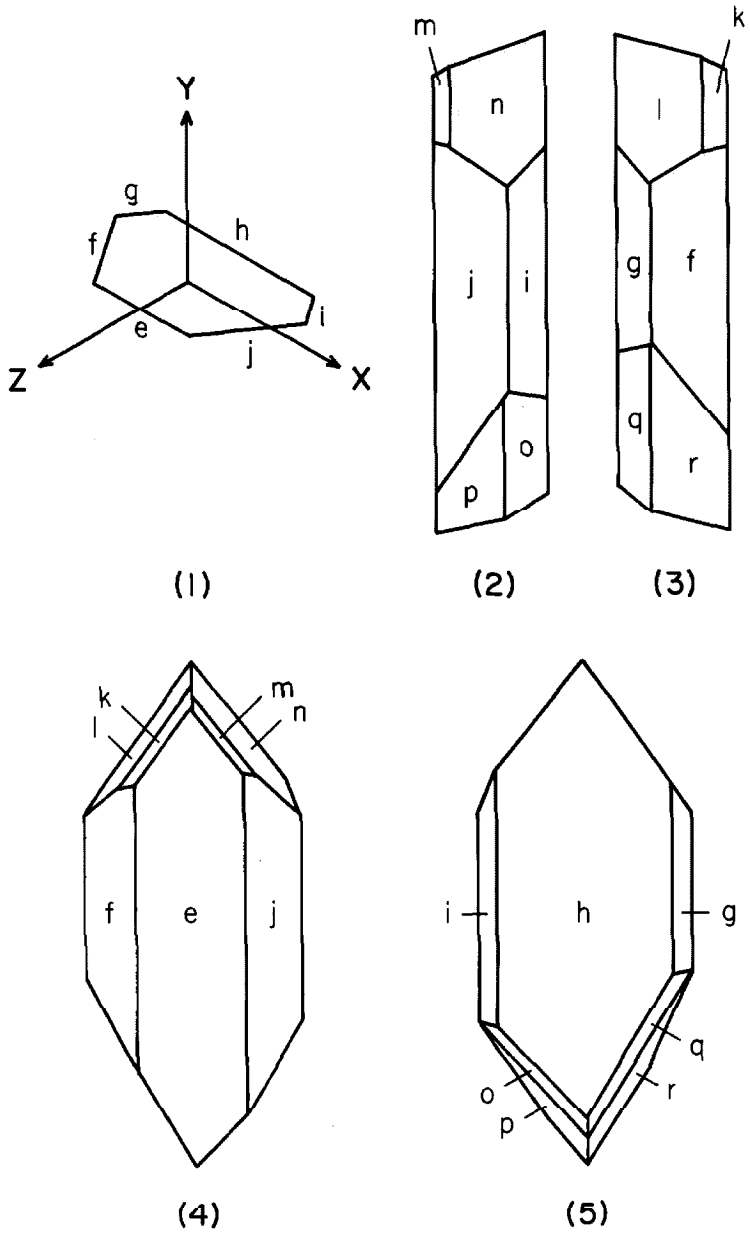

Figure 1

One typical habit of the fumaric acid-urea crystal (1). The definition of the axis system with respect to the crystal morphology. (2)-(5) The views of the crystal along the x, -x, z, and -z directions, respectively.

TABLE I

INTERFACIAL ANGLES OF THE FUMARIC ACID-UREA CRYSTALS

Angle[a]	Intersecting Faces[b]
13° 40'	l:k, n:m, p:o, r:q
32° 55'	f:k, m:j, i:o, q:g
40° 25'	l:f, j:n
56° 25'	g:h, h:i, j:e, e:f, g:l, n:i, r:f, j:p
65° 20'	k:e, m:e, o:h, q:h
67° 25'	f:g, i:j
100° 55'	h:n, h:l, e:p, e:r
107° 15'	l:n, k:m, o:q, p:r

[a] The exterior angles (± 15') formed by the lines normal to the two intersecting faces.

[b] The faces are those of the habit illustrated in Fig. 1.

found to be 1.0:2.0 ± .2. Furmaric acid-urea crystals were also grown from water, and were obtained as needles elongated along the y axis. The ESR spectra obtained from crystals grown in different solvents or with varying ratios of fumaric acid to urea in solution, were essentially equivalent. Crystals of the other dicarboxylic acids investigated were grown from methanol by slow evaporation.

A Varian X-band spectrometer was used to obtain the ESR data and the crystals were mounted in the microwave cavity by means of optical goniometer techniques. By this means, the orientations of the crystalline axes with respect to the magnetic field were known to within ± 30'. The room-temperature ESR spectra of the fumaric acid-urea crystals were complicated by the presence of more than one type of free radical, and several features of the spectra changed with time (due to the changing concentrations of the free radicals present[12]). Heating to 50°-70°C simplified the ESR spectra (Fig. 2), and we will consider here only the ESR spectra of the crystals which were heat-treated prior to obtaining the ESR spectra. Prolonged heat-treatment only diminished the ESR signal intensity and did not change the splittings or relative intensities of the major lines of the spectra.

C. RESULTS

The ESR spectra obtained with the magnetic field along the x, y, and z crystalline directions are given in Fig. 2. The g-value

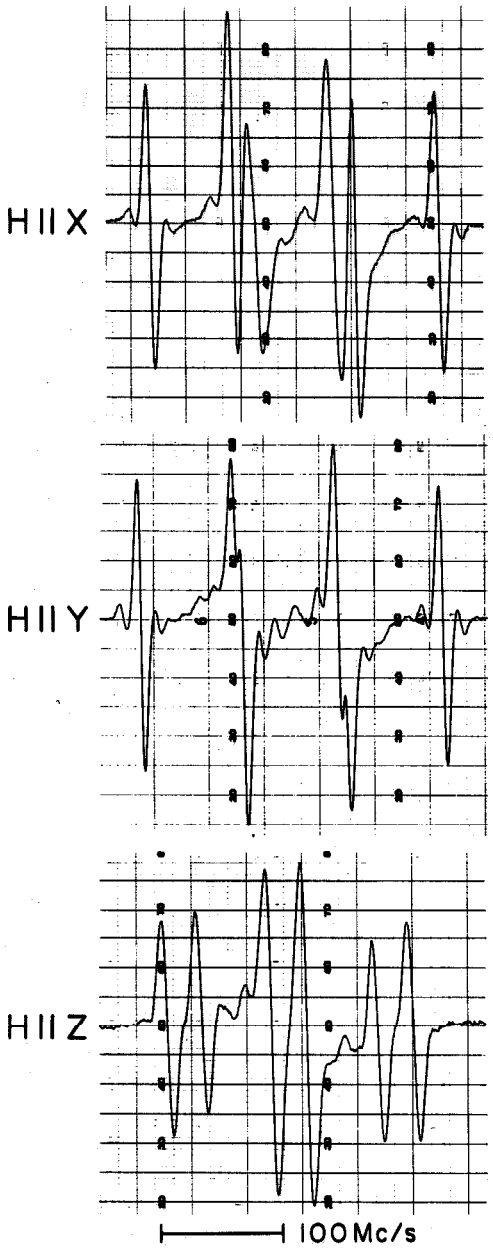

Figure 2
The ESR spectra of an X-irradiated fumaric acid-urea crystal with the magnetic field parallel to the x, y, and z crystalline axes, respectively. The crystal was heated (50° to 70°C) for one hour prior to recording these spectra. Continued heating decreased the intensity but left the major features of the spectra unchanged.

of the ESR spectra was nearly isotropic, and the maximum range for the xy, yz, and xz planes was from 2.0027 to 2.0046 ± .0003. The spectra of Fig. 2, and all other ESR spectra obtained from the (heat-treated) crystals are attributed to the radical

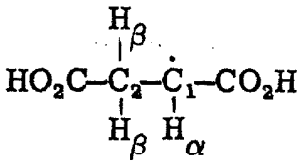

This radical has previously been produced by the removal of one α-proton from succinic acid[15,16] and from dl-aspartic acid[17] (by X- or γ-irradiation). However, in X-irradiated fumaric acid-urea crystals the above radical is formed by the addition of a hydrogen to an undamaged fumaric acid molecule. Observations of free radicals formed by H-atom addition at room temperature are relatively infrequent compared to observations of radicals produced by removal of H-atoms (or carboxyl groups, etc.). H-atom addition has, however, been observed in X-irradiated tiglic acid[18] and in X- and γ-irradiated furoic acid[18,19].

The ESR spectra of X-irradiated fumaric acid-urea crystals are complex for arbitrary orientations of the magnetic field, and there are apparently several magnetically-distinguishable orientations of the above radical. However, the spectra are always dominated by at most two orientations of the radical, and these two orientations account for at least two thirds of the total ESR signal intensity. We will be concerned here with the two major orientations

of the radical, and will not discuss further the multiple orientations which produce low-intensity ESR spectra (it was not possible to resolve completely these low-intensity signals).

The two major orientations of the fumaric acid radical gave the same ESR spectra in the yz plane and approximately the same spectra in the xz plane. These were the only two planes for which reasonably accurate coupling constant data could be obtained. As shown in Fig. 2, the ESR spectra of all radical orientations are approximately superimposed when the magnetic field is along the x, y, or z crystalline axes. Along these three directions the values of the approximately magnetically equivalent β-proton coupling constants are 86, 85, and 84 Mc/sec ($\pm$3 Mc/sec), respectively. The β-proton splittings for other orientations of the magnetic field differ at most by a few Mc/sec from these values.

The α-proton data were reduced to tensor form using the usual spin Hamiltonian[2] (neglecting the nuclear Zeeman term). It was found that the spectra arising from the major orientations of the radical could be reconstructed to within $\pm$ 1.5 Mc/sec for an arbitrary direction of the magnetic field provided two α-proton tensors were used. These two tensors are related by a two-fold rotation about the x axis and are given, along with the eigenvectors and eigenvalues, in Table II. (Two tensors related by a two-fold rotation about the y axis reproduce the major features of the spectra, but the agreement is much poorer than it is for the tensors of Table II). Although the tensors of Table II reproduce the α-proton coupling

TABLE II

α-PROTON TENSOR OF THE $HO_2CCH_2\dot{C}HCO_2H$ RADICAL IN THE FUMARIC ACID-UREA CRYSTAL [a-c]

	Tensor	Eigenvalues	Eigenvectors
	$+65.9 \pm 19.1 \pm .5$	(-) 92.2	$(-.586, \mp .809, \pm .040)$
(-)	$\pm 19.1 + 78.2 - 3.5$	(-) 52.2	$(+.808, \mp .580, \pm .104)$
	$\pm .5 - 3.5 + 28.9$	(-) 28.5	$(-.061, \pm .094, \pm .994)$

[a] The tensor is in the x, y, z crystalline coordinate system defined in Fig. 1

[b] All tensor elements are reported in Mc/sec. The absolute values only are determined (the eigenvalues are known to be negative[2]).

[c] The direction cosines relative to the x, y, z axes.

constants to within ± 1.5 Mc/sec, the absolute accuracy is limited to ± 3 Mc/sec because of the imperfect superposition of the multiple orientations of the radical. Laue X-ray diffraction patterns of the fumaric acid-urea crystal indicate the crystal structure is monoclinic and that the two-fold axis lies along the x direction. This confirms the results obtained from the anisotropic α-proton ESR data.

Electron spin r esonance data were also recorded for the succinic acid-urea crystals in order to compare the radical orientations with those of the fumaric acid-urea system. The morphology of the succinic acid-urea crystals is very similar to that of the fumaric acid-urea crystals (for example, f:g and g:h are 68°5' ± 15' and 55°55' ± 15', respectively, for the succinic acid-urea crystal). After X-irradiation at room temperature the only free radical observed is the one resulting from the removal of one α-proton from the succinic acid molecule, and it is therefore the same as the fumaric acid radical. The values of the α-proton coupling constants along the x, y, and z axes of the succinic acid-urea crystal are 69, 81, and 29 Mc/sec and are identical, within the limits of experimental accuracy, with the values 69, 80 and 29 Mc/sec along the corresponding axes of the fumaric acid-urea crystal. The β-proton coupling constants of the radicals in the two crystals are very nearly the same along the x, y, and z axes, respectively, and the ESR spectra with the magnetic field in an arbitrary direction are qualitatively the same for the two crystals.

The crystals formed between adipic acid and urea, and pimelic acid and urea were also briefly investigated. In both cases X-irradiation produced the usual long-lived free radical formed by the removal of one α-proton from the parent dicarboxylic acid. The morphology and radical orientations of the adipic acid-urea crystals are similar to those of the fumaric acid-urea and succinic acid-urea systems. However, the two β-protons of the adipic acid radical are nonequivalent, typical coupling constants being 105 and 83 Mc/sec, and the ESR spectra due to a second radical are observed (this latter observation has been briefly mentioned elsewhere[10]). The two β-protons of the pimelic acid radical are also magnetically nonequivalent, and the ESR spectra exhibit the usual anisotropy associated with an α-proton (in the absence of molecular motion). The crystals of pimelic acid-urea obtained from methanol had poorly developed faces and no radical orientation study of this system was attempted.

D. DISCUSSION

a. The Relation Between the Free Radical Axes and the Crystal Coordinates

Free radicals of the type $R\dot{C}HCO_2H$ have been extensively studied by ESR in X-irradiated crystalline dicarboxylic acids and the diagonal tensor elements of all of these radicals are approximately the same[2]. From a comparison of the eigenvalues of the α-proton tensor (TableII) with the values reported for similar radicals in crystals with known crystal structures, it is readily seen that the

eigenvalues 28, 52, and 92 Mc/sec correspond, respectively, to (1) the direction along the C_1–H_α bond, (2) the axis of the 2p orbital on C_1, and (3) a direction perpendicular to (1) and (2). These directions are commonly referred to as the molecular cartesian z', x', and y' axes, respectively. The direction cosines of the x', y', z' axes with respect to the crystalline x, y, z axes are given in Table II. From Table II it is seen that the C_1-H_α bonds of both radical orientations lie nearly along the crystalline z direction and the 2p orbitals containing the unpaired electrons lie approximately in the xy plane, and are inclined $\sim 36^\circ$ to the x axis of the crystal.

b. The β-Proton Coupling Constants

The β-proton coupling constants a_β, in the absence of molecular motion are given by the approximate relation $a_\beta = R(\theta)\rho C^\pi = \rho C^\pi B^0 \cos^2\theta$ where B^0 is a constant, ρC^π is the spin density in the $2p_{x'}$ orbital on C_1, and θ is the angle between the axis of the $2p_{x'}$ orbital on C_1 and the projection of the C_2–H_β bond onto a plane which is perpendicular to the C_1–C_2 bond [15]. [$R(\theta)$ is just the constant of proportionality between ρC^π and a_β.] If there exist small amplitude oscillations about the C_1–C_2 bond, then the principal effects on the above equation relating a_β and θ are to decrease the apparent value of B^0 and to add a small constant term, A^0 [20, 21]. However, if there exist very large molecular motions about the C_1–C_2 bond (e.g., free rotation) then the θ dependence will be averaged out and $a_\beta \simeq \rho C^\pi B^0/2$.

Therefore, the equivalence of the two β-protons of the fumaric acid radical indicates that one of the four following situations exist: (1) The value of θ for each β-proton is 30°, (2) the value of θ for each β-proton is 60°[22], (3) the β-protons are undergoing limited torsional motion about the 30° or 60° positions, or (4) the β-protons are undergoing very large amplitude oscillations about the C_1–C_2 bond. The choice between these possible explanations is made by comparing the values of a_β calculated from the above equation with the experimentally observed a_β, assuming a known value of $\rho C^\pi B^0$. Taking $\rho C^\pi B^0$ to be in the range 130 to 140 Mc/sec obtained from similar radicals with rotating methyl groups attached to C_1[2, 21] a_β for $\theta = 30°$ ranges from 97 to 105 Mc/sec. The observed values lie somewhat below this range, suggesting that the β-protons of the fumaric acid radical are undergoing limited motion about the 30° equilibrium positions. Therefore, the time-average positions of all four carbon atoms and the α-proton lie in one plane, and the β-protons are inclined 60° to this plane. The orientation of this plane is obtained from the α-proton tensor data of Table II.

c. Comparison of the Fumaric Acid-Urea Crystal with Other Dicarboxylic Acid-Urea Crystals

Urea has been found to form mixed crystals with a wide variety of molecules and these crystals have been the subject of numerous investigations. The urea inclusion compounds are the best known of

these systems and they are formed between urea and the derivatives of the straight-chain hydrocarbons. The inclusion compounds are hexagonal crystals in which the hydrocarbon molecules fit loosely into cavities formed by hydrogen-bonded urea molecules. The centers of the oxygen atoms of the urea molecules lie in the edges of a regular hexagonal prism, and the unit cell is composed of six urea molecules spiraled about the prism[23, 24]. Because of the absence of strong interactions between the urea molecules and the hydrocarbon molecules, the latter undergo a high degree of complex molecular motion in the tubular cavaties[21,25]. Another distinguishing property of the inclusion compounds is that the urea and hydrocarbon molecules do not, in general,crystallize in whole-number ratios[11,24,26]. This follows from the fact that the tubular structures have more or less fixed dimensions, whereas the hydrocarbon molecules may vary in length. These three properties of the urea inclusion compounds: (1) hexagonal crystal structures, (2) large degree of motion of the guest molecule, and (3) definite, but (in general) nonintegral composition, provide convenient means of identifying the urea-inclusion compounds.

Urea also forms crystals which are not of the inclusion compound type. Schlenk[11] has found that crystals formed between urea and acetone (1:2.8), adiponitrile (1:1), suberonitrile (1:5.7), trichloroacetic acid (1:1), malonic acid (1:2), succinic acid (1:2), adipic acid (1:2), and several dihalogenated hydrocarbons of short-chain length exhibit X-ray powder diffraction patterns unlike those

of the hexagonal urea inclusion compounds. Oxalic acid-urea crystals (1:2) and dioxane-urea crystals (1:1, 1:2) also differ from the hexagonal inclusion crystals[23, 27]. (The numbers in parentheses following all of these compounds are the mole ratios of the hydrocarbon derivatives to urea.) Most of these crystals are composed of whole-numbered ratios of the two components and are often referred to as "molecular compounds". The only one of the above crystals which has been studied in detail by X-ray crystallography is the oxalic acid-urea crystal[27]. Oxalic acid-urea crystals are monoclinic (space group $P2_1/c$) and possess a layer structure in which the oxalic acid molecules and urea molecules are held together by strong hydrogen bonds. The layers are held together by Van der-Waals forces and there is no indication that the crystal is a salt formed between the acid and urea molecules.

It is evident from the ESR data and Laue X-ray data that the fumaric acid-urea crystals are not urea inclusion compounds of the type discussed above. The crystal structure is not hexagonal, the motion of the fumaric acid radical is very limited, and the composition of the crystal is $\sim$1:2. Although our data does not permit a detailed analysis of the structure of these crystals, it is of interest to compare the ESR data with those of the other dicarboxylic acids. The orientations of the free radical in the fumaric acid-urea crystals are essentially the same as those of the succinic acid-urea crystal. Since the free radicals normally remain in nearly the same positions as the undamaged molecules, this is a strong indication that the

orientations of the undamaged molecules in the two crystals are the same.

The ESR spectra of adipic acid-urea crystals and of pimelic acid-urea crystals indicate that the radical orientations are not related by hexagonal (or trigonal) symmetry operations and therefore the crystals are not hexagonal urea inclusion compounds. Sebacic acid-urea crystals, on the other hand, are hexagonal and the ESR spectra indicate that the sebacic acid radical is undergoing large amplitude oscillations[21]. This motion removes the α-proton anisotropy in a plane perpendicular to the hexagonal needle axis, and produces an easily recognizable isotropic spectrum in this plane. Similar results are obtained for 1,12-dodecanedioic acid, and crystals of sebacic acid-urea and 1,12-dodecanedioic acid-urea are apparently urea inclusion compounds. Therefore, there is a transition from hexagonal urea inclusion crystals to crystals of lower symmetry as the saturated dicarboxylic acid chain length is shortened[28]. From the ESR data it is evident that some of the short-chain length acid molecules have similar orientations in the non-hexagonal crystals. In particular it is interesting to note that the orientations of the acid radicals are the same in the two crystals, succinic acid-urea and fumaric acid-urea. The positions of the urea molecules cannot be determined from ESR data since urea does not produce stable paramagnetic damage sites at room temperature.

E. ACKNOWLEDGMENTS

We wish to thank Professor J. Holmes Sturdivant for his advice and help concerning this work, especially in relation to the Laue X-ray photography. We are also greatly indebted to Professor Harden M. McConnell for the generous use of his laboratory facilities.

F. REFERENCES

(1, a) Supported by the National Science Foundation under Grant No. GP-930. (b) Contribution No. 3111. (c) National Science Foundation Predoctoral Fellow.

(2) For a review see: R. G. Shulman, Ann. Rev. Phys. Chem., 13, (1962).

(3) R. B. Mesrobian, P. Ander, D. S. Ballantine, and G. J. Dienes, J. Chem. Phys., 22, 565 (1954).

(4) A. J Restaino, R. B. Mesrobian, H. Morawetz, D. S. Ballantine, G. J. Dienes, and D. J. Metz, J. Am. Chem. Soc., 78, 2939 (1956).

(5) G. W. Griffen, J. E. Basinski, and A. F. Vellturo, Tetrahedron Letters No. 3, 13 (1960).

(6) G. W. Griffen, J. E. Basinski, and L. I. Peterson, J. Am. Chem. Soc., 84, 1012 (1962).

(7) G W Griffen, A. F Vellturo, and K. Furukawa, ibid., 83, 2725 (1961).

(8) R. J. Cook, J. R. Rowlands, and D. H. Whiffen, J. Chem. Soc., 1963, 3520.

(9) We have observed certain features of the ESR spectra of X-irradiated cis-12-ethylenedicarboxylic acid (maleic acid) which suggest that similar radicals are produced in this system (no detailed investigation of maleic acid is planned in this laboratory).

(10) The initial results of this work were briefly mentioned in a note reporting uses of X-ray-damaged urea inclusion compounds. [O. H. Griffith and H. M. McConnell, Proc. Natl. Acad. Sci. U.S., 48, 1877 (1962).]

(11) W. Schlenk, Jr., Ann., 565, 204 (1949).

(12) In addition to the lines attributed to the $HCO_2CH_2\dot{C}HCO_2H$ radical (I), the freshly X-irradiated fumaric acid-urea crystals exhibited four to eight partially resolved lines which probably arise from just one other type of radical (II). The maximum splitting attributed to II is 175 Mc/sec and the g-value of II is similar to that of I. It is possible that II is related to the vinyl radical, which has been observed by Fessenden and Schuler[13] in solution and by Adrian, Cochran, and Bowers[14] in an argon matrix. Radical II could also be a conformational isomer of I in which the value of θ (see discussion of β-proton coupling constants) of one of the β- protons is nearly 90°. (This could be caused, for example, by hydrogen addition perpendicular to the plane containing the carbon atoms of fumaric acid. II might then be a precursor to I.) The protons of urea and the carboxyl groups of fumaric acid were simultaneously exchanged for deuterium by repeated recrystallization from D_2O. The ESR spectra of the X-irradiated deuterated crystals did not provide positive identification of II due to extensive overlapping of lines. However, a large concentration of the radical $DO_2CCH(D)\dot{C}HCO_2D$ relative to the concentration of radical I was observed in the deuterated crystal. In view of the fact that the α-proton tensors of the minor orientations of radical

I could not be obtained, further work on this system would more profitably await a complete X-ray crystallographic investigation of the fumaric acid-urea crystals. (Multiple twinning or the presence of crystal defects, for example, would hinder the identification of additional radicals and are not always easily recognizable from the ESR spectra.)

(13) R. W. Fessenden and R. H. Schuler, J. Chem. Phys., 39, 2147 (1963).

(14) F. J. Adrian, E. L. Cochran, and V. A. Bowers, Free Radicals in Inorganic Chemistry (American Chemical Society, Washington, D.C., 1962), p.50. See also footnote 48 of reference 13.

(15) C. Heller and H. M. McConnell, J. Chem. Phys., 32, 1535 (1960).

(16) D. Pooley and D. H. Whiffen, Mol. Phys., 4, 81 (1961).

(17) T. S. Jaseja and R. S. Anderson, J. Chem. Phys., 36, 2727 (1962).

(18) A. L. Kwiram and H. M. McConnell, Proc. Natl. Acad. Sci. U.S., 48, 499 (1962).

(19) R. J. Cook, J. R. Rowlands , and D. H. Whiffen, Mol. Phys., 7, 57 (1963).

(20) E. W. Stone and A. H. Maki, ibid., 37, 1326 (1962).

(21) O. H. Griffith, J. Chem. Phys., in press.

(22) Throughout this discussion it is assumed that the σ bonds involving carbon atom 1 are sp^2 hybridized. Therefore the $H\text{-}C_2\text{-}H$

dihedral angle is taken to be 120°, and (in the absence of motion) the values of θ must be either 30° or 60° in order for the β-protons to be magnetically equivalent. These points have been discussed extensively in the literature. See for example: (a) T. Cole, H. O. Pritchard, N. R. Davidson, and H. M. McConnell, Mol. Phys., 1, 406 (1958); (b) H. M. McConnell, C. Heller, T. Cole and R. W. Fessenden, J. Am. Chem. Soc., 82, 766 (1960); (c) Reference 13; and (d) J. R. Rowlands and D. H. Whiffen, Mol. Phys., 4, 349 (1961).

(23) A. E. Smith, Acta. Cryst., 5, 224 (1952).

(24) K. A. Kobe and W. G. Domask, Petroleum Refinier, 31, No. 3, 106 (1952).

(25) D. F. R. Gilson and C. A. McDowell, Mol. Phys., 4, 125 (1961).

(26) O. Redlich, C. M. Gable, A. K. Dunlop, and R. W. Miller, J. Am. Chem. Soc., 72, 4153 (1950).

(27) J. H. Sturdivant, A. Schuch, and L. L. Merritt, Jr., Structure Reports, 13, 477 (1950). (Also, J. H. Sturdivant, unpublished results.)

(28) This transition was first noted in the series of acids: succinic acid, adipic acid, and sebacic acid by Schlenk[11] from X-ray powder diffraction data. Of course, neither the powder diffraction data nor the single crystal ESR data are a substitute for a (single crystal) X-ray crystallographic investigation. However, electron spin resonance does provide a method for investigating the structure, positions, and molecular motion of the X-ray produced free radicals

in the crystals.

V. MAGNETIC RESONANCE OF THE TRIPLET STATE OF ORIENTED PYRENE MOLECULES[1a]

O. Hayes Griffith[1b]

Gates and Crellin Laboratories of Chemistry[1c]
California Institute of Technology
Pasadena, California

Bree and Vilkos[2] have recently completed an optical polarization study of the lower singlet states of pyrene in a fluorene matrix at 77°K. The crystal structure of fluorene is orthorhombic, the space group is Pnam, and there are four molecules per unit cell.[3] This crystal is a convenient matrix because the long axes of the fluorene molecules are all parallel to the crystalline c axis. We report here the observation of electron spin resonance of the lowest triplet state of pyrene in a fluorene matrix.

The fluorene ($C_{13}H_{10}$), kindly supplied by D. E. Wood, was prepared from commercial reagent grade fluorenone. The fluorenone was purified by column chromatography (column: alumina, wash: spectral quality cyclohexane) and was reduced with hydrazene hydrate.[4] The resulting fluorene was then chromatographed as above and sublimed.[5] The pyrene ($C_{16}H_{10}$) was prepared by zone refining (30-50 zones) commercial reagent grade pyrene. The crystals of pyrene-doped fluorene were grown from a melt initially containing 1.0 mole % pyrene but the actual concentrations of pyrene in the crystals were not determined.[6] These crystals were found to cleave in the (001) plane and the positions of the a, b

and c axes were determined by X-ray crystallographic techniques. The actual crystal fragments used in the e.s.r. experiments were initially oriented with a polarizing microscope and were not subjected to X-irradiation until after the e.s.r. experiments were complete. The crystals were illuminated <u>in situ</u> with a General Electric BH-6 Hg arc lamp and the temperature of the sample was maintained at 100°K throughout the experiments with a conventional nitrogen gas flow system. A Varian X-band spectrometer was used to obtain the spectra. Magnetic fields corresponding to the extrema (or near extrema) splittings were measured with a rotating coil gaussmeter and the remainder of the fields were measured with a Hall effect probe.

The e.s.r. spectra were recorded with the magnetic field, $\underset{\sim}{H}$, in the ac, bc, and ab planes of the pyrene-doped fluorene crystals. Two e.s.r. lines displaced symmetrically about $g \approx 2.0030$ were observed with H in the ac or bc planes and the maximum splitting between these two lines occurred when H was perpendicular to the cleavage plane. In general, four lines were observed with H in the crystallographic ab plane. All of the e.s.r. lines decayed rapidly upon removal of the light source (lifetime $<$ 1-2 sec).

Using the method of Hutchison and Mangum,[7,8] the g values and zero field splitting parameters of the Hamiltonian $\mathcal{H} = \beta \underset{\sim}{H} \cdot \underset{\sim}{g} \cdot \underset{\sim}{S} + DS_z^2 + E(S_x^2 - S_y^2)$ were found to be $g_{xx} = 2.0033$, $g_{yy} = 2.0026$, $g_{zz} = 2.0033$, $D(xy)/hc = \pm 0.0806\ cm^{-1}$, $D(z)/hc = \pm 0.0810\ cm^{-1}$,

and $E/hc = \mp 0.0182\ cm^{-1}$. The estimated errors in the g values, D, and E are ± 0.0005, ± 0.0012, and ± 0.0009, respectively. The limits of error are uncomfortably large because the e.s.r. signals were very weak, frequently being only a factor of 1.5 to 8 above the noise level. Employing these values of the parameters in the above spin Hamiltonian and allowing for the symmetry properties of the fluorene lattice, the positions of all observed lines can be predicted within experimental error. Therefore, it is clear that the e.s.r. signals result from one type of molecule and this molecule occupies a substitutional site in the fluorene lattice. It remains to show that this molecule is pyrene.

Single crystals of fluorene exhibited a faint blue-green phosphorescence at boiling nitrogen temperatures and corresponding weak lines were present in the phosphorescence emission spectra of these crystals. However, under the same experimental conditions that the e.s.r. spectra were obtained from the pyrene-doped fluorene crystals, no e.s.r. signals were observed from single crystals of fluorene and therefore it is highly unlikely the above e.s.r. spectra are due to either fluorene or an impurity in fluorene. The zone refined pyrene undoubtedly contains impurities, the most troublesome of which is probably naphthacene[9] ($C_{18}H_{12}$). A single crystal of naphthacene-doped fluorene was grown from a melt containing 0.01 mole % of naphthacene and no e.s.r. signals were observed at 100°K in these crystals. The pyrene-doped fluorene crystals exhibited a reddish phosphorescence at low temperatures similar to

the phosphorescence of pyrene in a hydrocarbon glass. The maximum of the only line observed in the 77°K phosphorescence spectra of the pyrene-doped fluorene crystals occurred at 16,750 $cm^{-1} \pm 60\ cm^{-1}$, which is in good agreement with the phosphorescence maximum reported for pyrene in glasses at 77°K.[10] The emission lines observed in the fluorene crystal were apparently quenched in the pyrene-doped fluorene crystal. All of the above evidence supports the conclusion that the e.s.r. spectra observed in the pyrene-doped fluorene crystals arise from (the lowest) triplet state of pyrene.

Further splitting of the fine structure e.s.r. lines into hyperfine lines was not observed in any of the spectra recorded[11] and, therefore, it is not possible to uniquely determine the orientations of the pyrene molecules in the fluorene lattice. However, one of the principal magnetic axes of pyrene lies approximately along the crystalline c axis (the long axis of fluorene) and the other two magnetic axes correspond to the short axis and a normal to the molecular plane of fluorene. It appears, therefore, that the molecular plane and long axis of the pyrene molecule are oriented with respect to the fluorene lattice in the same manner as the displaced fluorene molecule. If we assume this to be the case then the molecular z, y, and x axes of pyrene would be parallel to the long axis, the short axis, and the normal to the molecular plane of the pyrene molecule, respectively.[12]

We are indebted to Professor Harden M. McConnell for the generous use of his laboratory facilities. We are also indebted to

Dr. Richard E. Marsh for help concerning the X-ray photography, to Professor Melvin W. Hanna for helpful discussions, and to Mrs. Lelia M. Coyne for obtaining the optical spectra.

REFERENCES

(1) (a) Supported by the National Science Foundation under Grant No. GP-930. (b) National Science Foundation Predoctoral Fellow. (c) Contribution No. 3181.

(2) A. Bree and V. V. B. Vilkos. J. Chem. Phys., 40, 3125 (1964).

(3) D. M. Burns and J. Iball, Proc. Roy. Soc. (London), A227, 200 (1955).

(4) J. H. Weissberger and P. H. Grantham, J. Org. Chem., 21, 1160 (1956).

(5) Fluorene prepared by this procedure exhibited far lower phosphorescence intensity at 77°K than did zone refined commercial reagent grade fluorene. According to D. E. Wood (private communication), some samples of fluorene prepared by this technique (with additional zone refining in some cases) produced a negligible phosphorescence.

(6) Cold traps were used during the crystal preparations to prevent possible contamination from stopcock grease and the chemicals were melted only under reduced pressures of prepurified nitrogen gas to minimize oxidation and decomposition.

(7) C. A. Hutchison, Jr., and B. W. Mangum, J. Chem. Phys., 34, 908 (1961).

(8) D(xy) is the value of D obtained along with E from the (extrema) splittings corresponding to the molecular x and y directions and D(z) is the value of D obtained using E and the (extremum) splitting corresponding to the molecular z direction. The agreement of these two values of D constitutes a partial verification of the proper choice of molecular axes. Using these values of D and E, $(D^2 + 3E^2)^{\frac{1}{2}} = 0.0868 \pm 0.002$. This value is in only fair agreement with the value 0.0929 cm^{-1} obtained by Smaller [B. Smaller, J. Chem. Phys., 37, 393 (1963)] (and confirmed by us) from the $\Delta m = \pm 2$ transition of randomly oriented pyrene molecules.

(9) However, the zone refined crystalline pyrene appeared white rather than the yellow, characteristic of small concentrations of naphthacene.

(10) McClure reports [D. S. McClure, J. Chem. Phys., 17, 910 (1944)] that for pyrene in a rigid glass at 77°K the phosphorescence maximum occurs at 16,800 cm^{-1}, the ratio of phosphorescence yield to fluorescence yield is 0.001, and the mean lifetime is about 0.2 seconds.

(11) The lack of resolution is presumably due to the large number of protons interacting with the electron and to crystal disorder. Laue photographs disclosed that the first crystals obtained were badly disordered. The crystals used for the e.s.r. study were of much better quality but could have been sufficiently disordered to reduce resolution of the hyperfine structure.

(12) By convention,[7] D and E for pyrene were arbitrarily chosen to have opposite signs. If D and E were chosen to have the same sign then the x and y axes would be interchanged. This indeterminancy affects only the relative signs of D and E and not their magnitudes. We are indebted to Dr. J. H. van der Waals for a discussion on this point.

VI. TRIPLET EXCITONS AND MAGNETICALLY DILUTE RADICALS IN $(\varphi_3PCH_3)^+(TCNQ)_2^-$ AND $(\varphi_3AsCH_3)^+(TCNQ)_2^-$ ION RADICAL SALTS[†]

Free radical impurity ESR lines in two ion radical salts of TCNQ were found to homogeneously broaden and change from a Gaussian to a Lorentzian line shape as the temperature was increased from 77°K. This is interpreted as resulting from an exciton-radical exchange interaction. The radical exciton exchange activation energies are of the same order of magnitude as the exciton-exciton activation energies. The 77°K exciton and radical line width anisotropies were investigated in $(\varphi_3AsCH_3)^+(TCNQ)_2^-$ crystals. The line width of the exciton is proportional to the free radical impurity line width, which suggests that nuclear hyperfine interactions dominate the exciton line width at this temperature.

A. INTRODUCTION

Several studies of $(\varphi_3PCH_3)^+(TCNQ)_2^-$ (I), $(\varphi_3AsCH_3)^+(TCNQ)_2^-$ (II), and other ion radical salts based on the strong electron acceptor tetracyanoquinodimethane[1] (TCNQ)

[†]Unpublished results of O. H. Griffith and H. M. McConnell.

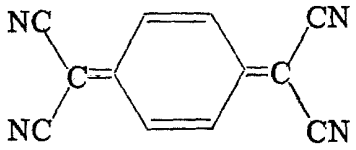

TCNQ

have been reported. The electron spin resonance (ESR) spectra of these salts exhibit triplet state behavior. The fine structure splittings of I and II are represented by the spin Hamiltonian

$$\mathcal{H} = \underset{\sim}{H} \cdot \underset{\sim}{g} \cdot \underset{\sim}{S} + DS_z^2 + E(S_x^2 - S_y^2) \qquad (1)$$

with $|D/hc| = 0.0062\ cm^{-1}$, $|E/hc| = 0.00098\ cm^{-1}$, $g_{xx} = 2.004$, $g_{yy} = 2.003$, and $g_{zz} = 2.003$.[2] (The parameters of I and II are identical within experimental error). The temperature dependence of the ESR signal intensity, I, for an excited triplet state separated from the ground singlet state by an energy J is

$$I \propto T^{-1} \left[\exp(J/kT) + 3 \right]^{-1} \qquad (2)$$

Chesnut and Phillips[2] found that the ESR intensities of I and II obey Eq. (2) (with J = 0.065 ev) and therefore the unpaired electrons correlate; giving rise to a ground singlet and a thermally accessible triplet state. The two 77°K high field lines broaden, move together, and collapse into one central line as the temperature is raised. This effect has been attributed to exchange interactions between triplets[2,3] and, more specifically, between triplet excitons.[4] The exciton concept provides a natural explanation of the absence of nuclear hyperfine

structure in the spectra of I and II.[5] The existence of triplet excitons also accounts for the zero field splittings, since the exciton Hamiltonian $\mathcal{H}_k$ reduces to Eq. (1) for a sufficiently small exciton band width.[6] D. D. Thomas, A. W. Merkl, A. F. Hildebrandt, and H. M. McConnell[7,8] have recently reported the zero-field exciton magnetic resonance of II. Here we are concerned with the relation between high field ESR spectra of triplet excitons and magnetically dilute free radicals in I and II.[10]

B. EXPERIMENTAL

The ESR spectra were obtained with a Varian X-band spectrometer. The crystals were mounted in a microwave cavity which forms part of the vacuum chamber of a metal dewar. Roughly half of the low temperature data were obtained by slow cooling of warm crystals and the other half were obtained by slow warming of cold crystals. Cold nitrogen gas was passed through the dewar to cool the system. The warming was accomplished simply by allowing the dewar to slowly return to room temperature. The average temperature change which occurred during the time necessary to obtain one ESR spectrum was ~ 2.5°K. All temperature effects were reversible.

C. RADICAL-EXCITON SPIN EXCHANGE

The ESR spectra of an arbitrarily oriented $(\varphi_3 PCH_3)^+(TCNQ)_2^-$ crystal are shown in Fig. 1. The orientation of the crystal and the

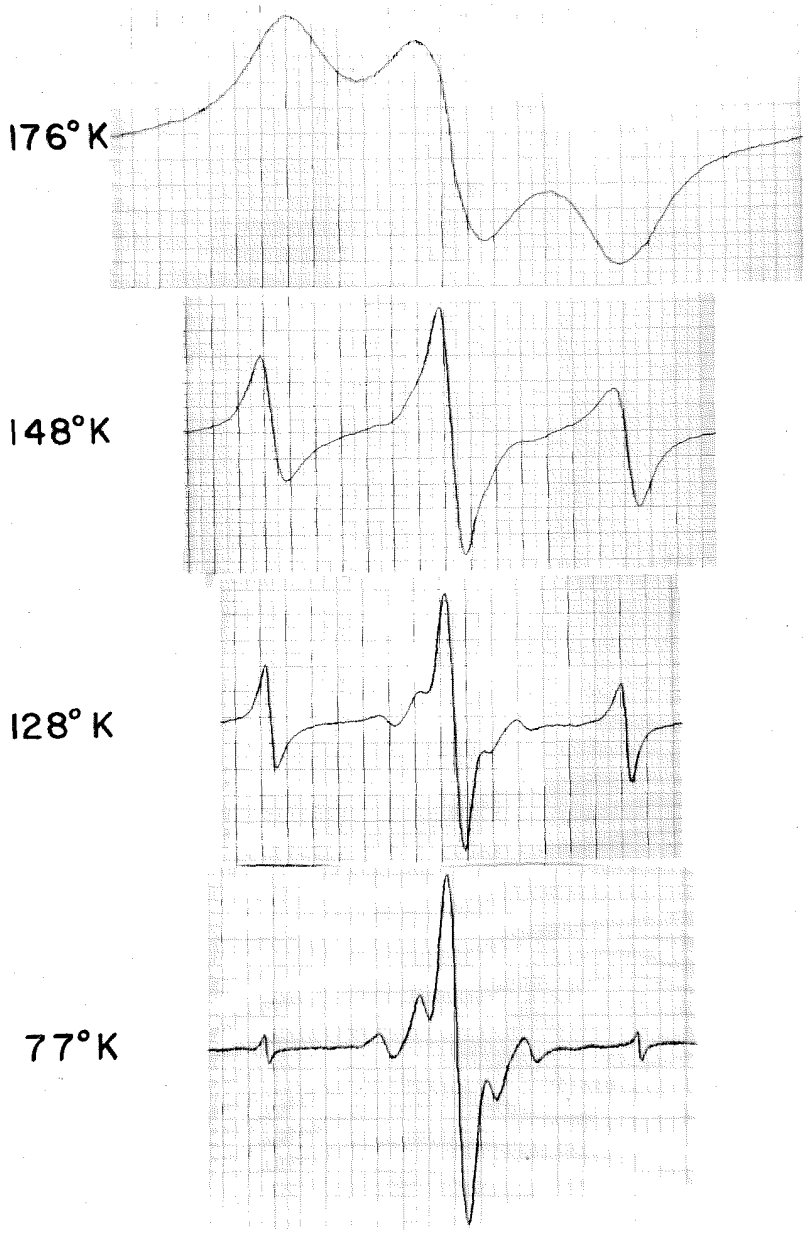

Figure 1

The temperature dependence of the exciton (outside doublet) and radical ESR signals of a $(\phi_3PCH_3)^+ (TCNQ)_2^-$ crystal. The exciton 77°K fine structure splitting is 73 gauss. These spectra were obtained at different spectrometer gain settings.

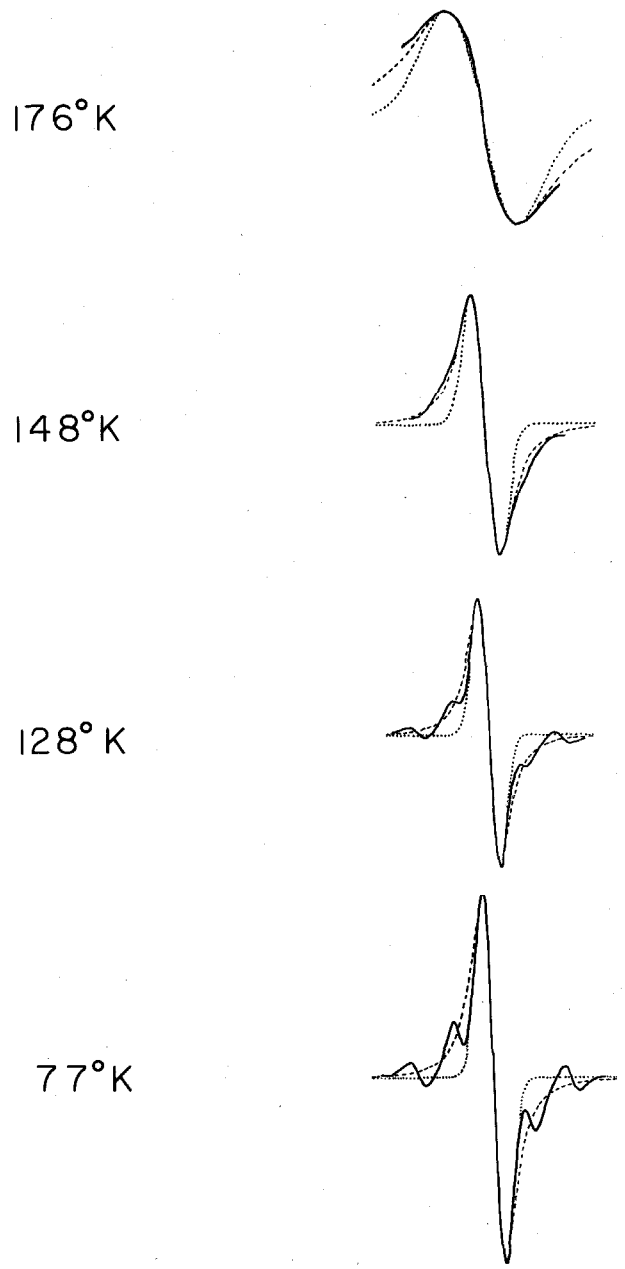

Figure 2

The retraced radical spectra of Fig. 1 and the reconstructed Lorentzian (---) and Gaussian (···) line shapes for the central radical line.

magnetic field scan rate were the same for all four spectra. The outside two lines result from a triplet exciton fine structure splitting[2,4] and the inner lines are free radical signals. The radical concentration was increased by X-irradiation prior to obtaining the spectra. In addition to the broadening of the exciton lines, there is a pronounced temperature effect on the free radical signals. At 77°K there are at least seven resolved hyperfine lines in the spectra of Fig. 1. As the temperature is increased the lines broaden until at 150°K only one structureless line is observed. This effect is apparently caused by a exciton-radical exchange interaction.

The exciton signals are Lorentzian.[11] The line shape of the radical changes with temperature as illustrated in Fig. 2. The Lorentzian and Gaussian lines of Fig. 2 were chosen to match the peak heights and widths of the observed central radical line. The central radical line at 77°K is Gaussian. As the temperature is increased this line changes shape until at ~ 150°K the line is Lorentzian. The smaller radical lines add intensity to the experimental derivative curves causing the 148°K spectra to appear to have more intensity in the wings than is characteristic of a Lorentzian line. The effect of temperature on the radical line shape is even more clearly illustrated in Fig. 3. In this case the crystal was not X-irradiated before recording the ESR spectra. The 77°K radical spectrum of Fig. 3 is obviously Gaussian. At 130°K the line shape is intermediate and at 150°K the Lorentzian curve coincides exactly with the experimental curve. The 167°K radical line (and the 176°K line of Figs. 1 and 2) appears to be Lorentzian even

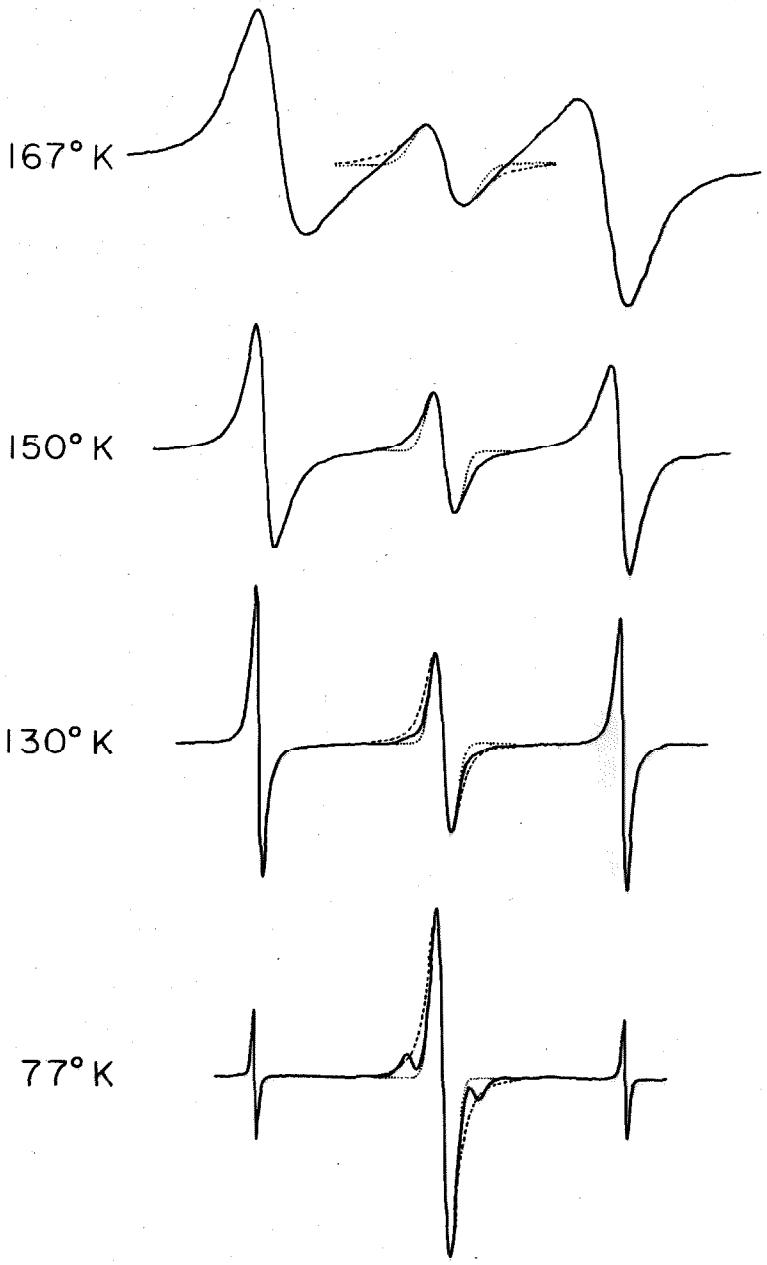

Figure 3

The retraced ESR spectra of a second $(\phi_3PCH_3)^+ (TCNQ)_2^-$ crystal. The Lorentzian (---) and Gaussian (· · ·) approximations to the central line are superimposed on the spectra. The exciton splitting of the 77°K spectrum is 70 gauss and each spectrum was obtained at a different gain setting.

though the shape is complicated by the overlapping of exciton and radical lines. At higher temperatures the exciton concentration increases to such an extent that the exciton lines completely dominate the radical line. The overall transition from a Gaussian line at low temperatures to a Lorentzian line at higher temperatures (higher exciton concentrations) provides strong evidence that the radical is undergoing spin exchange collisions with the excitons.

In the limit that the exchange frequency ν is much smaller than the separation between the ESR lines (slow exchange limit),

$$\nu = 3^{-\frac{1}{2}}\gamma(\Delta H - \Delta H_0) \tag{3}$$

where ΔH and ΔH_0 are the line widths in gauss measured from peak points of the derivative of the absorption in the presence and absence of exchange, respectively.[3] Jones and Chesnut[3] found that the exciton-exciton exchange frequencies have a temperature dependence given by

$$\nu = \nu_0 \exp(-\Delta E/kT) \tag{4}$$

where ΔE is 0.13 ± 0.01 ev and 0.11 ± 0.02 ev for I and II, respectively. In Fig. 4 the semilog plots of $\Delta H - \Delta H_0$ vs $1/T^\circ K$ are given for the same $(\varphi_3 PCH_3)^+(TCNQ)_2^-$ crystal used to obtain the spectra of Fig. 1. The ΔH_0 for the exciton and radical are 1.00 gauss and 3.75 gauss, respectively. The exciton-exciton and radical-exciton exchange frequencies are

$$\nu = 3^{-\frac{1}{2}}\gamma\ 1.3(\pm 1.0)\ \text{gauss}\ 10^4 \exp[-0.10(\pm 0.01)\ \text{ev}/kT]$$

and

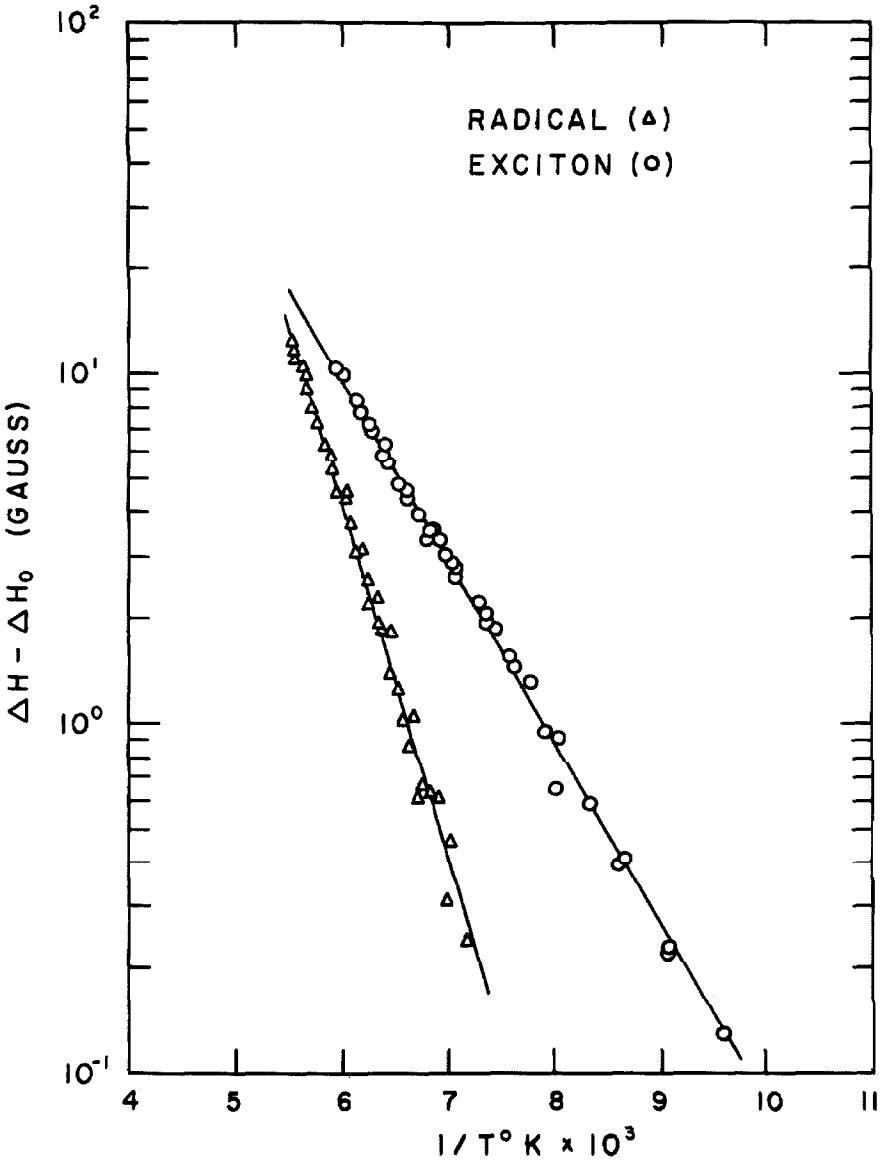

Figure 4

A semilog plot of $\Delta H - \Delta H_0$ vs $1/T^\circ K$ for the same $(\phi_3 PCH_3)^+ (TCNQ)_2^-$ crystal and magnetic field orientation used to obtain the spectra of Fig. 1.

$$\nu = 3^{-\frac{1}{2}}\gamma\, 4.0\,(\pm\, 5.0)\ \text{gauss}\ 10^{6}\ \exp[-0.20\,(\pm\, 0.03)\ \text{ev/kT}]$$

respectively. The errors given for ν_0 are associated with the extrapolated value ($T = \infty$). The temperature dependence of the line widths of one X-irradiated $(\varphi_3 AsCH_3)^+ (TCNQ)_2^-$ crystal was also measured. In this case the exciton-exciton and radical-exciton exchange frequencies are

$$\nu = 3^{-\frac{1}{2}}\gamma\, 2.2\,(\pm\, 2.0)\ \text{gauss}\ 10^{4}\ \exp[-0.10\,(\pm\, 0.02)\ \text{ev/kT}]$$

and

$$\nu = 3^{-\frac{1}{2}}\gamma\, 8.0\,(\pm\, 5.0)\ \text{gauss}\ 10^{4}\ \exp[-0.14\,(\pm\, 0.02)\ \text{ev/kT}]$$

respectively. The ΔH_0 values for the exciton and radical are 1.50 gauss and 10.0 gauss, respectively. The orientations of both crystals were arbitrary. The exciton-exciton spin exchange activation energies are the same for the two crystals, within experimental error, and agree with the values reported by Jones and Chesnut. The exciton-radical spin exchange activation energies are more difficult to consider quantitatively. The radical ΔH_0 was measured from a Gaussian curve and the ΔH were obtained from curves which varied in shape from Gaussian to Lorentzian. No corrections were introduced to compensate for this change in line shape. The radical-exciton exchange activation energies are of the same order of magnitude as the exciton-exciton exchange activation energies. The important observation is that there is an exchange interaction between the excitons and radicals.

The exciton concentrations and radical concentrations may be calculated using the singlet triplet activation energy, J. The exciton

concentration, C_t, is

$$C_t = \frac{N_t}{N_t + N_S} = \frac{3}{3 + \exp(J/kT)} \approx 3 \exp(-J/kT) \qquad (5)$$

where N_t and N_S are the number of triplets and singlets present and $J = 0.065$ ev. The number of radicals present may be determined by comparing the integrated free radical ESR signal intensity, I_r, with the exciton signal intensity, I_t; providing the signals are not saturated. The ESR signal intensities are not, of course, proportional only to the number of excitons and radicals present, but are also proportional to the ESR transition probabilities and the population differences of the energy levels involved. The number of radicals, N_r, is given by the relation

$$N_r = N_t (8 I_r / 3 I_t) \qquad (6)$$

where the factor of 8/3 or $1(1 + 1)/\frac{1}{2}(\frac{1}{2} + 1)$ represents the combined effects of the transition probabilities and Boltzman population differences on the radical and triplet state ESR signal intensities (neglecting the small fine structure and hyperfine structure perturbations on the Zeeman Hamiltonian).[10] The exciton signal intensity, I_t, includes both high field lines (the doublet of Fig. 1) but does not include the half field line.

The definition of the radical concentration, C_r, which we will use is

$$C_r \equiv N_r/(N_t + N_S) = C_t (8 I_r / 3 I_t) \qquad (7)$$

This is an arbitrarily defined spin concentration. A more conventional definition of C_r is the number of radicals divided by the total number of

centers which could produce radicals. If the free radical is derived from one TCNQ molecule the radical concentration, by this definition, is $N_r/4\,(N_t + N_s) = C_t\,(2\,I_r/3\,I_t)$ because each exciton is associated with four TCNQ molecules.[12] If, however, the radical is associated with two TCNQ units or with the phosphorous or arsenic atoms, then this ratio is increased slightly.

The ratio I_r/I_t may be obtained from peak to peak widths (w) and heights (h) of the ESR derivative spectra, since the radical and exciton line shapes are known. At 77°K the central radical line is Gaussian and the exciton lines are Lorentzian, so that

$$I_r/I_t = 0.517\ w_r^2 h_r/1.814\ w_t^2 h_t \qquad (8)$$

where r and t refer to the radical and triplet exciton, respectively, and the multiplicative constants are the standard absolute intensity conversion factors for these line shapes. Using Eq. (7) and Eq. (8) the radical concentrations in the crystals of Figs. 1 and 3 are 1.6% and 0.3%, respectively. The radical concentration in the X-irradiated $(\varphi_3 AsCH_3)^+(TCNQ)_2^-$ crystal is 0.8%. The exciton concentrations at 77°, 128°, 148°, and 176°K are 0.02%, 0.8%, 1.8%, and 4.0%, respectively. Although no detailed discussion is presented here, these results support the idea that the triplet excitons are mobile; if the triplets were immobile and localized, it is difficult to account for the homogeneous broadening of the entire free radical signal at these radical and triplet concentrations.

D. ANISOTROPY OF EXCITON AND RADICAL LINE WIDTHS

The radical and high field exciton line widths are plotted as a function of angle in Fig. 5. The line widths were measured from the peak positions of the derivative curves. The crystal was rotated about its long diagonal and $\theta = 0°$ corresponds roughly to the magnetic field being perpendicular to the large face of the crystal. Some points were recorded over the entire range, $0° \leq \theta \leq 360°$. Most of the points of Fig. 5, however, were recorded over the range $0° \leq \theta \leq 180°$ and plotted twice; once for θ and once for $180° + \theta$. To determine the experimental line shape, Gaussian and Lorentzian lines with the same w and h as the experimental spectra were calculated at intervals of $\theta = 30°$ over the range $0° \leq \theta \leq 360°$. The exciton fine structure splitting became small in the regions $30° < \theta < 60°$ and $120° < \theta < 150°$ (and corresponding $\theta + 180°$ regions) and no line shape information was obtained because of the overlapping of lines. Some of the ESR spectra at other orientations were slightly asymmetric but there is little doubt that the radical lines are Gaussian and the exciton lines are Lorentzian. The exciton line of Fig. 6, for example, coincides with the Lorentzian curve and the radical line of Fig. 6 coincides with the Gaussian curve. The Gaussian and Lorentzian lines are obviously poor approximations to the experimental exciton and radical lines, respectively, of Fig. 6. This $(\varphi_3 AsCH_3)^+ (TCNQ)_2^-$ crystal was not X-irradiated and the radical concentration calculated from Eqs. (7) and (8) is 0.04%.

The striking feature of Fig. 5 is that the exciton and radical line

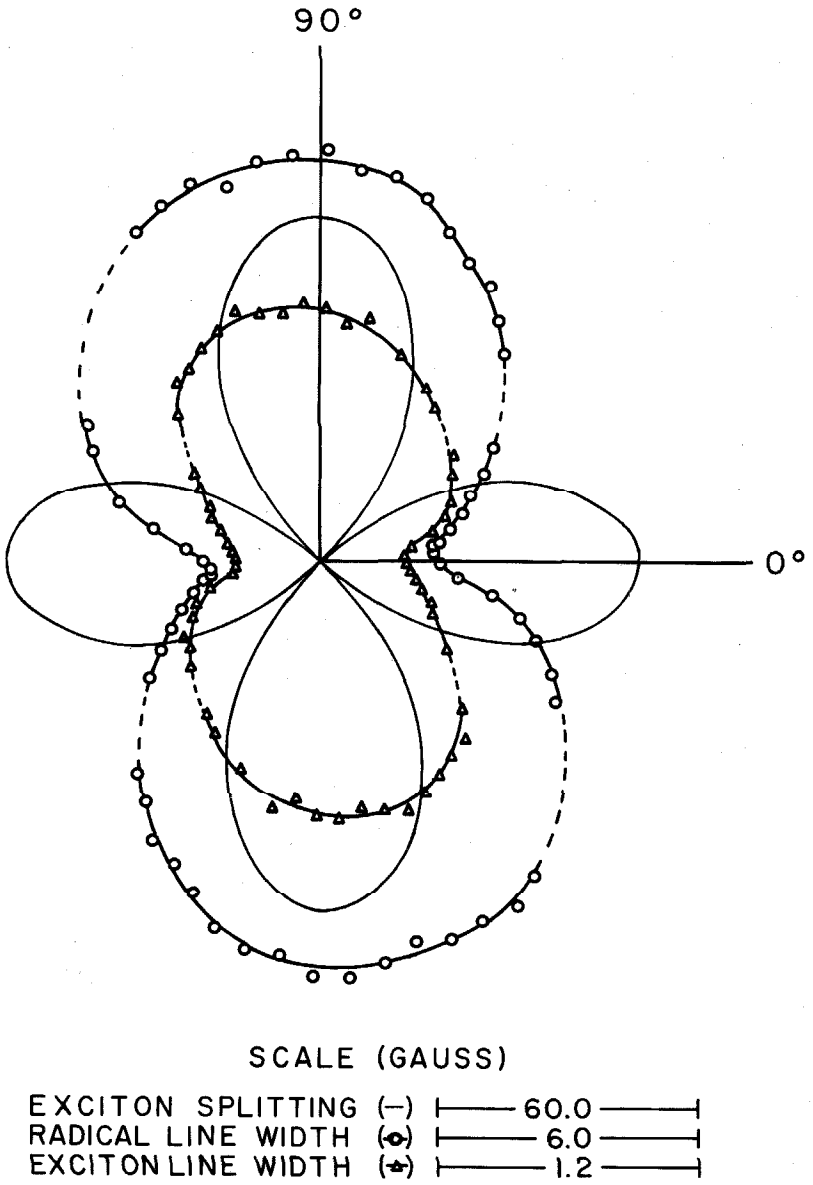

Figure 5

The 77°K exciton and radical line widths as a function of angle in an arbitrary plane of a $(\phi_3 AsCH_3)^+ (TCNQ)_2^-$ crystal.

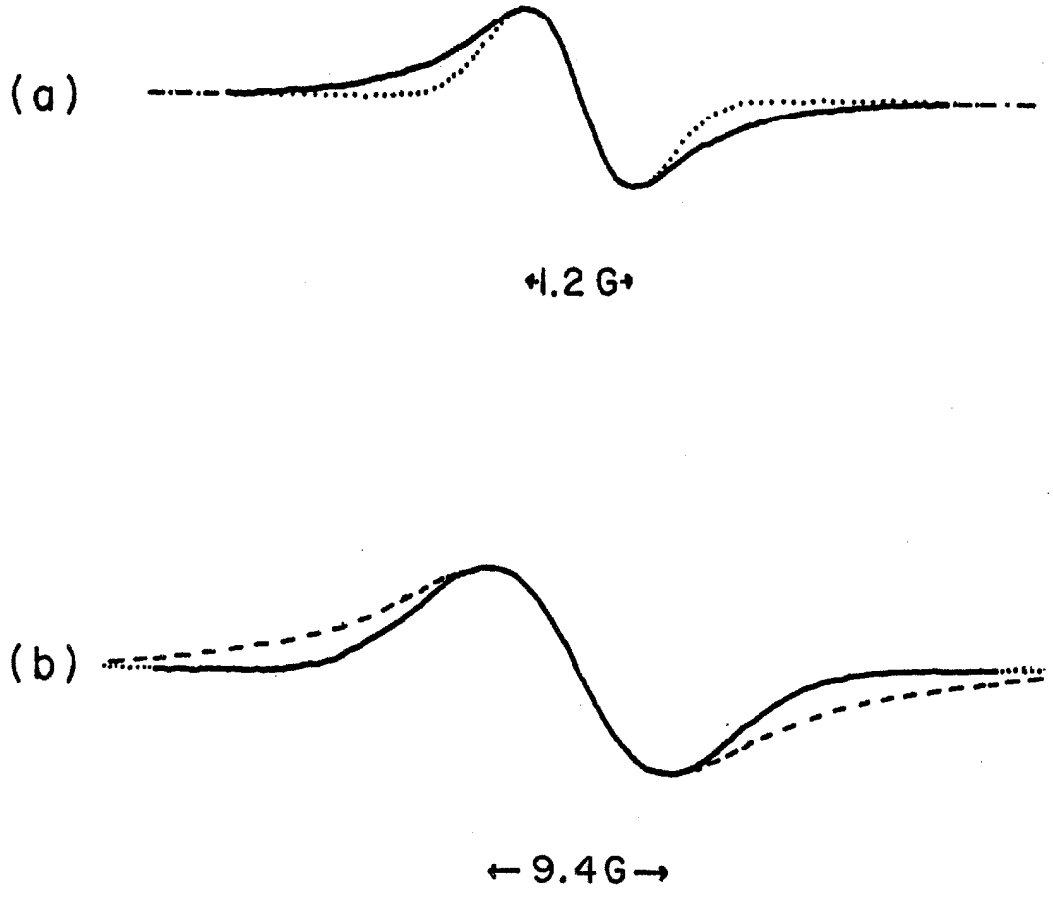

Figure 6

The (a) exciton and (b) radical ESR lines at the 90° orientation of Fig. 5. The Lorentzian (---) and Gaussian (···) lines are superimposed on both ESR spectra.

width anisotropies are approximately the same. If the radical is associated with the TCNQ units this observation strongly suggests that nuclear hyperfine interactions contribute to the exciton line width. Another possible source of exciton line width anisotropy is crystal disorder. The exciton lines will be inhomogeneously broadened if the angle between the magnetic field direction and the molecular axes are not the same for all molecules of the lattice [see Eq. (21) of Appendix III]. This effect will be most pronounced when the fine structure splitting is changing most rapidly with angle. In Fig. 5 this corresponds, for example, to the ~ 40° orientation. The minimum inhomogeneous broadening occurs near the 0° and 90° positions where the rate of change of the fine structure splitting with angle is small. The maximum exciton line width corresponds to the 90° position, however, and therefore crystal disorder does not account for the line width anisotropy and probably does not contribute significantly to the exciton line width.

The precise nature of the radical (or radicals) is not known. Small concentrations of free radical impurities are always present in crystals of I and II. The impurity could be TCNQ or $(TCNQ)_2$ radicals which did not pair up to form triplets. The impurity signals are apparently not associated with φ_3PCH_3 or φ_3AsCH_3, since the hyperfine structure in I and II are very similar. The X-irradiation of I and II had very little effect on the radical hyperfine structure. One possible result of the X-irradiation is to create $S = \frac{1}{2}$ damage sites which pair up with one of the two (initially paired) TCNQ units to form a singlet state plus the other TCNQ radical. The observation of very little change in hyper-

fine structure is consistent with this mechanism.[12] In any case, the radicals appear to be either TCNQ, $(TCNQ)_n$ or some impurity which is derived from TCNQ.

If one assumes that the instantaneous nuclear hyperfine structure of the exciton is the same as the hyperfine structure of the radical (e. g. TCNQ) and that this structure determines the exciton line width, an estimate of the diffusional exciton jump rate τ^{-1} can be obtained from the relation $\tau^{-1} \approx 3^{\frac{1}{2}} \pi A^4/W_{hf}^3$, where A is the hyperfine line width of an excitation on a single site and W_{hf} is the observed exciton line width (defined as one half the width at the peak points of the derivative curve).[7] From Fig. 5, $W_{hf} \sim 1$ Mc/sec and for TCNQ, A ~ 30 Mc/sec, giving $\tau^{-1} \sim 10^{12}$ sec^{-1}.[7] The same estimate is obtained from zero field data by an independent method.[7] Deuteration experiments are in progress which should test whether the dominant contribution to the exciton line width is nuclear hyperfine structure.

ACKNOWLEDGEMENTS

We are indebted to Dr. D. B. Chesnut and Dr. H. Keller for crystals of $(\varphi_3AsCH_3)^+(TCNQ)_2^-$ and $(\varphi_3PCH_3)^+(TCNQ)_2^-$. We wish to thank Dr. D. Pooley for assistance during the first stages of this work and Dr. D. D. Thomas for helpful discussions.

REFERENCES

1. D. S. Acker and W. R. Hertler, J. Am. Chem. Soc. 84, 3370 (1962).

2. D. B. Chesnut and W. D. Phillips, J. Chem. Phys. 35, 1002 (1961).

3. M. T. Jones and D. B. Chesnut, J. Chem. Phys. 38, 1311 (1963).

4. H. M. McConnell and R. Lynden-Bell, J. Chem. Phys. 36, 2392 (1962).

5. H. Sternlicht and H. M. McConnell, J. Chem. Phys. 35, 1793 (1961).

6. R. M. Lynden-Bell and H. M. McConnell, J. Chem. Phys. 37, 794 (1962).

7. D. D. Thomas, A. W. Merkl, A. F. Hildebrandt, and H. M. McConnell, J. Chem. Phys. 40, 2588 (1964).

8. D. D. Thomas, Ph. D. Thesis, California Institute of Technology (1964).

9. A preliminary account of this work has been published [H. M. McConnell, O. H. Griffith, and D. Pooley, J. Chem. Phys. 36, 2518 (1962)].

10. D. J. E. Ingram, Free Radicals as Studied by Electron Spin Resonance (Butterworths Scientific Publications, London, 1958).

11. The exciton lines are Lorentzian near liquid nitrogen temperatures. As the temperature is increased the lines become asymmetric because of the overlapping of lines. Although no checks were made,

the individual exciton lines at these higher temperatures are almost certainly Lorentzian.

12. This is a result of the stoichiometry of the crystal and does not imply that the exciton is delocalized over four units.

13. It is desirable to determine the increase in radical concentration after X-irradiation. This was not done in these preliminary experiments because the method used to mount the crystal made it difficult to perform two experiments on the same crystal (one before and the other after X-irradiation).

APPENDIXES

I. SUPPLEMENTARY REMARKS ON APPARATUS AND METHODS

The general apparatus used for these experiments included a vacuum system, several crystal growers and zone refiners, a low temperature gas flow system, X-ray equipment, two metal dewars, and other auxiliary equipment. Much of this apparatus was not designed by any one individual. When appropriate, we will attempt to mention the names of the contributors and to cite references in which some of the apparatus is described in more detail. The basic commercial equipment used was a Varian X-band ESR spectrometer and a General Electric XRD-5 X-ray unit.

The vacuum system was of conventional design except that low-temperature U-tubes were used to prevent contamination of the samples by pump oil and stopcock grease. The use of the zone refining technique was suggested to us by S. B. Berger. The zone refiners consisted of alternating heating elements and water-cooled copper coils. The theory and applications of zone refiners are discussed by W. G. Pfann.[1] Two heating elements housed in an insulated box (usually a drying oven) were used to grow crystals from the melt. These crystal growers are merely devices to insure the existence of equilibrium conditions between a solid-liquid interface. The basic rule in the design of crystal growers of this type is that a large temperature gradient across the interface produces the best crystals. This may be easily achieved by passing the compound, sealed in glass,

through two heated metal tubes placed end to end; one maintained at temperatures well above and the other at temperatures well below the melting point of the compound. D. E. Wood was also involved in the research requiring these techniques and drawings of typical zone refiners and crystal growers may be found in his thesis.[2] Low speed (approximately one revolution per day) synchronous motors suitable for drawing the Pyrex sample tubes through the zone refiners or crystal growers may be purchased from the Minarik Electric Co. of Los Angeles.

These crystal growers and zone refiners were used only in Section V of this thesis (and in a depressing number of unsuccessful experiments involving single crystals of purified aromatic hydrocarbons). The crystals of Sections I through IV were grown either by evaporation or by slow cooling of solutions. The slow cooling was easily achieved by placing a flask filled with the saturated solution in a Pyrex dewar. The dewar was partially filled with an alcohol-water mixture to increase the heat capacity of the system and was then placed in a refrigerator or cold room. The rate of cooling was controlled by varying the heat capacity and dimensions of the dewar. The room temperature solutions were usually cooled to 273°K in a quart dewar over a period of three days. Single hexagonal crystals 3mm x 15mm frequently were obtained by this method.

The crystals were subjected to X-irradiation from a tungsten target AEG-50S Machlett Tube powered by the GE-XRD-5 X-ray unit. Frequently it was desirable to X-irradiate the crystals at liquid

nitrogen temperatures and the device used for this purpose is shown in Fig. 1. Basically this is a copper platform soldered to a good heat conductor which is surrounded by liquid nitrogen. The ring near the bottom of the copper tube centers the heavy tube and prevents the platform from crushing the glass dewar when the dewar is tilted. There is a teflon collar on the bottom of the tube to protect the dewar. The holes in the side of the tube are necessary to allow the nitrogen gas to escape. The groove in the platform was used in early powder experiments; a portion of the sealed quartz tube holding the powder was shielded from the X-rays by the copper block and the powder was transferred to this part of the tube after X-irradiation (otherwise the color centers of quartz would dominate the ESR spectra). For single crystals the dewar was filled with liquid nitrogen, the copper platform was lowered into the dewar using the handle shown in Fig. 1, more liquid nitrogen was added, and the crystal was placed on the platform. A thin disk of Styrofoam insulated all of the top except the X-ray path and the entire top was covered with Saran Wrap to prevent ice from forming around the crystal.

The two liquid-helium dewars used are shown in Figs. 2 and 3. The basic design of the stainless steel cylinders of these dewars was provided by Professors G. W. Robinson and H. M. McConnell. The dewar of Fig. 1 was used for variable temperature studies of Sections I and VI. The evacuated microwave cavity is located near the bottom of this dewar and the waveguide tubing passes up through the liquid helium reservoir. A vacuum space and nitrogen reservoir surround

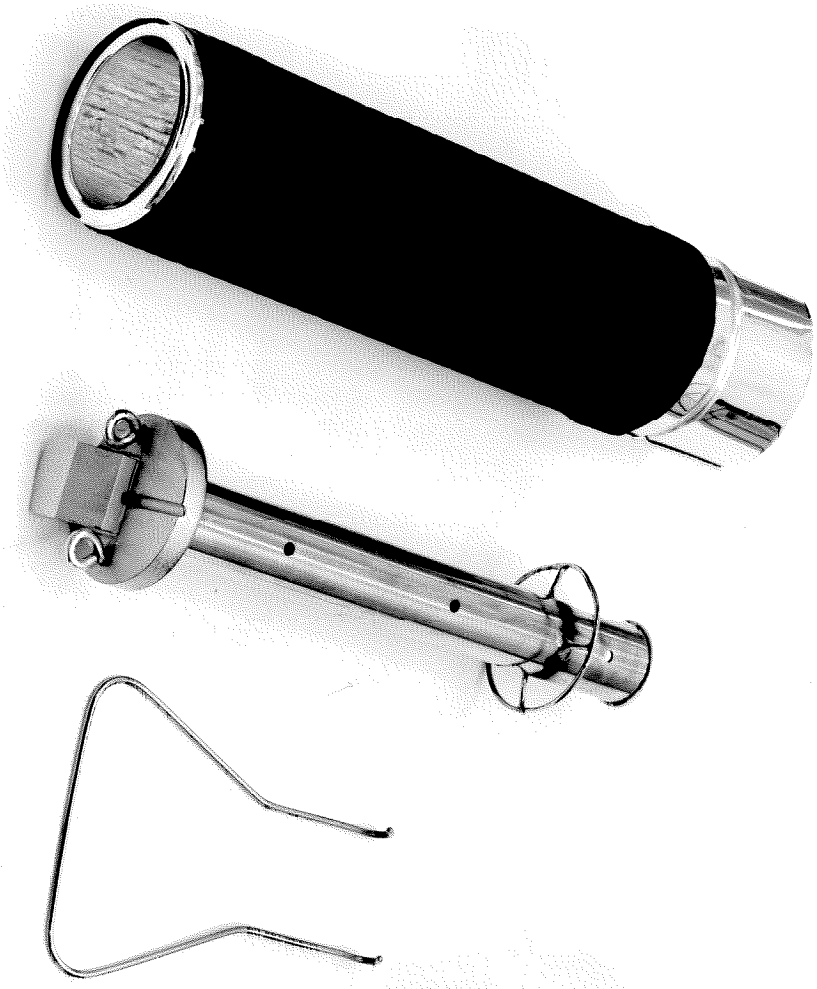

Figure 1

Copper platform for the X-irradiation of crystals at 77°K.

the helium reservoir. The cavity and iris tuning screw are mounted on the bottom of the helium reservoir and are, therefore, subject to drastic changes in temperature. This creates a serious noise problem because snug-fitting components loosen at low temperatures and undergo mechanical vibration. At the suggestion of A. F. Hildebrandt, a double modulation scheme was used to decrease the noise level. D. E. Wood later made very significant improvements in the cavity and crystal mounting scheme.[2] A. L. Kwiram and W. W. Schuelke contributed many suggestions during all phases of dewar design and modification.

The cold finger dewar of Fig. 3 has the advantage that the cavity and tuning screw are always at room temperature. It is only useful, however, for experiments performed at the boiling points of nitrogen, helium, or a few other liquids. A. L. Kwiram designed the base of the dewar, a metal cold finger which forms part of the helium reservoir, and a copper heat shield which is fastened to the nitrogen reservoir. The heat shield, quartz outer jacket, and brass base plate are shown, along with the lower portion of the dewar, in Fig. 3. Drawings of these and other parts may be found in A. L. Kwiram's thesis.[3] For experiments involving organic crystals, radiative heating of the sample mounted on the metal cold finger proved to be a serious problem. We therefore substituted a quartz finger for the metal finger (Fig. 3) and mounted the sample, on a rod extending through the dewar to the lower part of the cold finger. The quartz finger is attached through a quartz-Pyrex graded seal to a

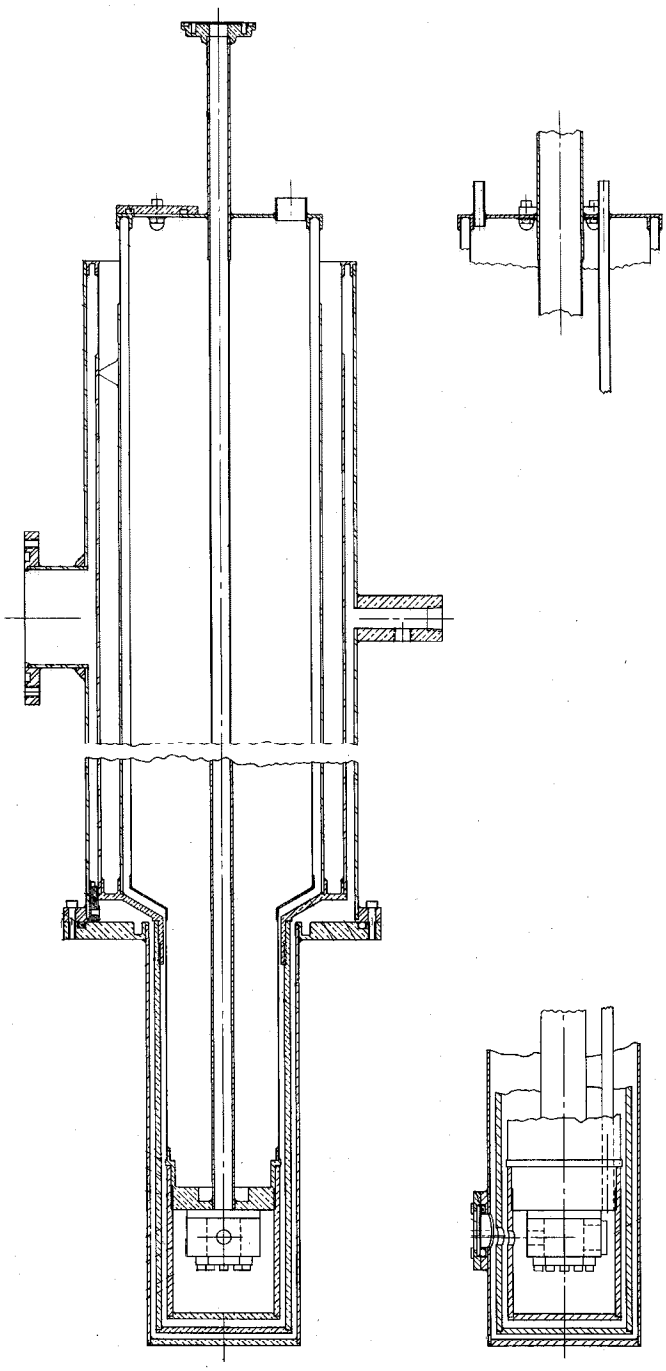

Figure 2

Magnetic resonance dewar.

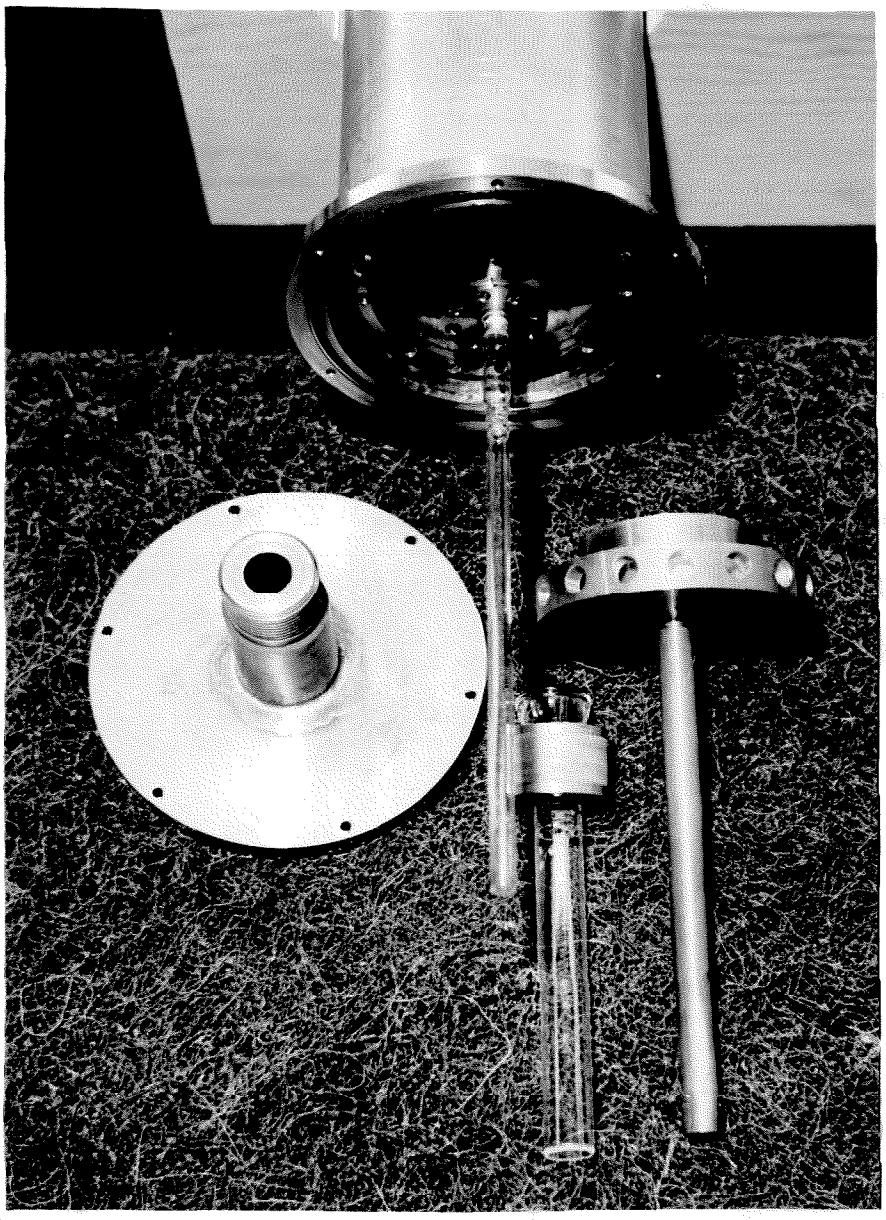

Figure 3

Cold finger dewar.

Pyrex-Kovar seal. Kovar metal-to-glass seals vary in durability. We obtained excellent results using seals made by Glass Instruments of Pasadena. The quartz finger was etched with hydrofluoric acid to reduce the outside diameter (the quartz jacket, copper shield, and cold finger must fit into the microwave cavity). The closed end of the finger consists of a quartz window which is fused onto the finger. This window was originally designed for use with u.v. irradiation from beneath the dewar. However, we found that it was almost impossible to avoid trapping a few crystals of ice on the inside of the window and these crystals, of course, scattered the light. In subsequent experiments, the light was passed through the side of the cold finger.

The cold finger is soldered to a flange and the flange is screwed onto the dewar. An indium wire gasket forms a helium-tight seal between the flange and the dewar. Soldering the cold finger onto the flange presents a problem because the cylinders of the dewar are not exactly concentric. This makes it difficult to center the long cold finger inside the nitrogen hear shield (which is screwed into a different set of cylinders). The problem was solved by soldering the finger into the flange with the flange, finger, and nitrogen shield all in place. A low-temperature, somewhat flexible solder was needed and indium solder (or indium wire) obtained from the Indium Corporation of America was quite satisfactory. A heating element was placed inside the upper end of the cold finger and the dewar was assembled. The indium was melted, the cold finger centered, and

the seal was allowed to cool. The heating element was then removed through the top of the dewar leaving the dewar ready for use.

The cold finger dewar was used for some preliminary experiments of Sections I and V, and several experiments not reported in this thesis. A few of these experiments required X-irradiation of the sample at liquid helium temperatures. In order to do this, a small portion of the nitrogen shield was removed and the X-rays were directed through the thin quartz walls of the jacket and cold finger and onto the sample. The sample was then lowered to the bottom of the cold finger for the ESR experiments. The majority of the ESR results of Sections II - V were, however, obtained with a conventional gas-flow system. Nitrogen gas was passed through a copper coil immersed in liquid nitrogen. The cold gas then passed through a small quartz dewar containing the crystal. Pressure differentials across the copper coil are to be avoided. When the pressure inside the coil becomes excessive, some of the nitrogen liquefies and the spray of nitrogen droplets creates an extremely high noise level. This may be easily avoided by using shorter coils or larger diameter tubing (we used four to six feet of 1/4" O.D. copper tubing). The helium gas-flow system mentioned in Section II was also frequently used. G. R. Liebling has designed a small quartz dewar and sample holder for use with gas-flow systems[4] and many of the results were obtained with this dewar.

The numerical calculations were performed with an IBM 7094 computer. The C.I.T. library matrix diagonalization subroutine

EIGVV[5] was used for the Hückel and McLachlan calculations of Section II. EIGVV uses Share subroutine NYEVV of Share Distribution 339 to accomplish the solution (see Share NYEVV write-up for details of the method). The procedure followed in these spin density calculations was to advance the parameter $\underline{h}$ in incremental units over the range $0 \leq \underline{h} \leq 3$. For each value of $\underline{h}$, the value of $\underline{k}$ was advanced over the range $0 \leq \underline{k} \leq 3$ (using a nest of DO loops). The computer then diagonalized one 3×3 matrix for each of these combinations of $\underline{h}$ and $\underline{k}$. It was a simple matter to manually pick out the desired spin density values from the range of values listed in the computer output.

The penetration integrals of Section III were evaluated by summing over nuclear attraction integrals and coulomb integrals obtained from programs generously made available by R. M. Pitzer. The overlap integral program was kindly provided by M. S. Itzkowitz. The zero field parameter calculations of Section V were performed with the aid of C.I.T. library subroutine MULLER.[5] This subroutine finds the real and complex roots of a polynomial with real coefficients. All other calculations associated with this thesis were made with short routines written in Fortran IV.

REFERENCES

1. W. G. Pfann, Zone Melting (John Wiley and Sons, New York, 1958).
2. D. E. Wood, Ph.D. Thesis, California Institute of Technology, (1964).

3. A. L. Kwiram, Ph.D. Thesis, California Institute of Technology, (1963).

4. G. R. Liebling, Ph.D. Thesis, California Institute of Technology, (1965).

5. Programmers' Manual (Booth Computing Center, California Institute of Technology, 1964).

II. ETHER RADICAL CI MATRIX ELEMENTS

From Eqs. (7), (8), and (12) of Section III, the matrix elements of the linear variational function (III - 11) are:

$$H_{11} = \langle \Psi_1 | H | \Psi_1 \rangle = 2I_1 + I_2 + J_{11} + 2J_{12} - K_{12}$$

$$H_{22} = \langle \Psi_2 | H | \Psi_2 \rangle = I_1 + 2I_2 + J_{22} + 2J_{12} - K_{12}$$

$$H_{12} = \langle \Psi_1 | H | \Psi_2 \rangle = -I_{12} - L_{12} - L_{21}$$

where

$$I_1 = \langle \phi_1(1) | \mathcal{H}_{CORE}(1) | \phi_1(1) \rangle = 2^{-1}(1 + S)^{-1} \times [\alpha_C^{CORE} + \alpha_O^{CORE} + \beta_{CO}^{CORE} + \beta_{OC}^{CORE}]$$

$$I_2 = \langle \phi_2(1) | \mathcal{H}_{CORE}(1) | \phi_2(1) \rangle = 2^{-1}(1 - S)^{-1} \times [\alpha_C^{CORE} + \alpha_O^{CORE} - \beta_{CO}^{CORE} - \beta_{OC}^{CORE}]$$

$$I_{12} = \langle \phi_1(1) | \mathcal{H}_{CORE}(1) | \phi_2(1) \rangle = 2^{-1}(1 - S^2)^{-\frac{1}{2}} \times [\alpha_C^{CORE} - \alpha_O^{CORE} + \beta_{CO}^{CORE} - \beta_{OC}^{CORE}]$$

$$J_{11} = \langle \phi_1(1)\phi_1(1) | \frac{1}{r_{12}} | \phi_1(2)\phi_1(2) \rangle = 2^{-2}(1 + S)^{-2} \times [(CC|CC) + (OO|OO) + 2(CC|OO) + 4(CC|CO) + 4(OO|CO) + 4(CO|CO)]$$

$$J_{22} = \langle \phi_2(1)\phi_2(1) | \frac{1}{r_{12}} | \phi_2(2)\phi_2(2) \rangle = 2^{-2}(1 - S)^{-2}$$

$$\times \; [(CC|CC) + (OO|OO) + 2(CC|OO) - 4(CC|CO)$$

$$-4(OO|CO) + 4(CO|CO)]$$

$$J_{12} = \langle \phi_1(1)\phi_1(1) | \frac{1}{r_{12}} | \phi_2(2)\phi_2(2) \rangle = 2^{-2}(1 - S^2)^{-1}$$

$$\times \; [(CC|CC) + (OO|OO) + 2(CC|OO) - 4(CO|CO)]$$

$$K_{12} = \langle \phi_1(1)\phi_2(1) | \frac{1}{r_{12}} | \phi_1(2)\phi_2(2) \rangle = 2^{-2}(1 - S^2)^{-1}$$

$$\times \; [(CC|CC) + (OO|OO) - 2(CC|OO)]$$

$$L_{12} = \langle \phi_1(1)\phi_1(1) | \frac{1}{r_{12}} | \phi_1(2)\phi_2(2) \rangle = 2^{-2}(1 + S)^{-1}(1 - S^2)^{-\frac{1}{2}}$$

$$\times \; [(CC|CC) - (OO|OO) + 2(CC|CO) - 2(OO|CO)]$$

$$L_{21} = \langle \phi_2(1)\phi_2(1) | \frac{1}{r_{12}} | \phi_2(2)\phi_1(2) \rangle = 2^{-2}(1 - S)^{-1}(1 - S^2)^{-\frac{1}{2}}$$

$$\times \; [(CC|CC) - (OO|OO) - 2(CC|CO) + 2(OO|CO)]$$

and, for example,

$$(CC|OO) \equiv \langle \chi_C(1)\chi_C(1) | \frac{1}{r_{12}} | \chi_O(2)\chi_O(2) \rangle$$

$$\alpha_C^{CORE} \equiv \langle \chi_C(1) | \mathcal{H}_{CORE}(1) | \chi_C(1) \rangle$$

$$\beta_{CO}^{CORE} \equiv \langle \chi_C(1) | \mathcal{H}_{CORE}(1) | \chi_O(1) \rangle$$

There are similar definitions for the remaining integrals.

The normalized coefficients of the linear variational function are

$$C_1 = [H_{12}^2 + (H_{11} - E)^2]^{\frac{1}{2}}(-H_{12})$$

$$C_2 = [H_{12}^2 + (H_{11} - E)^2]^{\frac{1}{2}}(H_{11} - E)$$

where E is the energy appearing in the secular determinant. Applying the Mulliken approximation and collecting terms, one finds

$$H_{12} = 2^{-1}(1 - S^2)^{-\frac{1}{2}}[\alpha_O^{CORE} - \alpha_C^{CORE} + (OO|OO) - (CC|CC)]$$

and

$$(H_{11} - E) = \beta + (\beta^2 + H_{12}^2)^{\frac{1}{2}}$$

The problem has now been reduced to the evaluation of the atomic core, overlap, and coulomb integrals. These integrals may be estimated by the method of Goeppert-Mayer and Sklar (reference 21 of Section III). It is well known, however, that the results obtained for hydrocarbons are unreliable and there is every reason to believe they would also be unreliable for the ether radical. Therefore, an extension of the method of Parisier and Parr was used. This approach is outlined in Section III.

III. RADICAL AND TRIPLET SPIN HAMILTONIANS

A. RADICAL HYPERFINE STRUCTURE HAMILTONIAN

The electron nuclear hyperfine Hamiltonian is

$$\mathcal{H} = |\beta|\underset{\sim}{S}\cdot\underset{\sim}{g}\cdot\underset{\sim}{H} - g_N\beta_N\mathrm{III}_H + hS_HI_Ha_0 + h(\underset{\sim}{S}\cdot\underset{\sim}{b}\cdot\underset{\sim}{I}) \qquad (1)$$

(see reference 16 of Section I). $\underset{\sim}{H}$,$\underset{\sim}{S}$, and $\underset{\sim}{I}$ are the magnetic field vector, electron spin angular momentum operator, and nuclear spin angular momentum operator, respectively. S_H and I_H are the components of $\underset{\sim}{S}$ and $\underset{\sim}{I}$ along $\underset{\sim}{H}$, and $\underset{\sim}{g}$ is the spectroscopic splitting factor tensor. The four terms of the Hamiltonian are, from left to right, the electron Zeeman term, the nuclear Zeeman term, the isotropic electron-nuclear contact term, and the anisotropic electron-nuclear dipolar term. The Hamiltonian matrix may be diagonalized by a procedure similar to the one used with the general triplet state Hamiltonian (see below). For the π-electron radicals in a magnetic field of $\sim$ 3 kilogauss, however, $\nu_e \gg |a|, |b|$ (where $\nu_e = h^{-1}g|\beta|H$) and therefore it is convenient to quantize the electron spin along the magnetic field direction. The Hamiltonian appropriate for the "intermediate magnetic field" case is

$$\mathcal{H} = g|\beta|HS_H - g_N\beta_NHI_H + hS_HI_Ha_0 + hS_H(\underset{\sim}{e_H}\cdot\underset{\sim}{b}\cdot\underset{\sim}{I}) \qquad (2)$$

where $\underset{\sim}{e_H}$ is a unit vector in the direction of the magnetic field. The g value of Eq. (2) has been taken to be isotropic because the g value

anisotropies of π-electron radical spectra are small and do not appreciably affect the magnitude of the ESR splittings.

McConnell, Heller , Cole, and Fessenden have determined the splittings from Eq. (2). The interested reader is directed to reference 16 of Section I for the details on the method (see also reference 3 of Appendix I). The hyperfine splitting d is given by

$$d^2 = \underset{\sim}{e}_H \cdot \underset{\sim}{\underset{\sim}{T}}^2 \cdot \underset{\sim}{e}_H \tag{3}$$

where

$$T = \begin{pmatrix} B & O & O \\ O & C & O \\ O & O & A \end{pmatrix}$$

and B, C, and A are the diagonal elements of the dipolar tensor plus the isotropic coupling constant, a_o . For an α proton bonded to a carbon atom having unit π-electron spin density, B, C, and A are on the order of -60, -90, and -30 Mc/sec. In Eq. (3) we have omitted the contribution from the nuclear Zeeman term because it has only a small effect on the splittings discussed in Sections I-IV. In polar coordinates, Eq. (3) becomes

$$d^2 = \sin^2\theta(B^2\cos^2\phi + C^2\sin^2\phi) + A^2\cos^2\theta \tag{4}$$

where θ is the angle between the $\dot{C}$-H_α bond and $\underset{\sim}{e}_H$, and $\phi$is the angle between the axis of the carbon 2p orbital and the projection of $\underset{\sim}{e}_H$ onto a plane perpendicular to the C-H_α bond.

In the "ultra high field" region where ν_e, $\nu_n \gg |a|, |b|$ (and

$\nu_n = h^{-1} g_n \beta_n H$), Eq. (2) becomes

$$\mathcal{H} = g|\beta| H S_H + h S_H I_H a_0 + h S_H I_H (\underset{\sim}{e}_H \cdot \underset{\sim}{b} \cdot \underset{\sim}{e}_H) \tag{5}$$

and for this case,

$$d \approx \underset{\sim}{e}_H \cdot \underset{\sim}{T} \cdot \underset{\sim}{e}_H \tag{6}$$

Although Eq. (6) is not strictly applicable for the ~3 KG magnetic field used in X-band ESR, Eq. (7) is frequently a good approximation to the ESR splittings. The α-proton coupling constant formulas in Sections I, II, and III are obtained from Eq. (4) or Eq. (6). In Section IV the tensor was obtained from the ESR splittings by essentially the reverse of the above procedure. The details of this method are given in reference 3 of Appendix I.

B. TRIPLET STATE FINE STRUCTURE HAMILTONIAN

The spin Hamiltonian which adequately describes the electron spin resonance fine structure splittings of a molecule in the triplet state is[1,2]

$$\mathcal{H} = (H_x g_{xx} S_x + H_y g_{yy} S_y + H_z g_{zz} S_z) + D S_z^2 + E(S_x^2 - S_y^2) \tag{7}$$

where D and E are the dipolar zero field splitting parameters. The three spin functions

$$\Psi_a = 2^{-\frac{1}{2}} (\alpha\alpha + \beta\beta)$$

$$\Psi_b = 2^{-\frac{1}{2}} (\alpha\beta + \beta\alpha)$$

and $$\Psi_c = 2^{-\frac{1}{2}}(\alpha\alpha + \beta\beta)$$

are eigenfunctions of $DS_z^2 + E(S_x^2 - S_y^2)$ with eigenvalues D + E, O, and D - E, respectively. These three functions form a convenient basis set for diagonalizing the Hamiltonian matrix. For example, if H is parallel to the x axis, the secular determinant becomes

$$\begin{array}{c|ccc|} & \Psi_a & \Psi_b & \Psi_c \\ \Psi_a & (D+E) - E & g_{xx}\beta H & O \\ \Psi_b & g_{xx}\beta H & -E & O \\ \Psi_c & O & O & (D-E) - E \end{array} = 0$$

Solving gives

$$E_0 = (D\text{-}E)\ ,\quad E_{\pm} = \tfrac{1}{2}(D + E) \pm [(g_{xx}\beta H)^2 + \tfrac{1}{4}(D + E)^2]^{\frac{1}{2}} \qquad (8)$$

hence

$$h\nu = \Delta E = (E_+ - E_0) = -\tfrac{1}{2}(D - 3E) + [(g_{xx}\beta H)^2 + \tfrac{1}{4}(D + E)^2]^{\frac{1}{2}} \qquad (9)$$

$$h\nu = \Delta E = (E_0 - E_-) = -\tfrac{1}{2}(D - 3E) + [(g_{xx}\beta H)^2 + \tfrac{1}{4}(D + E)^2]^{\frac{1}{2}} \qquad (10)$$

Expanding the square root in a Taylor's series and subtracting Eq. (9) from Eq. (10) gives the useful Eq. (11). Similarly, adding Eq. (9) to Eq. (10) yields Eq. (12). Similar results are obtained with H ∥ y and H ∥ z. We have restricted the discussion to the transitions occurring between E_0 and E_+ and between E_- and E_0. These $\Delta m = \pm 1$ transitions are allowed when the r.f. magnetic field is perpendicular to the constant field (as is the case for all of the experiments

reported in this thesis). The half field transition between E_- and E_+ ($\Delta m = \pm 2$) is allowed when the r.f. field is polarized parallel to the H field. The $\Delta m = \pm 2$ transitions have been observed for the TCNQ ion radical salts of Section VI but were not investigated in this work (see reference 1 of Section VI). The $\Delta m = \pm 2$ transitions have been extensively discussed by van der Waals and de Groot.[3,4]

All of the energy levels and equations used to obtain the zero field parameters from experimental $\Delta m = \pm 1$ transitions are listed below.

H ∥ x

$$E_0 = (D - E), \quad E_\pm = \tfrac{1}{2}(D + E) \pm [(g_{xx}\beta H)^2 + \tfrac{1}{4}(D + E)^2]^{\frac{1}{2}} \tag{8}$$

$$(D - 3E) = g_{xx}\beta(H_2 - H_1) + \frac{(D + E)^2}{8g_{xx}\beta}\left(\frac{H_1 - H_2}{H_1 H_2}\right) + \ldots \tag{11}$$

$$g_{xx} = \frac{2h\nu - \frac{(D + E)^2}{8g_{xx}\beta}\left(\frac{H_1 + H_2}{H_1 H_2}\right)}{\beta(H_1 + H_2)} + \ldots \tag{12}$$

H ∥ y

$$E_0 = (D + E), \quad E_\pm = \tfrac{1}{2}(D - E) \pm [(g_{yy}\beta H)^2 + \tfrac{1}{4}(D - E)^2]^{\frac{1}{2}} \tag{13}$$

$$(D + 3E) = g_{yy}\beta(H_2 - H_1) + \frac{(D - E)^2}{8g_{yy}\beta}\left(\frac{H_1 - H_2}{H_1 H_2}\right) + \ldots \tag{14}$$

$$g_{yy} = \frac{2h\nu - \frac{(D - E)^2}{8g_{yy}\beta}\left(\frac{H_1 + H_2}{H_1 H_2}\right)}{\beta(H_1 + H_2)} + \ldots \tag{15}$$

$\underline{H \parallel z}$

$$E_0 = 0, \quad E_{\pm} = D \pm [(g_{zz}\beta H)^2 + E^2]^{\frac{1}{2}} \tag{16}$$

$$D = \frac{g_{zz}\beta}{2}(H_1 - H_2) + \frac{E^2}{2g_{zz}\beta}\left(\frac{H_2 - H_1}{H_1 H_2}\right) + \ldots \tag{17}$$

$$g_{zz} = \frac{2h\nu - \frac{E^2}{2g_{zz}\beta}\left(\frac{H_1 + H_2}{H_1 H_2}\right)}{\beta(H_1 + H_2)} + \ldots \tag{18}$$

In Eqs. (11) through (18), H_1 and H_2 are the magnetic fields corresponding to the two $\Delta m = \pm 1$ transitions.

To obtain D and E one first locates the three extreme splittings of the ESR spectra. These three extrema lie in mutually perpendicular directions and correspond to the magnetic x, y, and z axes of the molecule. All six permutations of the axes are assigned to the three extrema and crude values of D and E are calculated from Eqs. (11), (14), and (17) (retaining only the first terms of the expansions and assuming g = 2.0). Four permutations of the axes are immediately eliminated because the value of D (D_{xy}) obtained from Egs. (11) and (14) does not approximately equal the D (D_z) obtained from Eq. (17). The other two permutations differ only in the assignment of the x and y axes and one may accurately obtain D and E using either choice of axes. The crude values of D and E are used to obtain g_{xx}, g_{yy} and g_{zz} from Eqs. (12), (15), and (18). These g values and the initial D_{xy}, D_z, and E are substituted into the right hand side of Eqs. (11), (14), and (17) to obtain improved values of D and E (reference 7 of Section V). This iterative

process produced constant values of D_{xy}, D_z, E, g_{xx}, g_{yy}, and g_{zz} within four or five cycles in the case of pyrene (Section V). The values of D_{xy} and D_z should, of course, be equal within experimental error.

The relative signs are not determined uniquely because an interchange of the x and y axes in Eq. (7) changes the sign of E. One of the two possible choices of axes corresponds to D and E having the same sign and the other choice corresponds to D and E having opposite signs. It is important to assign the correct set of axes once the sign convention has been chosen. This may be done using only one additional orientation of the magnetic field in the xy plane providing the direction of H is not 45° from the x and y axes. One merely compares the calculated splitting at this orientation with the experimental value. Only one choice of the axes will give the correct splitting.

Obtaining the fine structure splitting at an arbitrary orientation of the magnetic field is slightly more complicated because no terms of the secular determinant vanish. Expanding the secular determinant one obtains the general cubic equation

$$E^3 - 2DE^2 + [D^2 - E^2 - (\beta H)^2 (g_{xx}^2 \sin^2\theta \sin^2\phi + g_{yy}^2 \sin^2\theta \cos^2\phi + g_{zz}^2 \cos^2\phi)]E + [(\beta H)^2 \sin^2\theta(\langle D - E\rangle g_{xx}^2 \sin^2\phi + \langle D + E\rangle g_{yy}^2 \cos^2\phi)] = 0 \qquad (19)$$

where θ is the angle between the z axis and $\underset{\sim}{H}$, and ϕ is the angle between the x axis and the projection of $\underset{\sim}{H}$ onto the xy plane. This

cubic equation is easily programmed for a computer. The H field is scanned over a wide range and the quantities $E_+ - E_0$ and $E_0 - E_-$ (and $E_+ - E_-$) are calculated for each choice of H by the computer. Since these energy differences must be equal to $h\nu$, one has only to compare the computed energy differences with the laboratory microwave cavity resonance frequency. This process is needed only once to determine the choice of axes, but was repeated at intervals of every 30° in the xy, yz, and xz planes to compare the calculated splittings of pyrene with the experimental splittings (Section V).

The zero field parameters of the $(\phi_3PCH_3)^+(TCNQ)_2^-$ and $(\phi_3AsCH_3)^+(TCNQ)_2^-$ salts are so much smaller than the microwave quantum (compare 0.006 cm^{-1} to 0.3 cm^{-1}) that a first order perturbation method may be used to simplify the calculation of the fine structure splitting. The details of the method are given in references and of Section VI. One first quantizes the electron spin along the magnetic field direction and relates this new set of axes (x' y' z') to the xyz system using polar angles. Neglecting g-value anisotropies, Eq. (17) becomes in the x' y' z' coordinate system

$$\mathcal{H} = g\beta H S_{z'} + [\tfrac{1}{2}(3\cos^2\theta - 1)D + \tfrac{3}{2}(\sin^2\theta\cos^2 2\phi)E]S_{z'}^2 +$$

$$\text{terms involving } (S_{x'}^2 - S_{y'}^2),\ S^2,\ S_{x'}S_{z'},\ S_{z'}S_{x'},$$

$$S_{y'}S_{z'},\ S_{z'}S_{y'},\ \text{and } (S_{x'}S_{y'} + S_{y'}S_{x'}). \qquad (20)$$

The basis functions used in this case are the three eigenfunctions of S_z

$$|1,1\rangle = \alpha\alpha$$

$$|1,0\rangle = 2^{-\frac{1}{2}}(\alpha\beta + \beta\alpha)$$

$$|1,-1\rangle = \beta\beta$$

The only term of Eq. (20) yielding nonzero first-order corrections to the energy is the S_z^2, term. The fine structure splitting is easily seen to be

$$d = |(3\cos^2\theta - 1)D + 3(\sin^2\theta\cos 2\phi)E| \qquad (21)$$

REFERENCES

1. A. D. McLachlan, Mol. Phys., 6, 441 (1963).
2. H. J. Silverstone, Ph.D. Thesis, California Institute of Technology (1964).
3. J. H. van der Waals and M. S. de Groot, Mol. Phys. 2, 333 (1959).
4. M. S. de Groot and J. H. van der Waals, Mol. Phys. 3, 190 (1960).

PROPOSITIONS

PROPOSITION I

The ion radical salts of tetracyanoquinodimethane (TCNQ) have thermally accessible triplet states removed 0.03 to 0.4 ev from the ground singlet state.[1] The ESR spectra are consistent with the behavior of triplet exciton states rather than localized and immobile triplet states.[2,3] However, since there have been only a few observations of triplet excitons, further experimental evidence for such states is desirable. In this proposition a nuclear magnetic resonance experiment is suggested which should distinguish between localized triplet states and mobile triplet exciton states in ion radical salts.

Nuclear magnetic resonance techniques have been used to determine the magnitudes and signs of the isotropic hyperfine coupling constants, a, of several paramagnetic systems.[4,5] The effective nuclear Hamiltonian is

$$\mathcal{H} = -g_n\beta_n H I_z + a h I_z S_z \qquad (1)$$

If the lifetime τ of the electron spin in a given state is sufficiently short so that $a\tau \ll 1$, the proton will see a single average hyperfine magnetic field $\langle S_z \rangle$ much smaller than the instantaneous value.[6,7] The Hamiltonian becomes in this case

$$\mathcal{H} = -g_n\beta_n H I_z + a h I_z \langle S_z \rangle \qquad (2)$$

and if $kT \gg g_e|\beta_e|H$

$$\langle S_z \rangle = -g_e|\beta_e|S(S+1)H/3kT \qquad (3)$$

Combining Eqs. (2) and (3) one obtains for the constant frequency experiment

$$\Delta H = -ag_e^2 \beta_e^2 S(S+1)H/g_n\beta_n 3kT \qquad (4)$$

where

$$\Delta H \equiv H - H_o$$

and H_o is the magnetic field of the unshifted (a = 0) line.

Consider first the possibility that the thermally accessible triplet states are populated by immobile and localized triplet excitations. The proton isotropic hyperfine splitting constant of the $TCNQ^-$ radical in solution is 1.39 gauss. If the triplet spin density is delocalized over two TCNQ molecules, the coupling constant is approximately 0.70 gauss. Assume that strong exchange interactions of the form $JS_1 \cdot S_2$ exist between neighboring triplets and shorten the lifetime of the spin states. No hyperfine structure is resolved at 77°K, so evidently $a\tau \ll 1$ for all $T \geq 77°K$. This inequality probably also holds for some $T < 77°K$.

From Eq. (4) one would predict a line shifted by an amount ΔH, the shift increasing linearly with decreasing temperature. Thus in a field of 14 kilogauss the shifts are 2.1 and 7.5 gauss for 273°K and 77°K respectively. There also exists one unshifted line which corresponds to protons of molecules in the singlet state. The intensity of the unshifted line is approximately independent of temperature and

the intensity of the shifted line follows the relation $I \propto 1/T \times [\exp(J/kT) + 3]$ where J is the singlet-triplet energy separation. For the salt $(\phi_3PCH_3)^+(TCNQ)^-$ (I), for example, J = 0.065 ev. The signal intensity of this shifted line is sufficient for observation above liquid nitrogen temperatures by a standard wide line NMR spectrometer.

Second, consider the possibility that the thermally accessible triplet state is populated by mobile triplet excitations.[8] If the exciton is moving fast enough so that $a\tau \ll 1$, the electron's field at the nucleus is again averaged and a temperature-dependent shift of the nuclear signal is predicted. Since each proton effectively sees the same average exciton spin density, the shift is related to the magnetic susceptibility. The following formula is readily obtained[9]

$$\Delta H = -2ag_e^2\beta_e^2 H/g_n\beta_n kT[\exp(J/kT) + 3] \qquad (5)$$

A maximum shift occurs when $T \sim J/1.6k$ or $\sim 470°K$ for I. Above this temperature the shift drops off roughly as 1/T and below it decreases more rapidly. There is no unshifted line. In a field of 14 kilogauss the shifts obtained from Eq. (5) are 0.2 and $\sim 10^{-4}$ gauss for 470°K and 77°K respectively.

These experiments are somewhat marginal since even the larger predicted shifts are of the same order of magnitude as the line widths. However, other systems, for example the radical α,α-diphenyl-β-picryl hydrazyl, have been studied under conditions in which the shifts were approximately equal to the line widths.[7, 10] The above

experiments should, therefore, also be feasible.

Added Note. This suggestion was originally submitted as a candidacy proposition in March of 1962. Since this time the ion radical salt Wurster's Blue Perchlorate (WBP) has been extensively investigated by ESR [D.D. Thomas, H. Keller, and H. M. McConnell, J. Chem. Phys., 39, 2321 (1963)]. WBP undergoes a phase transition at 186°K. Below 186°K the cation radicals pair up to form ground singlet states and thermally accessible triplet states. The ESR spectra indicate that the electronic excitations are triplet excitations. Very recently Kawamori and Suzuki [A. Kawamori and K. Suzuki, Mol. Phys., 8, 95 (1964)] have performed wide line NMR experiments on WBP similar to those proposed above. The WBP NMR shift roughly obeys Eq. (4) from room temperature to ~190°K. Below this temperature the shift is in qualitative agreement with Eq. (6). These NMR results are consistent with the exciton interpretation given by Thomas, Keller and McConnell.

REFERENCES

1. D. B. Chesnut and W. D. Phillips, J. Chem. Phys., 35, 1002 (1961).
2. H. Sternlicht and H. M. McConnell, J. Chem. Phys., 35, 1793 (1961).
3. H. M. McConnell and R. Lyndon-Bell, J. Chem. Phys., 36, 2393 (1962).

4. W. D. Phillips and R. E. Benson, J. Chem. Phys. 33, 607 (1960).

5. M. E. Anderson and G. E. Pake, J. Chem. Phys. 33, 1581 (1960).

6. H. M. McConnell and D. B. Chesnut, J. Chem. Phys. 28, 107 (1958).

7. T. H. Brown, D. H. Anderson, and H. S. Gutowsky, J. Chem. Phys. 33, 720 (1960).

8. For the purpose of this discussion, a distributed excitation is equivalent to a moving excitation.

9. The isotropic coupling constant is in units of Mc/sec in Eqs. (1) and (2) and is in units of gauss in Eqs. (4) and (5). An anisotropic contribution to the proton coupling constant will broaden the resonance line if a powdered sample is used but it will add no complications if a single crystal is used.

10. H. S. Gutowsky, H. Kusumoto, J. H. Brown, and D. H. Anderson, J. Chem. Phys. 30, 860 (1959).

PROPOSITION 2

The catalytic or radiation-induced polymerizations of acetylenes in solution (or in the gas phase) give poor yields and polymers of poor quality. Most of the polymeric products are liquid and tarry substances of an aromatic nature.[1,2] The mechanisms of these reactions have not been completely elucidated.[3] Several authors have suggested that the fragment CH=CH-CH=CH-CH=CH forms from acetylene and rapidly cyclizes to yield benzene (or benzene derivatives).[1] Other products observed are divinylacetylene (CH_2=CH-C≡C-CH=CH_2) and polymers which probably contain cyclobutane and cyclobutene rings.[1,2] If only linear additions were allowed, however, long unsaturated polymers might result. We propose a synthesis of semi-infinite polyenynes , semi-infinite polyenes, and a new class of organic semiconductors using a helical template to orient the acetylenic monomer molecules during the polymerization.

The word "synthesis" is used here in the biological sense and we will find it convenient to discuss the reactions in terms of templates, substrates, and a source of energy to initiate the reaction. The template in all cases is a helical urea or thiourea structure. The substrate is, of course, the unsaturated monomer and the source of energy is a photon or electron. There are an average number of "ifs" in the following discussion. However, a great number of "ifs" have been removed by the recent work of Brown and White,[4,5,6] and a review of the pertinent aspects of their work is necessary in order to discuss the synthesis of unsaturated polymers. Brown and White

prepared the urea and thiourea inclusion compounds of a great number of molecules containing double bonds by using well known methods. The crystalline inclusion compounds were then subjected to x-irradiation. The ensuing polymerization my be schematically represented as follows.[6]

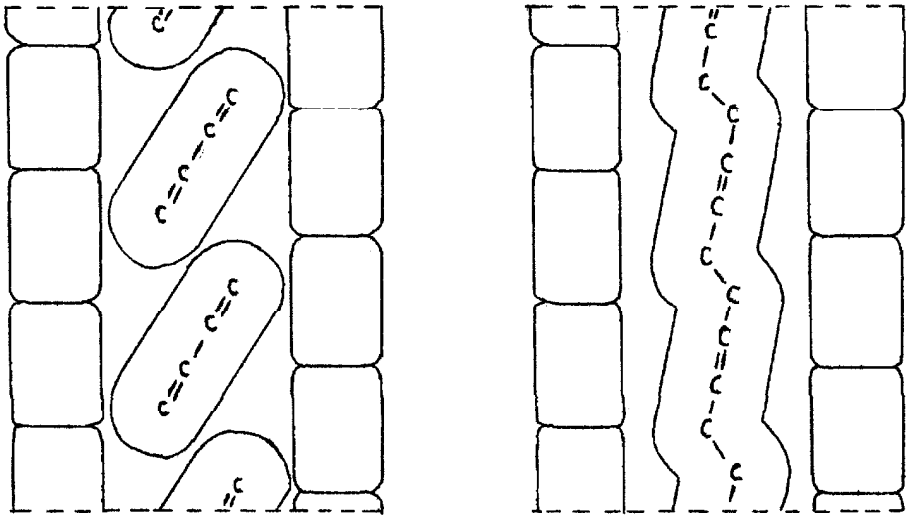

After the inclusion compounds were irradiated, the substrate was removed with water (or other solvents) and the polymers were studied by the usual methods.

The important results are: (1) Long chains resulted from the polymerizations. In a typical dimethylbutadiene polymerization, a short burst of high intensity (2.3×10^5 r/sec) irradiation caused a 70% conversion to polymer in thiourea. The yield and quality of the polymer were independent of temperature over the range -78° to

+30°C. (2) under similar conditions and irradiation doses no polymerization occurred in any monomer in the liquid phase. This dramatically illustrates the importance of the template. (3) The chain growth in the canals probably occurs very rapidly; during irradiation a sharp temperature rise associated with the heat of polymerization was observed. (4) The highest molecular weights obtained in urea were ~ 100,000. and in thiourea ~ 10,000. These polymers may be considered short by polymer chemists, but they do indicate that vacancies and impurities in the canals are not a major problem. (5) In all cases where a solid polymer was produced, the product left after template extraction consisted of small needles with well defined crystal faces. X-ray diffraction patterns of the needles indicate that the chains are lined up parallel to the axis of the needle and that the polymers are highly crystalline (perhaps pseudomorphic). The needles showed well defined extinctions when rotated between crossed polaroids. In the words of Brown and White: "Apparently, when the thiourea (or urea) is extracted from a polymerized complex, the polymer chains collapse together but do not loose the parallel alignment which they had in the complex." (6) In several cases the crystalline polymers crosslinked on standing at room temperature after the template had been removed. (7) The polymers formed are apparently all <u>trans</u>. (8) And finally, copolymers could be formed by including more than one substrate into the template. As in any template reaction, substrate specificity limits the molecules which can be reacted. The classes of compounds are now well known,

however, and linear molecules nearly always include in either urea or thiourea (or both).

Turning now to polyenynes, it is evident that acetylenes rather than ethylenes must be employed in the synthesis. We first note that there has been no published work on polymerizing acetylenes in inclusion compounds. Acetylene itself probably will not form urea or thiourea inclusion compounds because of its short length. (It may be possible to utilize molecular sieves for this purpose and this should be attempted. However, it is unlikely that the acetylene molecules would be held end to end and cyclic polymers would probably result.) A much more likely candidate is butadiyne and we suggest that this compound be investigated initially (although the higher "n-ynes" would be equally interesting). The desired polymer is $(-C\equiv C-HC=CH-C\equiv C-HC=CH-)_n$. Butadiyne polymerizes in solution above about 0°C.[1] However, the inclusion compound may be formed at temperatures well below 0°C and if the inhibitor (present in many industrial samples) is sufficiently bulky, it may be left in solution since it will not be included in the template. The solubility of molecules forming inclusion compounds is greatly increased when urea is added to the solution. This implies a degree of association between the template and substrate in solution and this in turn should aid in reducing the tendancy for random polymerization during inclusion compound formation. Finally, we may add that acetylenes are known to form inclusion compounds.[7]

A similar route to polyenes is proposed. In this case, the

monomer is 1,5-hexadiyne. The initial polymer will probably be $(-HC{=}CH-CH_2-CH_2-C{\equiv}C-)_n$ and the question arises as to whether this polymer can be isomerized to the linear polyene. It is possible that the linear polyene is actually formed during, or soon after, the polymerization. It is even more likely that this isomerization could be accomplished by the application of heat or some other form of energy (unlike the solution case, the polymer is isolated and should exhibit a reasonable thermal stability). For example, an electric discharge could cause a permanent dielectric breakdown of the individual insulating units. A third possibility is chemical isomerization. Recently Sondheimer, Ben-Efraim, and Wolovsky[8] have discovered that 1,5-enynes can be isomerized to linear polyenes by means of potassium t-butoxide in t-butyl alcohol. By this method these authors were able to sunthesize linear polyenes containing as many as ten carbon atoms. The chemical route to long polyenes would, of course, require partial or total solution of the polymer. If successful, these synthetic routes could be extended to substituted polyenes.

The long polyenynes and polyenes are of great interest in absorption spectroscopy.[9] Perhaps of more importance is the possibility of obtaining one, two and three dimensional organic semiconductors. All presently known purely organic semiconductors except polyphenyls and related compounds, are in a sense, zero dimensional. That is, the electronic forces between adjacent molecules are relatively weak and there is no direct π-electron conduction path through the crystal. The poly-p-phenyls are one-dimensional conductors

in that there are one-dimensional conduction paths along the phenyl rings of the polymer. However, these polymers are infusible amorphous powders and are apparently unsuitable as semiconductors.[10,11] The polyenynes and polyenes are also one-dimensional semiconductors. It is doubtful that a macroscopic crystal of unbroken chains could be formed because of impurities and irregularities in the lattice. However, the single polymer strand conduction path in one direction could be quite long, perhaps on the order of 100,000 Å. Since all conduction paths are parallel, this class of organic polymers could easily have carrier mobilities much larger than those of any previously reported organic semiconductor. Two and three dimensional organic semiconductors are possible in the case of enyne polymers through crosslinking of the linear chains. This could provide a macroscopic number of unbroken π-electron paths through a large single crystal.

REFERENCES

1. H. Mark and R. Raff, High Polymeric Reactions (Interscience New York, 1941), p.298.
2. C.E.H. Brown, The Chemistry of High Polymers (Interscience, New York, 1948) p.16.
3. A. Chapiro, Radiation Chemistry of Polymeric Systems (Interscience, New York, 1962) p.89.
4. J.F. Brown, Jr. and D. M. White, J. Am. Chem. Soc., 82, 5671 (1960).

5. D. M. White, J. Am. Chem. Soc., 82, 5678 (1960).

6. J. F. Brown, Jr., Sci. Am., 207 No. 1 , 82 (1962).

7. J. Radell and J. W. Connolly, Advan. X-Ray Anal., 4, 140 (1960).

8. F. Sondheimer, D. A. Ben-Efraim, and R. Wolovsky, J. Am. Chem. Soc., 83, 1675 (1961).

9. H. H. Jaffe and M. Orchin, Theory and Applications of Ultraviolet Spectroscopy (John Wiley and Sons, New York, 1962) chapter 11.

10. J. J. Brophy and J. W. Buttrey, editors, Organic Semiconductors (Macmillan Co., New York, 1962).

11. M. J. S. Dewar and A. M. Talati, J. Am. Chem. Soc., 86, 1592 (1964).

PROPOSITION 3

The valence-state concept was introduced by Van Vleck.[1] Mulliken[2] constructed a table of valence-state energies and this table was later expanded by Skinner and Prichard.[3] Moffitt[4] has also made valuable contributions to the theory of valence states. Very recently Companion and Ellison[5, 6] have constructed tables (based on Moffitt's approach) which enable the rapid expansion of valence-state energies in terms of spectroscopic energies. The theory of valence states developed by these authors has been useful in relating the electronic properties of molecules to known atomic properties. For example, many of the integrals encountered in molecular calculations can be estimated from atomic spectroscopic data. We review here the development of semi-emperical one-center coulomb integrals in terms of valence state energies and suggest a modification of the method used to estimate the integrals when there are two π-electrons on one center.

Pariser[7, 8] estimates the carbon one center coulomb integral $(CC|CC)$ using the relation

$$(CC|CC) = I_c + A_c \qquad (1)$$

where I_c and A_c are the appropriate valence state ionization potential and electron affinity, respectively. The rationalization of this step is based on the simple charge transfer process

$$\dot{C} + \dot{C} \longrightarrow \dot{\ddot{C}}^- + C^+$$

The electrons shown are π electrons and the remainder of the electrons are in sp^2 hybrid orbitals. According to the Goeppert-Mayer and Sklar[9] (GMS) theory the total π-electron energy on the left is $-2I_c$ while on the right it is $-2I_c + (CC|CC)$. The energy difference is therefore $(CC|CC)$ and this may be equated to the value of $I_c - A_c$ obtained (indirectly) from experimental spectroscopic data. Eq. (1) is also used to evaluate integrals over oxygen and nitrogen orbitals, provided that each atom contributes one electron to the π-system. If the atom contributes two electrons to the π-system, however, the interpretation of the charge-transfer reaction is not as clear. Very few attempts have been made to obtain semiemperical coulomb integrals for the two electron case. Using nitrogen as an example, Paloni[10, 11] argues that the charge transfer process $2\dot{N}^{\cdot} \longrightarrow \dot{N}^{+} + \dot{N}^{-}$ should be replaced by the process

$$2\dot{N}^{+} \longrightarrow N^{++} + \dot{N}^{\cdot} \qquad (2)$$

This is a reasonable extension of the arguments of Pariser. To obtain a better understanding of the problem it is necessary to expand the valence-state energies in terms of spectroscopic energies and to quantitatively relate these energies to the coulomb and exchange integrals. For a specific example, we will discuss the semiemperical integral of oxygen.

To obtain the valence-state energies in terms of spectroscopic energies, one first writes down the valence-bond wave function, Ω, of a given structural formula as a linear combination of antisymmetrized product wave functions, D_i.[1-6, 12] Since configurational interaction is

neglected, only one valence bond function is considered. The D_i are then written as a partially antisymmetrized product of normalized determinantal wave functions D^M, one for each of the M atoms of the molecule.[13] The D^M are expanded in terms of the atomic eigenfunctions Φ_α^A of the atom A, and the coefficients $\Gamma_{j\alpha}$ of each product of the Φ_α^A are collected in a systematic fashion. One then imagines that the molecule is completely dissociated in such a manner that the coefficients $\Gamma_{j\alpha}$ retain their values for the equilibrium internuclear distances. The resulting nonstationary state of the atoms is therefore a simple product (without antisymmetrization) of the Φ_α^A's and atom A may be considered to be in the nonstationary valence state[4]

$$\Omega^A = \sum_\alpha \Phi_\alpha^A G_\alpha^A$$

where G_α^A is the sum of the $|\Gamma_{j\alpha}|^2$. The energy of the valence state is the sum of the products of the spectroscopic-state energies times the factors, G_α^A.

As an example, consider the $:\dot{\underset{\cdot\cdot}{O}}-H$ radical. One possible valence bond structure for this radical is

$$\Omega = \frac{1}{\sqrt{2}} |P_+ \overline{P}_+ P_- \overline{P}_0 h| - \frac{1}{\sqrt{2}} |P_+ \overline{P}_+ P_- P_0 \overline{h}|$$

where $P_{+,0,-}$ are the 2p orbitals with $m_\ell = +1, 0, -1$, h is the hydrogen 1s orbital, and the oxygen 1s and 2s filled shells have been omitted. Expanding the single determinantal wave functions, one obtains

$$|P_+ \overline{P}_+ P_- \overline{P}_0 h| = \frac{1}{\sqrt{5}} [1 - \sum_{i=1}^{4} P_{i5}] \; |P_+ \overline{P}_+ P_- \overline{P}_0| \; |h|$$

$$|P_+\overline{P}_+P_-P_0\overline{h}| = \frac{1}{\sqrt{5}}\left[1 - \sum_{i=1}^{4} P_{i5}\right] |P_+\overline{P}_+P_-P_0| \, |\overline{h}|$$

and from the tables of Companion and Ellison (or by the procedures given by Eyring, Walter, and Kimball[14])

$$|P_+\overline{P}_+P_-\overline{P}_0| = \frac{1}{\sqrt{2}}\left[-\Phi^0(^1D, 1, 0) + \Phi^0(^3P, 1, 0)\right]$$

$$|P_+\overline{P}_+P_-P_0| = \Phi^0(^3P, 1, 1)$$

$$|h| = \Phi^h(^2S, 0, \tfrac{1}{2}) \text{ and } |\overline{h}| = \Phi^h(^2S, 0, -\tfrac{1}{2})$$

The standard notation is used for the stationary-state functions $\Phi(^{2s+1}L, M_L, M_S)$ and the operator P_{ij} only permutes electrons between different determinants, D^M (electrons 1-4 and 5 are associated with oxygen and hydrogen, respectively). The valence bond function before dissociation is

$$\Omega = \frac{1}{\sqrt{5}}\left[1 - \sum_{i=1}^{5} P_{i5}\right]\left[-\tfrac{1}{2}\Phi^0(^1D, 1, 0)\Phi^h(^2S, 0, \tfrac{1}{2}) + \tfrac{1}{2}\Phi^0(^3P, 1, 0)\Phi^h(^2S, 0, -\tfrac{1}{2})\right.$$

$$\left. - \frac{1}{\sqrt{2}}\Phi^0(^3P, 1, 1)\Phi^h(^2S, 0, -\tfrac{1}{2})\right]$$

The energy of the oxygen atom in its valence state is therefore

$$E(O^0;\ s^2x^2yz,\ V_2) = E(O^0;\ s^2, p_+^2, p_-, p_0) = \tfrac{1}{4}E(^1D) + \tfrac{1}{4}E(^3P) + \tfrac{1}{2}E(^3P)$$

$$= \tfrac{3}{4}E(^3P) + \tfrac{1}{4}E(^1D)$$

likewise

$$E(O^+; s^2y^2z; V_1) = \tfrac{1}{2} E(^2D) + \tfrac{1}{2} E(^2P)$$

$$E(O^-; s^2x^2yz^2; V_1) = E(^2P)$$

Here V_i is the number of singly occupied orbitals and x, y, and z denote the 2px, 2py, and 2pz orbitals, respectively. These same valence-state energies may be obtained from the valence-bond functions of other molecules (H_2O, for example[4]). Numerical values for the valence-state energies are obtained from experimental spectroscopic data using these equations.

The valence-state energies may be further decomposed into the atomic I, J, and K (core, coulomb, and exchange) integrals by methods similar to those of Eyring, Walter, and Kimball.[14] The results are[15-17]

$$E(O^0; s^2x^2yz; V_2) = E_{core} + 4\,I_p + J_{xx} + 5\,J_{xy} - (5/2)K_{xy} \qquad (3)$$

$$E(O^+; s^2y^2z; V_1) = E_{core} + 3\,I_p + J_{xx} + 2\,J_{xy} - K_{xy} \qquad (4)$$

$$E(O^-; s^2x^2yz^2; V_1) = E_{core} + 5\,I_p + 2\,J_{xx} + 8\,J_{xy} - 4\,K_{xy} \qquad (5)$$

where x and y are the 2p functions which have vanishing components of angular momentum about the x and y axes, respectively, and $z \equiv p_0$. Using these relations the energies of the reactions

$$O^-(s^2x^2yz^2; V_1) \longrightarrow O^0(s^2x^2yz; V_2) + e^- \qquad \Delta E = A_0$$

$$O^0(s^2x^2yz;\ V_2) \longrightarrow O^+(s^2y^2z;\ V_1) + e^- \qquad \Delta E = I_0$$

are readily obtained in terms of I, J, and K. Collecting terms one obtains

$$J_{XX} = (OO|\,OO) = E(O^+;\ s^2y^2z;\ V_1) + E(O^-;\ s^2x^2yz^2;\ V_1) - 2E(O^0;\ s^2x^2yz;V_2)$$

$$= I_0 - A_0 \qquad (6)$$

or, from the valence-state data of Parks and Parr,[16]

$$(OO|\,OO) = (17.8) + (-2.2) - 2(0.49) = 14.6 \text{ ev}$$

The integral $(OO|\,OO)$ may also be developed in terms of the energies of the singly and doubly ionized atoms. The resulting expression is

$$(OO|\,OO) = J_{XX} = E(O^{++},\ s^2yz,\ V_2) + E(O^0, s^2x^2yz,\ V_2) - 2E(O^+,\ s^2xyz,\ V_3) \qquad (7)$$

or

$$(OO|\,OO) = (49.4) + (0.5) - 2\ (15.3) = 19.3 \text{ ev}$$

The 19.3 ev value results from the quantitative treatment of the charge transfer reaction (2) and the 14.6 ev value is the same as that obtained from Eq. (1). The difference arrises from the common orbital treatment rather than errors in spectroscopic measurements. We suggest that Eq. (6) leads to a more reliable estimate of the coulomb integral than does Eq. (7). Eq. (7), which involves the second ionization

potential of oxygen, is formally consistent with one extension of the GMS theory to the two π-electron (one one center) case. However, even the first ionization potential of the atom in the molecular environment is smaller than the value calculated from the valence-state theory. The effect on the second ionization potential is difficult to predict. Certainly the molecular properties of interest depend more critically on the first ionization potential of oxygen than on the second ionization potential. When using Eq. (6) in a modification of the GMS theory, it may be advisable to estimate the orbital energy by the first ionization potential (plus a coulomb term) rather than the second ionization potential. Improvements on the common orbital method should be made. Julg,[18] among others, is considering this problem and the results published so far are similar to those obtained from Eq. (1).

As a final comment, we suggest that equations similar to (6) be used in place of Eq. (1) to obtain the semiempirical value of the coulomb integral.[19] Formally the results are the same. It is relatively easy, however, to employ an incorrect valence-state energy when using Eq. (1). The only purpose in considering the quantity I - A is that, for a particular choice of three valence-state energies all core, J_{xy}, and K_{xy} integrals cancel leaving only J_{xx}. There are usually several valence-state energies to choose from. For example, one alternate choice for the first method given above is $E(O^{+1}; s^2xyz, V_3)$ and two alternate choices for the second method are $E(O^{+1}; s^2xyz, V_3)$ and $E(O^{+2}; s^2z^2, V_0)$. The energies do not always differ sufficiently to make the choice an obvious one. If the energies are systematically

expanded in terms of atomic integrals, however, the choice is obvious because the cancellation of all core, J_{xy}, K_{xy} integrals occurs for only one combination of the valence-state energies.

REFERENCES

1. J. H. Van Vleck, J. Chem. Phys. 2, 22 (1935).
2. R. S. Mulliken, J. Chem. Phys. 2, 782 (1935).
3. H. A. Skinner and H. O. Pritchard, Trans. Faraday Soc. 49, 1254 (1953).
4. W. Moffitt, Repts. Progr. Phys. 17, 173 (1954).
5. A. L. Companion and F. O. Ellison, J. Chem. Phys. 28, 1 (1958).
6. F. O. Ellison, J. Chem. Phys. 36, 3107 (1962).
7. R. Pariser, J. Chem. Phys. 21, 568 (1953).
8. R. G. Parr, Quantum Theory of Molecular Electronic Structure (W. A. Benjamin, New York, 1963).
9. M. Goeppert-Mayer and A. L. Sklar, J. Chem. Phys. 6, 645 (1938).
10. L. Paoloni, Nuovo Cimento 4, 410 (1956).
11. M. J. S. Dewar and L. Paoloni, Trans. Faraday Soc. 53, 261 (1957).
12. All spin-spin and spin-orbit terms are neglected in this approach (see references 1 through 5).

13. If the orbitals are hybridized they must first be expanded in terms of unhybridized orbitals. See references 4 and 5.

14. H. Eyring, J. Walter, and G. E. Kimball, Quantum Chemistry (John Wiley and Sons, New York, 1944), ch. 9.

15. J. M. Parks and R. G. Parr, J. Chem. Phys. 32, 1657 (1960).

16. J. M. Parks, Ph. D. thesis, Carnegie Institute of Technology, 1956.

17. It is a simple matter to obtain the energies by this method since one may expand directly the matrix element $\langle O^{\nu}(s^{\ell}p^{n}; V_{m})|\mathcal{H}|O^{\nu}(s^{\ell}p^{n}; V_{m})\rangle$ providing the number of K_{xy} integrals is always chosen to be one half the number of J_{xy} integrals (this corresponds to Moffitt's random spin argument). For example, $\langle (4!)^{-\frac{1}{2}} P_{ij} s\bar{s}x\bar{x}yz \left| \sum_i \mathcal{H}_{\text{core(i)}} + \sum_{i<j} 1/r_{ij} \right| (4!)^{-\frac{1}{2}} P_{ij} s\bar{s}x\bar{x}yz\rangle$ gives Eq. (3). One obtains better insight, however, by expanding the spectroscopic state wave functions into single determinantal functions and then expanding the matrix elements of these functions into atomic integrals by the methods of Eyring, Walter, and Kimball.[14] (One must, in general, expand the $J_{\pi\sigma}$, $K_{\pi\sigma}$, etc. into F and G functions and then collect terms.)

18. A. Julg, J. Chim. Phys. 57, 19 (1960).

19. This is undoubtedly done by many investigators.

PROPOSITION 4

The chemistry of micelles continues to be one of the more active fields of colloid and surface chemistry. A micelle may be defined as a thermodynamically stable association colloid formed by three or more amphipathic molecules.[1] Partly because of their importance to the soap and detergent industry, the overwhelming majority of papers published on micelles have delt with detergent micelles in aqueous solutions. There is also a growing literature on micelle formation in liquid hydrocarbons. Dramatic changes frequently occur in the physical properties of the colloid when small amounts of water are added to the nonaqueous solutions. The properties of the (semi) nonaqueous solutions are the subject matter of this proposition.

Many proposed structures and properties of nonaqueous micelles are deduced from the extensively-studied aqueous systems. In water, the ionic amphipaths (e. g. sodium dodecyl sulfate) cluster into micelles at concentrations exceeding the critical micelle concentration (c. m. c.). The hydrophilic parts are exposed to the water while the hydrophobic hydrocarbon chains extend into the interior of the micelle.[2] In nonaqueous solvents, just the opposite arrangement is presumed to exist; the polar heads of the amphipatic molecule are buried in the center of the aggregate and the hydrocarbon chains extend into the solvent.[2,3] Because of this inverted structure, the nonaqueous micelles carry no excess charge and therefore cannot be studied by the usual conductivity methods. Several physico-chemical techniques, including density,

viscosity, osmotic pressure, and ebullioscopic methods, have been frequently employed to investigate the size and shape of the micelles.[1-4] Most of the methods used, however, give only the average detergent content and average water content of a micelle. It is of interest to obtain information regarding the distribution of water molecules in the micelles and for this purpose a nuclear magnetic resonance experiment is proposed. Consider the typical oil-soluble surfactant bis-(2-ethylhexyl) sulfosuccinate (Aerosol OT), for example. In anhydrous dodecane Aerosol OT is present in micellar form. The c. m. c. of Aerosol OT has not been determined but the micelles are apparently present even for very low surfactant concentrations. Typical solutions contain 1-10 g. Aerosol OT in 90 g. of hydrocarbon solvent.[1, 4] The average number of Aerosol OT molecules per micelle is ~ 30 in a solution containing 1 g. Aerosol OT and 100 g. dodecane.[1] The micelle diameter is thought to be roughly twice the effective length of an Aerosol OT molecule.

As water is added to the solution it is solubilized by the detergent and presumably occupies a position near the center of the micelle. One observes that the average micelle size increases as the water is added to the system.[1, 4, 5] The position of the H_2O proton NMR signal should be sensitive to the ratio of the detergent concentration to the water concentration of a given micelle. For one water molecule, the down-field shift due to the ion is expected to be on the order of 4-10 ppm depending on the cation employed. There is also an up-field shift caused by the breaking of hydrogen bonds and the magnitude of this shift

will depend on the structure of the micelle.[6] It is highly unlikely that these two shifts will cancel. All H_2O protons on the interior of a given micelle will exchange rapidly, producing a single sharp line characteristic of the size and shape of the micelle. The resulting shifts will be difficult to calculate but one should be able to obtain a measure of the micelle uniformity from the line width data. The line will be inhomogeneously broadened if the water: detergent ratio varies greatly among the micelles. Initially, one should look for a difference in line width as a function of water and detergent concentrations. Temperature, pressure, and solvent studies would also be useful. Aromatic and aliphatic protons may, of course, be replaced by deuterium. A comparison of the NMR and X-ray data would be useful. From X-ray data on nonaqueous and aqueous micelles, Winsor[8] suggests that three types of micelles, spheroidal lipophilic, spheroidal hydrophilic, and lamellar, coexist in solution.

Density measurements have been reported on a series of solutions containing 0.1-20 g. water and 10 g. Aerosol OT dissolved in 90 g. n-dodecane.[5] The apparent specific volume of water is 0.91 for 0.1 g. water in the solution. As more water is added the apparent specific volume increases rather sharply. After 2 g. water has been added the specific volume increases more gradually and approaches a value of 1.00. Mathews and Hirschhorn[5] interpret these results as indicating that the initial increments of water strongly hydrate the polar groups of the detergent. Additional water is considered to retain its bulk density in the micelle. In view of these data we propose that an attempt

be made to freeze the solubilized water by increasing the pressure, lowering the temperature, or by a combination of these techniques. If a solid core of ~ 50-100 water molecules rotates sufficiently rapidly, a sharp line will be observed in the NMR spectrum. There will also be a shifted line from the water molecules surrounding the ions of the detergent. Nonrotating microcrystallites would not give high resolution NMR signals but in either case an effect on the NMR spectrum should occur as the crystallite forms. It may be possible to obtain information regarding the amount of water solvating the ions relative to the amount present in the central core.

These experiments are obviously nontrivial. There are, however, a large number of possible solvent-detergent combinations which could be studied. Several sulfonates have been reported other than Aerosol OT.[1-4, 8] Oil-soluble alkali metal phenylstearates are known to form micelles.[9] The viscosities of the lithium, sodium, potassium, and cesium salts of phenylstearic acid in benzene decrease sharply as water is added to the solution. Apparently spherical micelle formation occurs only after water has been added (in contrast to the sulfonate case). Several other soaps and detergents have been reported as detergent additives and corrosion inhibitors in lubricating oils.[1, 3]

REFERENCES

1. C. R. Singleterry, J. Am. Oil Chem. Soc. 32, 446 (1955).
2. K. J. Mysels, Introduction to Colloid Chemistry (Interscience, New York, 1959).

3. L. I. Osipow, Surface Chemistry (Reinhold, New York, 1962).

4. A. M. Schwartz, J. W. Perry, and J. Berch, Surface Active Agents and Detergents (Interscience, New York, 1958).

5. M. B. Mathews and E. Herschhorn, J. Colloid Sci. 8, 86 (1953).

6. J. A. Pople, W. G. Schneider and H. J. Bernstein, High-resolution Nuclear Magnetic Resonance (McGraw-Hill, New York, 1959).

7. P. A. Winsor, J. Phys. Chem. 56, 391 (1952).

8. R. W. Mattoon and M. B. Mathews, J. Chem. Phys. 17, 496 (1949).

9. J. G. Honig, and C. R. Singleterry, J. Phys. Chem. 60, 1108 (1956); 1114 (1956).

PROPOSITION 5

Many magnetic resonance investigations of aromatic hydrocarbons in their triplet states have been reported since the classic experiments of Hutchison and Mangum.[1] It is logical to extend this work to excitations confined to two molecules. Sternlicht and McConnell[2] have calculated the dimer excitation spectrum as a function of the excitation transfer rate between two translationally-nonequivalent sites. As the transfer rate is increased the monomer lines are homogeneously broadened. For very fast transfer rates the fine structure doublet is represented by the average of the two monomer spin Hamiltonians. Here we propose methods for distinguising the dimer signals (in the fast transfer limit) from the monomer and impurity signals. It is instructive to consider a specific system and we arbitrarily choose naphthalene in a durene lattice. The right-handed coordinate systems for the monomer and dimer are taken to be[3]

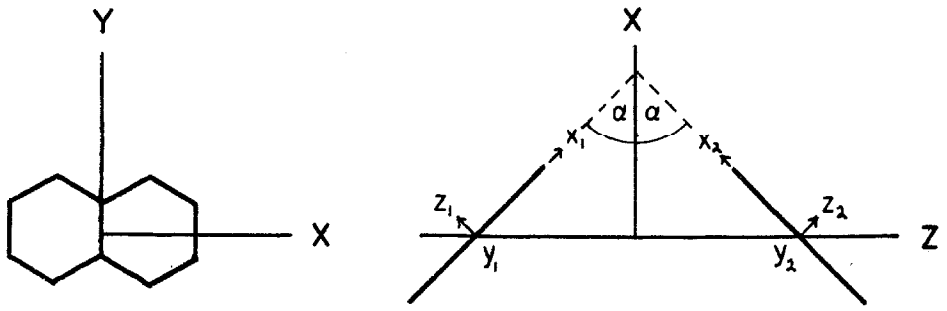

MONOMER DIMER

where x_1, y_1, z_1 and x_2, y_2, z_2 are the magnetic axes of the two naphthalene molecules.

The monomer spectra may be calculated by standard methods. To obtain the dimer spectra it is convenient to first calculate the effective zero field parameters, D_{12} and E_{12}, of the dimer. These parameters may then be used to obtain the dimer spectra by the usual methods. The individual dipolar Hamiltonians $\mathcal{H}_1$ and $\mathcal{H}_2$ for the two naphthalene molecules are

$$\mathcal{H}_1 = DS_{Z_1}^2 + E\,(S_{X_1}^2 - S_{y_1}^2) \tag{1}$$

$$\mathcal{H}_2 = DS_{Z_2}^2 + E\,(S_{X_2}^2 - S_{y_2}^2) \tag{2}$$

where $D/hc = 0.1003\ cm^{-1}$ and $E/hc = -0.0137\ cm^{-1}$. In the dimer coordinate system the dimer Hamiltonian $\mathcal{H}_{12}$ is

$$\mathcal{H}_{12} = \tfrac{1}{2}(\mathcal{H}_1 + \mathcal{H}_2) = [D - (D - E)\sin^2\alpha]\,S_Z^2 + [\tfrac{1}{2}(D - E)\sin^2\alpha]\,(S_X^2 + S_y^2) + [E + \tfrac{1}{2}(D - E)\sin^2\alpha]\,(S_X^2 - S_y^2) \tag{3}$$

Substituting $S_X^2 + S_y^2 = S^2 - S_Z^2$ and omitting the operator S^2, Eq. (3) reduces to

$$\mathcal{H}_{12} = [D - \tfrac{3}{2}(D - E)\sin^2\alpha]\,S_Z^2 + [E + \tfrac{1}{2}(D - E)\sin^2\alpha]\,(S_X^2 - S_y^2) \tag{4}$$

and D_{12} and E_{12} for the naphthalene dimer are

$$D_{12} = [D - \tfrac{3}{2}(D - E)\sin^2\alpha] \tag{5}$$

$$E_{12} = [E + \tfrac{1}{2}(D - E)\sin^2\alpha] \qquad (6)$$

for our model $\alpha = 45°$ and therefore $D_{12}/hc = E_{12}/hc = +0.01480\ cm^{-1}$.

Either or both the monomer and the dimer spectra may be observed experimentally. Consider first the case where both monomer and dimer signals are observed. The two translationally-nonequivalent monomer sites will give rise to a total of four $\Delta m = \pm 1$ transitions. The dimer will only have two $\Delta m = 1$ transitions and this aids in distinguishing the dimer signals from impurity signals (the impurities being other phosphorescing aromatic molecules in the lattice). Whenever "spurious" resonances are observed, we suggest that the positions of both the dimer and monomer lines be calculated and compared to the experimental line positions. A plot of the monomer and dimer splittings when the magnetic field is in the x_2y_2 monomer plane is shown in Fig. 1. The microwave quantum was chosen to be $0.3210\ cm^{-1}$ (typical X band). The $o°$ and $90°$ positions correspond to the magnetic field being parallel to the x_2 and y_2 axes, respectively. One interesting feature of Fig. 1 is that the center of the dimer (xxx) doublet is shifted up field from the center of the doublets of monomer one (---) and monomer two (- · -). Along the y_2 axis the magnitude of the dimer and monomer splittings are the same, but the dimer lines are again shifted to higher fields. Another distinguishing feature is that the dimer splitting vanishes when the two monomer splittings cross. We propose that this phenomenon be investigated for more general models. (This is algebraically tedious but may be accomplished using the definition of

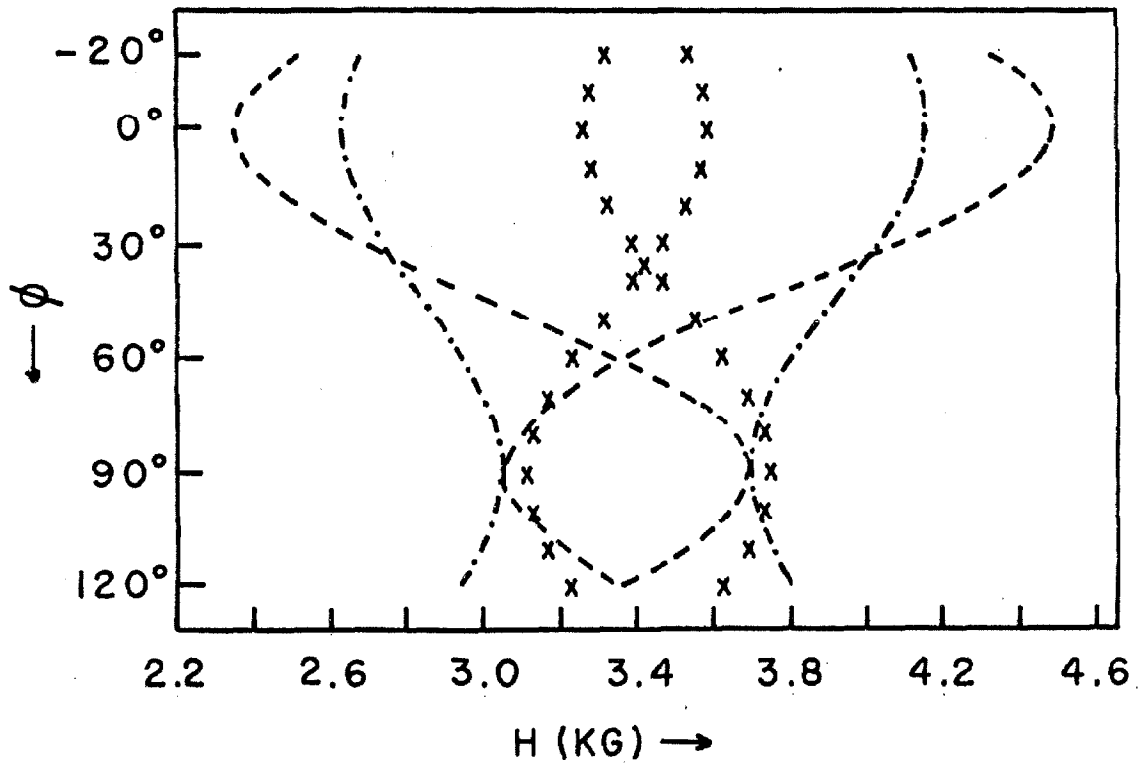

Figure 1. The fine structure splittings of the monomers (--, - ·) and of the dimer (xx) vs rotation of the magnetic field in the molecular plane of one of the monomers.

D_{12} and E_{12} and the general cubic equation given in Appendix III.) If it can be shown that the dimer lines coalesce whenever the monomer lines cross this would be a very useful rule in identifying dimer signals. In any case the splittings rather than the signal intensities must be considered because the relative concentrations of the monomers and dimers are not known. In some crystals it is conceivable that pairs of guest molecules are incorporated into the lattice, yielding a high dimer concentration. In other crystals (such as naphthalene in durene) the concentration of monomers is apparently much greater than the concentration of dimers.

If only the dimer lines are observed the problem becomes more difficult. As mentioned above, the dimer splittings will not have the symmetry of the displaced host molecules (when there are two translationally-nonequivalent lattice sites there is only one dimer). One principle magnetic axis of the monomer is perpendicular to the aromatic plane of the displaced host molecule and this is not in general true for the dimer. Both of these differences should help in identifying the dimer spectra. Unfortunately, if the guest molecules do not occupy substitutional sites it is remotely possible that neither the monomer nor the dimer signals would have the expected symmetry properties. We, therefore, propose the following experiment to distinguish between monomer and dimer signals (when only one doublet is observed). A mixture of 50% perdeuterated and 50% protonated guest molecules should be incorporated into the lattice. The triplet state of the perdeuterated molecule is lower than that of the protonated molecule by

$\sim 10^2$ cm^{-1}. At low temperatures, therefore, one would observe a large signal intensity from the deuterated monomer even though it is adjacent to a protonated monomer. The energy difference between the deuterated and protonated molecules can be controlled by the extent of deuteration, so that it should be possible to prepare a crystal which exhibits dimer signals at one temperature and a combination of dimer and monomer signals at a lower temperature.

REFERENCES

1. C. A. Hutchison, Jr., and B. W. Mangum, J. Chem. Phys. 34, 908 (1961).
2. H. Sternlicht, Ph. D. thesis, California Institute of Technology, (1963).
3. The model is somewhat idealized since we have ignored a 7° tilt of the y_1 axis away from the y axis. The angle α is taken to be 45° (it is roughly 43° for durene[4]).
4. J. Robertson, Proc. Roy. Soc. A141, 594 (1933); A142, 659 (1933).